

0149-704

Wm. A. G. 1963

0149-704 43
Little Joe

SOLID ROCKET PLANT

DIRECTOR
 ASSO DIR
 A DIR G 1
 A DIR G 2
 A DIR G 3
 T ASST
 SR ST SO
 R ASST
 ERD
 EDIT
 REC
 ACD
 AMPD
 APD
 DID
 FMED
 FSRD
 IRD
 SMD
 STRUC
 NASA
 ETS
 ENGR
 A DIR ADM
 P B AFF
 SECURITY
 FISC
 ASD
 PHOTO
 PERS
 PROC
 FROM

Final Report

LITTLE JOE II MOTOR DEVELOPMENT PROGRAM

Contract No. NAS 9-456

Report 0667-01F

25 October 1963

N66 267 62
 (ACCESSION NUMBER)
 131
 (PAGES)
 CR-75263
 (NASA CR OR TMX OR AD NUMBER)

(THRU)
 1
 (CODE)
 28
 (CATEGORY)

GPO PRICE \$

CFSTI PRICE(S) \$

Hard copy (HC) 4.00

Microfiche (MF) 1.00

ff 653 July 65



25 October 1963

Report 0667-01F

FINAL REPORT

LITTLE JOE II MOTOR DEVELOPMENT PROGRAM

Prepared by

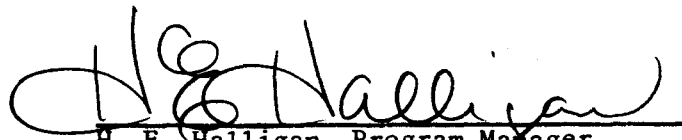
AEROJET-GENERAL CORPORATION
SOLID ROCKET PLANT
Sacramento, California

Contract No. NAS 9-456

Prepared for

National Aeronautics and Space Administration
Manned Spacecraft Center
Houston, Texas

Approved by:


H. E. Halligan, Program Manager
Little Joe II Propulsion Project

9665

AEROJET-GENERAL CORPORATION
A SUBSIDIARY OF THE GENERAL TIRE & RUBBER COMPANY

TABLE OF CONTENTS

	<u>Page</u>
I. Introduction	1
II. Summary	1
III. Program History	1
A. Contract History	1
B. Milestones	2
IV. Motor Development	2
A. Motor	2
B. Nozzle	2
C. Ignition System	3
D. Igniter Initiator	5
E. Destruct System	6
F. Weather Seals	7
V. Test Program	7
A. Full-Scale-Motor Firings	7
B. Subscale-Motor Firings	11
C. Igniter Tests	11
D. Destruct Tests	13
E. Weather-Seal Tests	15
VI. Motor Processing and Assembly	16
A. Motors Processed	16
B. Processing Operations	16
VII. Additional Technical Effort	22
A. Monte Carlo Computer Ballistic Performance Study	22
B. Environmental Temperature Gradient Study	27
VIII. Reliability and Quality Control	28
A. Reliability	28
B. Quality Control	31
IX. Ground Support Equipment	34
A. Items of Equipment	34
B. Description	34
C. Manuals	38

FIGURE LIST

	<u>Figure</u>
Little Joe II Program Milestone Completion Schedule	1
Little Joe II Motor Chamber	2
Straight Nozzle	3
Cantable Nozzle	4
High-Altitude Igniter	5
Comparison of Igniter Charge Weights vs Motor Free Volumes	6
Correlation of Total Igniter Energy vs Delivery Rate	7
Igniter Development Program Phases	8
Initiator Design Data	9
Schematic Drawing of Initiator	10
Destruct Unit for Algol ID Motor	11
Schematic Drawing of Motor Test Installation With Altitude Facility	12
Motor LJ-7, Prefiring Side View	13
Motor LJ-7, Prefiring Front View	14
Motor LJ-7, Prefiring View of Igniter and Transducers	15
Motor LJ-7, Prefiring Aft View	16
Instrumentation Locations, Motor LJ-7	17
Performance Characteristics, Motor LJ-1, -4, and -7	18
Thrust and Pressure vs Time, Motor LJ-1	19
Thrust and Pressure vs Time, Motor LJ-4	20
Thrust and Pressure vs Time, Motor LJ-7	21
Postfiring Side View, Motor LJ-1	22
Postfiring Side View, Motor LJ-1	23
Postfiring Aft View, Motor LJ-4	24
Postfiring Aft View, Motor LJ-7	25
Postfiring View of Nozzle, Motor LJ-7	26
Postfiring View of Top Destruct Cut, Motor LJ-7	27
Postfiring View of Bottom Destruct Cut, Motor LJ-7	28
Side-Force Data, Motor LJ-7	29
Jet-Deflection-Angle Data, Motor LJ-7	30
Nozzle Temperature at Locations TN4, TN6, and TN7; Motor LJ-7	31

FIGURE LIST (cont.)

	<u>Figure</u>
Chamber Temperatures at Locations TC13, TC17, and TC1; Motor LJ-7	32
Igniter Qualification-Test Results	33
Motor LJ-4 Ignition-Performance Data	34
Postfiring View, Motor LJ-4 Igniter	35
Postfiring View of Nozzle Throat Section, Motor LJ-1	36
Postfiring View of Aft-Closure Section, Motor LJ-1	37
Postfiring View of Nozzle Exit-Cone Section, Motor LJ-1	38
Sequence of Igniter Performance	39
Igniter Performance After Exposure to Extremes of Environmental Conditioning	40
Postfiring View of Altitude Igniter	41
Destruct-Unit Test Assembly	42
Witness Plates Cut During Destruct Test	43
Prefiring View of Motor Destruct-Test Setup	44
Postfiring View of Test Stand	45
Primacord Harness Assembly and Test Plates, Seven-Motor-Configuration Destruct Test	46
Close-up of Seven-Motor-Configuration Test	47
Excerpts From Film of Weather-Seal Break Test, Full-Igniter Charge Pressurization	48
Weather Seal Broken by Igniter Charge	49
Excerpts From Film of Weather-Seal Break Test, Igniter-Booster Charge Pressurization	50
Little Joe II Motor Fabrication and Processing Schedule	51
Little Joe II Motor Weight Summary	52
Algol ID Mod 1 Motor Assembly	53
Algol ID Mod 2 Motor Assembly	54
Algol ID Mod 1 Motor Envelope	55
Algol ID Mod 2 Motor Envelope	56
Values for Characteristics Used in Computer Program	57
Chamber Pressure vs Time at 70°F, 100 Runs	58
Sea-Level Thrust vs Time at 70°F, 100 Runs	59
Altitude Thrust vs Time at 70°F, 100 Runs	60

FIGURE LIST (cont.)

	<u>Figure</u>
Nominal Thrust and Pressure at 50, 70, and 90°F at Sea Level	61
Nominal Thrust and Pressure at 50, 70, and 90°F at Altitude	62
Three-Sigma Limits of Thrust and Pressure at 70°F and Sea Level	63
Three-Sigma Limits of Thrust and Pressure at 70°F and Altitude	64
Thrust and Pressure at 70°F From Sea Level to 100,000 ft	65
Hot-Season Grain-Temperature Gradients	66
Cold-Season Grain-Temperature Gradients	67
Rocket-Motor Semitrailer	68
Semitrailer Top	69
Principal Dimensions of Semitrailer	70
Semitrailer Equipment	71
Rocket Motor Lifting Beam	72
Auxiliary Hoist Control and Principal Dimensions of Lifting Beam	73
Transport and Erector Trailer	74
Principal Dimensions of Transport and Erector Trailer	75
Motor Storage Dolly	76
Rocket-Motor Borescope	77
Principal Dimensions of Rocket-Motor Borescope	78

ATTACHMENT

Little Joe II Program Process Flow Chart

I. INTRODUCTION

This report describes the design, development, fabrication, and delivery of motors and items of ground support equipment that Aerojet-General has accomplished in compliance with National Aeronautics and Space Administration Contract NAS 9-456.

II. SUMMARY

Under Contract NAS 9-456, Aerojet-General has designed and developed an igniter capable of operating at an altitude of 100,000 ft, a destruct system, and a cantable nozzle for the Algol ID motor. Seven motors were fabricated, three for cantable-nozzle testing and four for delivery. In addition, 11 items of ground support equipment were designed, fabricated, and delivered; associated program support was also provided. The program described herein was initiated in May 1962 and concluded in September 1963.

III. PROGRAM HISTORY

A. CONTRACT HISTORY

National Aeronautics and Space Administration (NASA) Contract NAS 9-456 was received 28 May 1962. The contract required design, proof testing, and delivery of 19 each adjustable cantable nozzles, igniters, and Algol ID motors; delivery of three Algol ID motor transporters; and the necessary program support functions. Associated support effort and hardware and the specific program details were to be in accordance with the program plan prepared by Aerojet-General and approved by NASA.

Following submittal of the program plan in July 1962, NASA redirected the program in October 1962. The number of deliverable motors was reduced to four with straight nozzles and the number of test motors for canted-nozzle development was reduced to three. In addition, support services and equipment requirements were reduced accordingly. Development of an igniter and a forward-head-mounted destruct system as specified in the program plan was included in the program redirection.

III, A, Contract History (cont.)

In January 1963, NASA changed the requirements for the destruct system from a forward-head-mounted system to a chamber-mounted system.

B. MILESTONES

The completion dates of program milestones from receipt of the letter contract in May 1962 through program completion in September 1963 are shown in Figure 1.

IV. MOTOR DEVELOPMENT

A. MOTOR

1. Chamber

The Little Joe II motor chamber design (Figure 2) is similar to the Algol ID motor chamber design except that the welded metal clips used for raceway attachment are omitted and the skirt-ring bolt hole size is increased from 0.500-20 UNF-2B to 0.625-18 UNF-2B.

B. NOZZLE

1. Straight Nozzle (Algol ID Mod II Motor)

The straight nozzle (Figure 3) used on deliverable Algol ID Mod II motors is the same nozzle used on previous Algol ID motors. More stringent inspection requirements are used for the welded steel housing, and Speer 875T graphite is substituted for the Speer 8500 graphite, which is no longer available.

2. Cantable Nozzle (Algol ID Mod I Motor)

The cantable nozzle (Figure 4) used on the developmental Algol ID Mod I motors was designed for the Little Joe II Program. The basic design criteria

IV, B, Nozzle (cont.)

for the nozzle are to provide performance equivalent to that of a straight nozzle and the capability for adjustment of the nozzle cant angle from 0 to 14 degrees. The nozzle consists of a movable throat and exit-cone assembly attached to a fixed closure assembly by trunnion arms and pins. A ball-and-socket type joint enables nozzle movement and an O ring between the parts provides the gas seal. The gas seal is protected from the flame front by a baffle ring. A micrometer assembly, located 90 degrees from the hinge axis, is used to set the nozzle cant angle.

The ball-and-socket joint and O-ring seal design used on the Little Joe II nozzle is similar to the movable seal design successfully used on other Aerojet motors. The throat and exit-cone assembly is similar to that successfully used on the Algol IIA nozzle assemblies. The throat insert is fabricated of RVA graphite; Refrasil-phenolic was used for the aft-closure insulator and exit cone; and the aft closure, throat housing, and small hardware were fabricated of 4130 or 4340 steel.

The four nozzles produced for the program were fabricated to the original design with minor changes to facilitate machining and inspection. The completed nozzles were proof-tested at 350 psig before installation on the motors. Nozzle-performance data are presented in Section V and in the Little Joe II Test Data Book.

C. IGNITION SYSTEM

A high-altitude igniter (Figure 5) was developed for the Algol ID rocket motor; 33 igniters were test-fired during the program. The first six igniters were fired to establish the igniter main-charge formulation. Ten igniters were subsequently fired to establish the size of the igniter charge and to determine the area of the gas ports in the main chamber required to maintain design igniter chamber pressure. Fourteen igniters of final design were fired to determine performance repeatability. Three igniters of the final configuration were used during the static firings of motors LJ-1, -4, and -7. Test results confirmed the ignition capability of the igniter for use in the Algol ID rocket motor.

IV, C, Ignition System (cont.)

The principal igniter components are the adapter, squibs, booster, and main charges. The igniter adapter, which holds all igniter components together, is used to assemble the igniter to the rocket motor. The squibs, which are actuated by electric bridgewires, fire a small charge, igniting the booster charge, which propagates the firing train and results in ignition of the main igniter charge. The booster charge consists of 90 gm of AGC-14046 Alclo powder, which contains aluminum powder, iron-carbonyl powder, lead powder, and potassium perchlorate. The main igniter charge consists of 3000 gm of AGC-14046 Alclo powder. A comparison of the main charge weight vs motor free volume of the Little Joe II igniter with that of igniters for other solid-rocket motors is shown in Figure 6. The total igniter energy delivered, compared with the igniter energy-delivery rate for other large-solid-rocket motors, is shown in Figure 7.

In establishing the final igniter design criteria, the following important changes were made:

1. Igniter Main-Charge Formulation

AGC-14046 Alclo powder rather than AGC-32014 Alclo powder was selected for the main igniter charge because of the greater reproducibility of burning characteristics.

2. Igniter Main-Charge Weight

A main charge weight of 3000 gm was selected following the review of the performance of igniters with 1950- and 3000-gm charge weights. The heavier charge weight provided the necessary thermal energy required to ignite the Algol ID rocket motor within the design limits at altitude conditions and low ambient temperatures.

IV, C, Ignition System (cont.)

3. Igniter Main-Chamber Port Size

The port size, which was increased from 3.76 to 6.90 sq in. when the igniter main charge weight was increased, was subsequently reduced to 5.51 sq in. In addition, four holes were drilled around the single axial hole of the port to provide wider distribution of igniter energy. The 5.51-sq-in. port maintains chamber pressure and controls the energy delivery rate, resulting in reproducible rocket-motor ignition.

4. Booster-Chamber Port Design

The original three-hole booster chamber operated at excessively high pressures and apparently contributed to burnthroughs of the igniter main chamber. Therefore, the port design was modified to a single axial hole with pellet retainer. The change enables the booster charge to burn completely without blocking the chamber port. The development of the igniter design is summarized in Figure 8.

Minor changes were also made to modify dimensional tolerances and simplify fabrication of the component parts. The final configuration of the igniter assembly is shown in Figure 5.

D. IGNITER INITIATOR

Design criteria for the igniter initiator were established from data obtained in the successful use of the squibs in the Aerojet Algol IIA motor igniter; the external configuration of the Algol IIA motor igniter squibs was slightly modified for use with the Algol ID igniter initiator, which has a different connector and is required to operate at altitudes up to 200,000 ft. The no-fire and functional design capability and the physical data for the squib are shown in Figure 9. The squib configuration is shown in Figure 10.

IV, Motor Development (cont.)

E. DESTRUCT SYSTEM

Three concepts were considered in the development of the destruct unit. In the first concept, proposed by Aerojet, two shaped charges were assembled in parallel lines 6 in. apart on the side of the chamber in a raceway assembly. The charges were designed to produce two parallel cuts approximately 10 ft long. The second concept, initiated at the direction of NASA, resulted in the design of a shaped charge assembled in a hoop configuration to enable separation of the forward dome from the chamber. Fabrication of this destruct system was started but was discontinued at the direction of NASA because of the hazard of possible damage to the Little Joe II re-entry vehicle when the head became separated from the chamber in flight. In the third concept, initiated at the direction of NASA, two 8-ft-long single linear shaped charges are mounted 180 degrees apart on the forward end of the chamber. These charges produce longitudinal perforations at least 100 in. long when actuated on an unpressurized motor.

The destruct unit (Figure 11) for the Algol ID motor was designed on the basis of experience gained in the Minuteman Motor Development Program. The two 8-ft-long shaped charges in a chevron configuration are enclosed in separate silicone rubber retaining tracks, which are attached to the chamber. The rubber retainer is bonded to the chamber and held in place by clamps and blocks, which may be used as reference points in assembling the destruct unit to the chamber during field installation. The shaped charge is initiated from both ends by Primacord connectors, which are actuated by an electrical signal to the Beckman-Whitley safety-arming device.

All of the explosive components used in the destruct unit, except for the safety-arming device, have been used on Minuteman motors and have a demonstrated minimum reliability of 0.995 at a 95% confidence level.

IV, Motor Development (cont.)

F. WEATHER SEALS

The weather-blast seal for the Little Joe II canted nozzle is designed to: prevent entry of dust, moisture, and foreign objects; resist the external-to-internal pressure differential and the heat effects of launching; prevent premature ignition of second-stage motors by adjacent first stage motors; withstand or relieve the internal-to-external pressure differential at altitude; blow off at ignition when the internal motor pressure reaches approximately 35 psig; provide access for grain inspection and leak tests; and enable installation of leads from the thermocouples that are located in the grain.

V. TEST PROGRAM

A. FULL-SCALE-MOTOR FIRINGS

1. Motor Performance

Three full-scale Algol ID Mod I motors, LJ-1, -4, and -7, were fired to demonstrate the propulsion system and to determine performance characteristics. The motors had the improved high-altitude igniters and variable cant-angle nozzles. A schematic drawing of the motor test setup is shown in Figure 12; Figures 13 through 16 show the motors in the test stand. Instrumentation locations for motor LJ-7 are shown in Figure 17. The performance characteristics of the three motors are summarized in Figure 18; curves of measured chamber pressure and thrust vs time for motors LJ-1, -4, and -7 are shown in Figures 19, 20, and 21, respectively. Postfiring views of the motors are shown in Figures 22 through 28.

The most significant factors in a comparison of data obtained from motor firings (Figure 18) are the average web thrust and the web burning time. The range of average thrust values was 201 lbf. The differences in the web burning times did not exceed 0.6 sec.

V, A, Full-Scale-Motor Firings (cont.)

Motor LJ-1 was fired with the nozzle in the zero-degree position; a force angle of 0.6 degrees was measured between the motor and the test stand. Motors LJ-4 and LJ-7 were fired with the nozzles canted at 14 degrees; the measured force angles between the motors and the test stand were 12.9 and 14.5 degrees, respectively. The difference in force angles is attributed to misalignment of the motor in the test stand during each of the tests. The side forces measured during the firing of motor LJ-7 are shown in Figure 29 and the resultant force angle is shown in Figure 30.

Motor LJ-7 was instrumented with a high-frequency pressure transducer and four crystal accelerometers to confirm the chamber-pressure fluctuations indicated during earlier tests. The chamber pressure remained essentially constant for 19 sec without evidence of oscillations; at 19 sec oscillations of 60 to 63 cps were recorded. The oscillations reached a maximum amplitude of about 6 psi and continued throughout the firing. Analysis of data from microphones positioned aft of the motor indicated sound levels of 148 db at 100 ft and 140 db 200 ft aft of the motor.

Recorded temperature data obtained from thermocouples (Figure 17) during the firing of motor LJ-7 showed that no significant temperature increases occurred on either the nozzle or chamber during the 100 sec of temperature recording. Typical temperature recordings on the nozzle and the chamber are shown in Figures 31 and 32, respectively.

2. Igniter Performance

The three igniters used on the full-scale test motors performed within the limits established during the igniter test and qualification program. Ignition performance data for the full-scale motors is presented in Figure 33. The ignition characteristics of motor LJ-4 (Figure 34) are typical of those of the three motors fired. Seventy-five percent of full operating pressure was achieved within 100 millisec during each of the tests. Motor LJ-1 was fired at sea-level conditions; motors LJ-4 and -7 were ignited at a simulated altitude in excess of 100,000 ft.

V, A, Full-Scale-Motor Firings (cont.)

A postfiring view of the igniter used in the test of motor LJ-4 is shown in Figure 35; the rough surface of the igniter was caused by deterioration of the rubber external insulation.

3. Nozzle Performance

The variable cant-angle nozzles performed satisfactorily during each of the three firings. Baffle ring performance was satisfactory; no hot gases reached the main O-ring seal. A summary of nozzle throat and aft-closure-insulator erosion is as follows:

Summary of Nozzle Throat and Aft-Closure-Insulator Erosion

	<u>Motor LJ-1</u>	<u>Motor LJ-4</u>	<u>Motor LJ-7</u>
Cant angle, degrees	0	14	14
Initial throat diameter, in.	14.950	14.950	14.950
Final throat diameter, in.	15.010	14.990	15.004
Initial aft-closure-insulator diameter, in.	18.340	18.340	18.340
Final aft-closure insulator diameter, in.	18.870	19.100	19.240

The initial throat diameter was measured to the ID of the zirconium oxide coating ($0.030 \pm .05$ in. thick). No trace of the coating remained after the firing. The observed throat erosion is attributed to loss of the protective zirconium oxide coating.

Two circumferential hairline cracks occurred at the same locations on each of the fired throat inserts. The cracks were approximately 3 in. forward of the aft edge of the graphie and near the middle. Analysis of the cracks did not indicate evidence of gas flow or erosion; therefore, the cracks apparently occurred late in the firing or were caused by the postfiring water quench.

V, A, Full-Scale-Motor Firings (cont.)

The Refrasil-phenolic aft-closure insulators were eroded; however, thermocouple data indicate that sufficient material remained to prevent heating of the metal parts. The flow of gases down the propellant rays contributed to nonuniform erosion of the aft-closure insulator during the first 15 sec of firing. These erosion patterns became more severe during the remaining 20 sec of firing following the burning of the rays. Examination of the sectioned nozzle of motor LJ-1 (Figures 36 through 38) revealed that up to 0.50 in. of material was eroded from the entrance side of the insulator. The minimum diameter of the entrance had increased by 0.90 in. on motor LJ-7; the increase was less on motors LJ-1 and -4. Examination also indicated that circumferential gas flow in the nonsymmetrical gap between the fixed and movable portions of the nozzle resulted in erosion pockets up to 1.25 in. deep opposite the propellant rays. The average erosion on the long sides of the entrance insulators of the nozzles canted at 14 degrees was 0.75 in.

Erosion of the exit cones was relatively uniform. Erosion was up to 0.25 in. deep adjacent to the throat insert and tapered to zero near the middle of the exit cone. Swelling of the plastic caused a reduction of the diameters over the aft quarter of the exit cone.

4. Destruct-System Performance

The destruct system of motor LJ-7 was activated 90 sec after fire switch, approximately 50 sec after motor tailoff. The time delay was selected to demonstrate the capability of the destruct unit to withstand continued chamber wall heating during operation of an adjacent second-stage motor without being actuated prematurely. The resultant two cuts, both the length of the shaped charge, are shown in Figures 27 and 28. Data indicate that the destruct unit would have ruptured a pressurized motor.

V, A, Full-Scale-Motor Firings (cont.)

5. Base-Heating-Insulation Performance

The protection against base heating provided by the nozzle insulating boot was demonstrated in the firing of motor LJ-7. The nozzle insulating boot (Figure 25) was blackened by soot; however, the boot showed no charring due to exposure during the sea-level firing of motor LJ-1.

B. SUBSCALE-MOTOR FIRINGS

Data for predicting full-scale motor operation were obtained in a series of 3KS-500 size motor tests. The average propellant burning rates for the batch-test motors fired were:

<u>Full-Scale Motor</u>	<u>Average Propellant Burning Rates of Batch-Test Motors, in./sec</u>
LJ-1	245
LJ-2	243
LJ-3	243
LJ-4	241
LJ-5	242
LJ-6A	239
LJ-7	238

C. IGNITER TESTS

Data obtained from the firing of four igniters (SN 14 through 17) to determine the final igniter configuration and 14 additional igniters (SN 18 through 35) to determine the performance repeatability of the selected design are summarized in Figure 33.

V, C, Igniter Tests (cont.)

Six igniters were fired at sea level and eight were tested at a simulated altitude of 175,000 ft. The igniters were conditioned at temperatures of 40, 80, and 100°F for at least 12 hr prior to test firing. Two of the igniter assemblies were subjected to random gaussian vibrations from 40 to 4000 cps and acceleration loads from 0 to 10 g. A single squib was used in two tests to demonstrate the redundancy of a backup, or second, squib. Data from these firings are summarized in Figure 33.

The repeatability of igniter performance characteristics (Figure 39) is essential to ensure successful motor ignition. Variations of conditioning temperature, firing altitude, number of squibs, and effects of vibration produced only slight changes in these repeatability factors.

Data obtained from the qualification tests indicate that the average igniter chamber pressure was 6960 psia, that the peak ignition pressure occurred at 0.034 sec, and that the average total igniter duration was 0.048 sec. The effects of extreme conditioning temperatures and firing at simulated altitudes are shown in Figure 40. Figure 41 shows an altitude igniter after test firing.

The igniter test series demonstrated that:

1. The final Little Joe II igniter assembly will ignite an Algol ID rocket motor successfully at simulated altitude conditions.
2. The duration of igniter performance is approximately 50 millisec and the ignition interval is approximately 70 millisec.
3. Temperatures from 40 to 100°F prior to ignition will cause no significant variation in igniter performance.
4. Prelaunch and launch vibrations will have no detrimental effect on igniter performance.
5. A single squib will initiate motor ignition.

V, Test Program (cont.)

D. DESTRUCT TESTS

A destruct unit for the Algol ID rocket motor was developed and satisfactorily tested during the program. The destruct unit consists of two linear shaped charges attached to the motor-chamber exterior 180 degrees apart. Actuation of the destruct unit cuts the chamber along the full length of each of the 100-in.-long charges; actuation of the unit on a pressurized chamber in one test resulted in rupture of the chamber.

A test program was conducted in four phases: (1) the destruct system cut witness plates to demonstrate the capability of the linear shaped charge; (2) a test firing of 14 destruct units and a harness assembly was conducted to simulate the destruct system on a seven-motor-configuration Little Joe II vehicle; (3) a pressurized chamber was destructed; and (4) the chamber of motor LJ-7 was cut by a destruct unit following the normal firing of the motor and subsequent chamber heating for a period equivalent to second-stage motor operation.

The manufacturing processes and lot-acceptance tests used for the Little Joe II destruct units were identical to those used in the Minuteman Program. Four percent of all the boosters manufactured were test-fired for lot acceptance. The 100-gr/ft Primacord was cut in 100-ft-long specimens, and a 1-ft specimen from each end was test-fired to determine end and side forces. The 200-gr/ft linear shaped charge was obtained in 14-ft specimens; each was weighed for load density and radiographically inspected for voids in the explosive train. A 1-ft section was removed from each 14-ft specimen of the linear shaped charge for test purposes. From each of the 1-ft specimens, a 3-in.-long specimen was cut for load determination and a 4-in.-long specimen was cut for velocity and severance testing.

The 4-in.-long specimens were mounted on witness plates of AISI 4130 steel, 0.200 in. thick, and heat-treated to 180- to 200-ksi ultimate tensile strength. Breakwire leads were attached to the test plates and the velocity of the detonation was measured. The average velocity of detonation in all tests was 8300 to 8400 meters/sec. All test plates were cut satisfactorily.

V, D, Destruct Tests (cont.)

The 3-in.-long segments of shaped charge were weighed and the RDX explosives were dissolved out of the tube. The empty tubes were reweighed to confirm the 200-gr/ft charge weight.

1. Single-Motor-Configuration Witness-Plate Tests

Six units were installed in the test device (Figure 42) and initiated with a Beckman-Whitley safety-arming device. The witness plates were 0.200-in.-thick 4130 steel that was heat-treated to 180- to 200-ksi ultimate tensile strength. The plates were cut as shown in Figure 43.

2. Destruct Test of Rocket Motor

Two destruct units were bonded to a fired motor chamber that had been used in the test of motor LJ-4. The chamber was pressurized to 450 psig with nitrogen, and the charges were initiated by a Beckman-Whitley safety-arming device attached to one of the wooden poles of the erecting stand. The test was recorded by high-speed motion-picture cameras. Actuation of the charges destructed the chamber; the largest segment of chamber recovered was approximately 4 by 5 ft. Examination of the recovered segments indicated that the charges had cut the chamber the full length of the charges. Segments of the chamber were recovered approximately 0.25 miles from the test site. Analysis of the motion-picture film indicated that the forward head was not blown upward toward the designated location of the re-entry vehicle of a Little Joe II missile in flight. Prefiring and postfiring views of the test setup are shown in Figures 44 and 45, respectively.

3. Seven-Motor Configuration Test

A simulated seven-motor destruct-test apparatus (Figures 46 and 47) consisting of 14 individual destruct units with a Primacord harness assembly was actuated by a Beckman-Whitley safety-arming device; all 14 destruct units performed satisfactorily. Twelve of the 36-in.-long witness plates were severed; one plate was

V, D, Destruct Tests (cont.)

cut 32.5 in. longitudinally and one plate was cut 27 in. longitudinally. The plates that were not severed completely had been cracked on the bottom surface.

4. Destruct Test Conclusions

The destruct-test series demonstrated the following:

- a. The destruct unit for the Algol ID motor will cut or crack the 4130 steel shell of the motor chamber when the charge is fired on an unpressurized chamber.
- b. When fired on a pressurized chamber, the destruct unit will destruct the entire chamber.
- c. The Primacord harness assembly for initiating a seven-motor-configuration destruct system performed satisfactorily.

E. WEATHER-SEAL TESTS

1. Full Igniter Charge Pressurization

One weather seal was broken by the firing of an igniter in the free-volume igniter test chamber. The test was recorded by a high-speed (4000 frames/sec) motion picture camera. A series of frames taken from the film strip are shown in Figure 48; remains of the weather seal are shown in Figure 49. The seal failed approximately 1.5 millisecc after fire switch at a pressure of approximately 100 psig as measured by a transducer located in the exit cone.

2. Igniter Booster-Charge Pressurization

A second weather seal was broken by the firing of an igniter booster charge of 90 gm (a full igniter charge is 3090 gm) in the free-volume igniter test chamber. A series of frames taken from the high-speed motion-picture

V, E, Weather-Seal Tests (cont.)

film are shown in Figure 50. The seal failed approximately 2.0 millisec after fire switch at a pressure of about 30 psig as measured by a transducer located in the exit cone.

VI. MOTOR PROCESSING AND ASSEMBLY

A. MOTORS PROCESSED

Figure 51 shows the motor fabrication and processing schedule for the seven Little Joe II motors; three Algol ID Mod I motors were fired at Sacramento and four Algol ID Mod II motors were delivered to White Sands Missile Range. A weight summary for these motors is shown in Figure 52. The deliverable motors were shipped without the destruct unit or igniter installed.

B. PROCESSING OPERATIONS

The manufacturing and processing of the Algol rocket motor, including the special tools used in each operation, PAIS (integrated planning numbers), and Aerojet and Navy quality-control-plan stop points are shown in Attachment A. Figures 53 through 56 show the motor assemblies and envelopes.

Integrated planning for inert parts is based on the shop planning sheet (AGC Form 3-009-019), which specifies the various steps in an operation and refers to shop sketches. The inspection planning and record sheet (AGC Form 3-390-1A(2A)) similarly follows the operation.

1. Chamber

The chambers (Figure 2) are fabricated from 4130 sheet steel, rolled and welded into cylindrical sections, and joined by girth welds. The machined aft head, spun forward head, forward and aft skirts, and skirt rings are attached by girth welds. The forward and aft halves of the chamber are heat-treated

VI, B, Processing Operations (cont.)

separately to 180,000 psi minimum ultimate tensile strength in the thin-walled sections and are then joined by a final girth weld. The completed chamber is subjected to radiographic and magnetic particle inspection. The chamber is then hydrostatically tested at 750 psig, cleaned, and painted.

2. Insulation

The chamber insulation is identical to that used in previous Algol ID motors. The insulation consists of asbestos cloth and epoxy resin. Sections of cloth are cut to size, impregnated, laid up, vacuum-bagged, and cured in the motor. No machining is required.

3. Release Boots

The release boots at the forward and aft ends of the chamber are identical to those used on the Algol ID motor. They are made of asbestos cloth sections that are sewn together. Prior to installation, the boots are impregnated with SD-723 Ta liner material. The boots are partially bonded in place with epoxy adhesive. Wax is applied to the release surfaces of the boots.

4. Chamber Liner

SD-723 Ta liner is spun in place on the walls of the boot-insulated chamber until the liner is cured. Additional SD-723 Ta liner is spun into the forward end of the chamber. The liner system is identical to that used in earlier Algol ID motors.

5. Propellant

The propellant, ANP-2639 AF, is mixed in accordance with specification WS-1013 and cast in an eight-point gear-tooth configuration with the same core used in earlier Algol ID motors.

VI, B, Processing Operations (cont.)

6. Straight Nozzle, (Algol ID Mod II)

The straight nozzle (Figure 3) supplied with a deliverable motor consists of a metal housing, an insulator, and an insert. The housing is welded and machined from AISI 1015-1022 steel. All welds are radiographically inspected and dye-checked after machining. The insulation is manufactured from phenolic-impregnated high-silica fabric molded at a minimum pressure of 2000 psi to a density of 100 lb/cu ft. The insert is machined from Speer graphite 875T with a minimum specific gravity of 1.72. The insert and insulator are bonded to the prepared surface of the metal housing with an epoxy adhesive.

7. Canted Nozzle (Algol ID Mod I)

The canted nozzle assembly (Figure 4) consists of aft-closure, throat and exit cone, and micrometer subassemblies.

The aft closure consists of the metal closure and the Refrasil-phenolic closure insulator. The aft closure is rough-machined from 4130 steel, welded, heat-treated, and final-machined. The insulator is assembled by bonding together laminated ring sections of Refrasil-phenolic fabric that are laid up perpendicular to the gas flow. The insulator is bonded to the closure and then final-machined.

The throat and exit-cone subassembly consists of a metal housing, the insulated throat insert, and the exit cone. The housing is rough-machined from 4130 steel, welded, heat-treated, and final-machined. The RVA graphite throat is partially machined, wrapped with Refrasil-phenolic cloth insulation, and then final-machined on the outside and bonded to the metal closure. The exit cone is fabricated by wrapping Refrasil-phenolic cloth, curing the laminate, and final-machining. The exit cone is then bonded to the throat housing and the assembly is overwrapped with glass cloth-phenolic and glass-filament epoxy to hold the exit cone in place. Finally, the inside contour of the throat is final-machined and the surface of the graphite is coated with zirconium oxide.

VI, B, Processing Operations (cont.)

The micrometer subassembly is fabricated from Type 416 steel and heat-treated. Each division on the micrometer scale represents 15 min of nozzle cant angle.

8. Igniter Assembly

The igniter assembly (Figure 5) consists of four main components, the igniter adapter, the booster chamber, the igniter chamber, and the squib.

The igniter adapter, fabricated from 4130 steel, consists of a 4.990-in.-dia 2.70-in.-thick steel plug. The forward side of the plug has two 0.75-in.-dia threaded holes to receive the igniter squibs. The forward side of the igniter plug has four 0.25-in.-dia threaded holes, two for installation of chamber pressure transducers. The booster chamber is fabricated from 4340 steel and lined with Polytherm 40SA. The igniter chamber is fabricated from 4340 steel. The squib is manufactured by Horex, Inc.

9. Destruct Assembly

a. Component Manufacture

(1) Booster Explosive

The boosters used to initiate the detonating cord are fabricated in accordance with AGC-STD-5037 (DOW). Type A, Class C RDX conforming to MIL-R-00398 is dried and loaded at a consolidation pressure of 1000 psi. The boosters are manufactured in sublots of 100 units, and are sampled and tested according to AGC-STD-5037 (DOW) for acceptance prior to use or storage.

VI, B, Processing Operations (cont.)

(2) Booster

The booster used to initiate the 200-gr/ft linear shaped charge are fabricated per AGC-STD-5036 (DOW). Type A, Class C RDX conforming to MIL-R-00398 is dried and loaded at a consolidation pressure of 3000 psi. The boosters are also manufactured in sublots of 100 units, and are sampled and tested according to AGC-STD-5036 (DOW) for acceptance prior to use or storage.

(3) Detonating Cord

Detonating cord is purchased to Specification Control Dwg 511604. The material has a core loading of 100 ± 10 gr/ft of Type B, Class C RDX (MIL-R-00398) and is jacketed with synthetic rubber (HYCAR). The detonating cord is accepted in accordance with Aerojet Component Specification 54045.

(4) Linear Shaped Charge

The linear shaped charge material is purchased to Source Control Dwg 511605, and Aerojet Component Specification 54046. The material has a core loading of 200 ± 20 gr/ft of Type B, Class C RDX (MIL-R-00398).

b. Assembly Procedures

(1) Detonating Cord Assembly

The detonating cord is cut to the desired length and a booster is crimped to each end. The contact between the explosive in the booster and explosive in the detonating cord is confirmed by radiographic examination.

VI, B, Processing Operations (cont.)

(2) Explosive-Connector Subassembly, PN 511624

This explosive-connector subassembly is assembled to a tube adapter and potted in accordance with Aerojet Component Specification 51069. The unit is inspected to ensure that the booster face is free of potting compound and that the recess of the booster into the tube adapter is within drawing limits.

(3) Explosive Connector Subassembly, PN 512665

This explosive connector subassembly is assembled to a tube adapter in a protective covering of heat-shrunk tubing designed to prevent damage to the detonating cord by atmospheric conditions. A ferrule is then bonded to the bare booster to increase the diameter of the booster so that it may be centered in the connector that mates with the linear-shaped-charge boosters.

(4) Linear Shaped Charge

The linear shaped charge is cut to the desired length, trimmed flush at the end, and inserted into the booster; the booster is then crimped to the linear shaped charge. Cement is applied to the crimped end of the booster to ensure a positive seal and the unit is then radiographically examined to verify the contact between the explosive in the linear shaped charge.

(5) Destruct Unit

The linear shaped charge assembly is first potted into the connector tube. When the potting material has cured, the detonating-cord assembly is inserted in the same connector and potted in the same manner. Contact of the linear-shaped-charge booster and the detonating-cord booster is then verified by radiographic examination. Adhesive is applied to the back of the linear shaped charge, and the linear shaped charge is then snapped into the retainer. Adhesive is then applied to the inside of the detonating cord retainer, and the detonating cord

VI, B, Processing Operations (cont.)

is snapped into place. The connector tubes are bonded into the holder and the bracket connector. When the bond has cured, the bracket cover and holder cover are bonded in place. After this bond has cured, identification labels are attached and the unit is packed in a shipping container.

VII. ADDITIONAL TECHNICAL EFFORT

A. MONTE CARLO COMPUTER BALLISTIC PERFORMANCE STUDY

1. General

The Monte Carlo study consisted of a series of ballistic evaluations to determine the effects of propellant variability on ballistic performance of Algol ID motors for the Little Joe II Program. To determine the performance variations, values of selected propellant ballistic properties were sampled randomly from a normally distributed population of known mean and standard deviation. One hundred ballistic evaluations of the randomly sampled properties were made, and performance curves were plotted.

2. Program Discussion

The mathematical model used for the Monte Carlo study consists of Aerojet Computer Program 1103 program deck and the input description of the Algol ID motor to provide an adequate simulation of motor LJ-4. This model was selected because it provided the best possible prediction of the ballistic behavior of the Little Joe II motors.

The characteristics below were subjected to random variation for the Monte Carlo Program. The standard deviations were computed from the 100 values of these characteristics used for the program.

VII, A, Monte Carlo Computer Ballistic Performance Study (cont.)

<u>Characteristic</u>	<u>Mean Value</u>	<u>Range</u>	<u>Standard Deviation</u>
Density, ρ	0.06034	0.06014 to 0.06054	0.0000670
Mass-flow coefficient, C_w	0.006600	0.006255 to 0.006945	0.000117
Burning-rate constant, C	0.08503	0.08033 to 0.09000	0.001546
Throat area, A_t	175.33	175.00 to 175.66	0.0320

These characteristics were selected for variation in the Monte Carlo program because they produce the only significant variations in motor-to-motor performance. Of these variables, burning-rate changes produce the greatest performance variations.

The range of values for the burning-rate constant (0.08033 to 0.09000) was taken from the propellant specification, WS-1013, which specifies burning-rate limits of 0.223 to 0.265 in./sec. The relationship $\dot{Y} = CP^n$ is used to convert the burning rate, r , to the burning-rate constant C , which is used in the computer program. The actual limits for the burning rate among the seven Little Joe II motors produced were 0.245 to 0.256 in./sec. These actual limits are equivalent to a burning-rate-constant range of 0.0833 to 0.0870, which is a narrower range of burning rates than allowed by the propellant specification and used in this Monte Carlo program. This motor-burning variation is explained by the number of batches of propellant in a batch-mixed rocket motor. The burning rates of the 10 batches of propellant may vary within the limits allowed by the propellant specification. However, the average burning rate of the 10 batches is used for the prediction of motor performance.

The range of values for the density (0.06014 to 0.06054 lb/cu in.) was taken from the propellant specification. The actual limits for the density of propellant among the seven Little Joe II motors produced were 0.06030 to 0.06037 lb/cu in. Again, the actual motors produced cover a much narrower band of values than that permitted by the specification. As with burning rate, the motor propellant density used for performance predictions is an average of the densities of the 10 batches of propellant in the motor.

VII, A, Monte Carlo Computer Ballistic Performance Study (cont.)

The range of values for the nozzle throat area was taken from actual measurements of nozzle throats that were used on Algol ID motors that were fired. The range of values for the mass-flow coefficient was taken from data on fired Algol ID motors.

The random normally distributed samples for the program were generated by a computer program that combines the method of congruences and the central limit theorem. The 100 values generated for the Little Joe II Monte Carlo Program are listed in Figure 57.

The standard deviations are based on batch variations, and therefore they describe the variability that would be expected if each motor were cast with one batch. However, since each Algol motor requires 10 batches of propellant, the standard deviation for each value (σ_m) should be

$$\sigma_m = \frac{\sigma_B}{\sqrt{10}}$$

where σ_B is the batch standard deviation listed in the chart above. Because it is possible that adjacent batches will be more nearly alike than batches cast at widely spaced intervals, there is probably a bias tending to increase the value of σ_m . Therefore, the true value of standard deviation falls somewhere between the batch standard deviation and σ_m calculated by the above equation.

The performance curves for the 100 simulated motor firings at 70°F are plotted in Figures 58 through 60. The nominal curves for 50, 70, and 90°F are shown in Figures 61 and 62. The three-sigma bands of thrust and pressure at sea level and altitude conditions are shown in Figures 63 and 64, respectively. The nominal thrust at 10,000-ft altitude increments from 10,000 to 100,000 ft is shown in Figure 65.

VII, A, Monte Carlo Computer Ballistic Performance Study (cont.)

From the preceding discussion it can be concluded that the dispersion observed in the Monte Carlo runs is greater than can be expected in actual firings and represents an extreme limit. Below is a list of significant ballistic factors, their mean values, and their standard deviations.

<u>Characteristic</u>	<u>Mean Value</u>	<u>Standard Deviation</u>
Initial pressure, psi	474.10	10.36
Maximum pressure, psi	484.90	10.75
Maximum thrust, lbf	123,030	3175.0
Duration, sec	34.41	0.676

The performance curves plotted in Figures 58 through 60 show one curve that is considerably higher than the others. This particular run is case 31, with an unusually high burning-rate constant of 0.090474. The four factors cited in the above table have the following values for this curve: 512.803 psi, 525,745 psi, 134,643 lbf, and 32 sec. These values are not within three-sigma standard deviations of the mean value; however, this is the only case that is not within the three-sigma band.

According to statistical theory, 99% of cases should be between plus and minus three sigma. Thus, it is not unexpected that one case out of one hundred would fall outside this range. The probability that one firing out of 100 would produce a curve this far from the mean is 0.168.

A study was made of the correlation between the four characteristics used as input and the four factors selected to evaluate the results. The following table lists the four output factors vertically, the four input characteristics horizontally, and the square of the correlation coefficient in the spaces. This value represents the fraction of the dispersion of each resulting factor that is attributable to each input characteristic. For example, in the first line, 99.37% of the dispersion in initial pressure is caused by variations in the burning-rate constant C. The total does not equal exactly one because of the limited sample.

VII, A, Monte Carlo Computer Ballistic Performance Study (cont.)

	<u>C</u>	<u>C_w</u>	<u>p</u>	<u>A_t</u>	<u>Total</u>
P _i	0.9937	0.0068	0.0086	0.0001	1.0092
P _{max}	0.9900	0.0066	0.0077	0.0001	1.0044
F _{max}	0.9908	0.0001	0.0084	0	0.9993
t _b	0.9482	0.0078	0.0001	0	0.9561

It is evident that the burning-rate constant C is the only value that significantly affects the pressure, thrust, and duration. The squares of the correlation coefficients for duration are less than one because the definition of burning time is inexact. A more careful definition of burning time will give a more satisfactory correlation.

3. Conclusions

(a) The standard deviations of the thrust, pressure, and duration as calculated from the Monte Carlo runs are undoubtedly higher than would be expected from a series of 100 actual motor firings because of the 10-batch factor discussed above. Therefore, the standard deviation of about 2% is perhaps high.

(b) The Monte Carlo technique represents the best method presently known for assessing the effects of variability in the components of a solid-rocket motor. The performance evaluations resulting from this study give a prediction of the behavior of 100 randomly sampled Algol ID motors produced within the specification limits noted. However, the seven Little Joe II motors produced were within a much narrower range of density and burning-rate values than allowed by specification.

(c) Individual motor predictions should be used for planning vehicle performance. Such predictions are based on nominal performance and modified by the average burning rate of the propellant in the individual motor. The validity of the prediction system has been demonstrated by the firing of motor LJ-7 and the first Little Joe II vehicle at White Sands.

VII, Additional Technical Effort (cont.)

B. ENVIRONMENTAL TEMPERATURE GRADIENT STUDY

The temperature gradients across the grain of the motor, when exposed to hot or cold temperature extremes, were computed. The environmental conditions considered were the Sacramento, California summer and the El Paso, Texas winter. For a typical Sacramento summer day, the ambient temperature was varied according to the following schedule:

<u>Time</u>	<u>Temperature, °F</u>
6 a.m.	60
12 p.m.	110
6 p.m.	110
12 a.m.	60
6 a.m.	60

For a typical El Paso day, the ambient temperatures were varied according to the following schedule:

<u>Time</u>	<u>Temperature, °F</u>
6 a.m.	8
12 p.m.	50
6 p.m.	50
12 a.m.	8
6 a.m.	8

The initial conditioning temperature was 70°F for both cases. A wind velocity of 10 mph was assumed, and the motor was not exposed to direct sunlight. The results of this study are shown in Figures 66 and 67.

VIII. RELIABILITY AND QUALITY CONTROL

A. RELIABILITY

1. Igniter Initiator Development and Test Program

To provide the necessary initiators for the Little Joe II program, a lot of 200 initiators of the selected design were fabricated by a vendor (Holex, Inc.). From the production lot of 200 units, 100 units were randomly selected for qualification testing. These tests were conducted at the vendor facility under the cognizance of a resident Aerojet representative.

All of the tests were successfully completed and the required reliability was demonstrated.

a.	Successful	100
b.	Failures	0
c.	Observed reliability	100%
d.	Demonstrated reliability	98.7% at the 90% confidence level

2. Igniter Test Program

Fourteen igniters were fired to determine performance repeatability of the selected igniter design, and four development units were added the total because they were essentially the same as the final selected design and produced similar results.

Three full-scale motors were statically fired and one was flight-tested with an igniter of the final configuration.

Indicated reliability for the Little Joe igniter is determined from the success-failure history as follows:

VIII, A, Reliability (cont.)

a. Development (4) and Qualification (14)
(Free-Volume Tests)

(1)	Successful	18
(2)	Failures	0
(3)	Observed reliability	100%
(4)	Demonstrated reliability	88.0% at the 90% confidence level

b. Motor Static Tests

(1)	Successful	3
(2)	Failures	0
(3)	Observed reliability	100%
(4)	Demonstrated reliability	46.4% at the 90% confidence level

c. Flight Tests

(1)	Successful	1
(2)	Failures	0
(3)	Observed reliability	100%
(4)	Demonstrated reliability	10% at the 90% confidence level

d. Total Tests

(1)	Successful	22
(2)	Failures	0
(3)	Observed reliability	100%
(4)	Demonstrated reliability	90.1% at the 90% confidence level

VIII, A, Reliability (cont.)

3. Destruct Unit

The destruct unit (Aerojet PN 369410) for the Little Joe II motor was designed on the basis of experience gained in the Minuteman Motor Development Program. All of the explosive components used in the destruct unit, except for the safety-arming device, have been used on Minuteman motors and have a demonstrated minimum reliability of 0.995 at a 95% confidence level.

4. Motor History

Twenty Algol I and Senior (33KS-120,000 size) motors were previously fired; one of these was excluded from reliability computations. Missile SN D8 was excluded because the guidance system malfunctioned at T + 26 sec.

Indicated reliability for the Algol I and Senior motors is as follows:

a.	Successful	20
b.	Failures	0
c.	Observed reliability	100%
d.	Demonstrated reliability	89.1% at the 90% confidence level

5. Indicated Reliability

Three Little Joe motors have been fired, at Aerojet Sacramento and one flight-test was conducted at White Sands.

Indicated reliability for the motors manufactured for this program is determined from the success-failure history on the four units tested.

VIII, A, Reliability (cont.)

a. Total Units Tested

(1)	Successful	4
(2)	Failures	0
(3)	Observed reliability	100%
(4)	Demonstrated reliability	56.2% at the 90% confidence level

6. Predicted Reliability

The predicted reliability for the three unfired motors will not be degraded since no major nondestructive-test discrepancies were discovered on these motors.

B. QUALITY CONTROL

The quality-control program established for the Little Joe II motors was in accordance with Document NPC 200-2 as amended. Prior to inception of the program, the existing quality-control program and the requirements of NPC 200-2 were compared. The requirements of the two programs were found to be basically in agreement. However, to enable maximum use of Aerojet experience and procedures established for compliance with other government quality-control specifications, specific exceptions to NPC 200-2 were requested and granted by NASA. The following is a list of the changes made to NPC 200-2 with the number preceding each paragraph referring to that of NPC 200-2.

2.2.1 This section requiring Qualification Status List, End-Item Test Plan, and End-Item Test and Inspection Procedures has been deleted.

2.2.2 The requirements for Reports of Special Measuring and Test Equipment Evaluations and Storage Procedures for End Items are deleted.

2.2.3 Monthly and Quarterly Quality Reports requirements of this section are deleted.

VIII, B, Quality Control (cont.)

3.1.1d This section is amended to read: "Quality Control and Top Management Organizational Charts."

3.1.1 The paragraph, concerning quality program plans is changed from "Further details, including changes and additions shall be submitted as prepared and two weeks prior to their implementation," to: "Further details, including changes and additions shall be submitted."

4.2.1 The second paragraph of the section requiring documentation of design reviews is deleted.

4.3.5 This section is deleted.

5.3.1d Paragraph (1) of this section requiring major subcontractors to follow NPC 200-2 is deleted.

7.4.2.1 This section is deleted.

7.4.2.2 The sentence reading, "Detailed end-items test and inspection procedures, documented per Paragraph 7.3.1 shall be submitted for approval prior to beginning their tests and inspections," of this section is deleted.

9.4 The last paragraph of this section, Test and Inspection Equipment Evaluation Report, is deleted.

9.7 The last sentence of this section requiring variables data on gage wear is deleted.

11.5 The second paragraph of this section requiring temporary storage procedures is deleted.

VIII, B, Quality Control (cont.)

14.2.1 The Monthly Quality Status Report requirement of this section is deleted.

14.2.4 The Narrative End-Item Report requirement of this section will be changed to a Motor Log Book. BuWepsResRep will recommend contents.

14.2.5 The Operational Data requirement of this section is deleted.

15.2 The last sentence of this section requiring quarterly summary reports is deleted.

IX. GROUND SUPPORT EQUIPMENTA. ITEMS OF EQUIPMENT

Eleven items of ground support equipment (GSE) were delivered to NASA, WSMR, for NASA Contract 9-456. A total of 17 pieces of GSE were included in the 11-item delivery as follows:

<u>ITEM</u>	<u>Part No.</u>	<u>Quantity</u>
Trailer, Rocket Motor, Transport and Erector	368549-9	1
Dolly, Rocket Motor, Storage	368550-9	4
Ring Set, Rocket Motor, Handling	368767-9	1
Plug, Nozzle, Rocket Motor	368807-9	1
Installing Tool, Rocket Motor, Igniter	368720-9	1
Borescope, Rocket Motor	368554-9	1
Semitrailer, Rocket Motor (Includes Cradles, Transport)	368515-9 360689-19	1
Electric Graph Line Temperature Recorder (Marshalltown Mfg Co.)	2200A	1
Ring, Handling	360690-3	4
Beam, Lifting, Rocket Motor (Includes Auxiliary Control Hoist)	368593-9 363147	1
Sling, Beam Type, Rocket Motor	368556-9	1

B. DESCRIPTION1. Rocket-Motor Semitrailer (PN 368515-9)

The rocket-motor semitrailer (Figure 68) is a standard two-axle, flatbed semitrailer modified for the special purpose of transporting one or two Algol rocket motors. The flooring and structural members of the trailer bed are drilled and tapped to receive the transport cradles, which support the rocket motors in a

IX, B, Description (cont.)

horizontal position during shipment. The trailer top (Figure 69), designed for quick removal or installation, contains the heating unit and ducts and the temperature recorder. Principal dimensions are shown in Figure 70.

Environmental conditions are maintained during motor shipment by the trailer top that is aluminum lined with 3-in.-thick thermal insulation. A 60,000 Btu/hr heater and heat-ducting system maintains a minimum temperature of 75°F. Access to the rocket motors is provided by an access door at each end of the trailer top. A ladder at each end of the trailer top provides access to the roof to connect the lifting beam. The heating unit, battery case, 50-gal fuel tank, electric fuel pump, and two CO₂ fire extinguishers (Figure 71) are mounted outside the forward bulkhead of the trailer top. The top is secured to the trailer with two toggle locks at each end and three locking pins on each side.

2. Rocket-Motor Lifting Beam, PN 368593-9 (Includes Auxiliary Control Hoist, PN 363147)

The rocket-motor lifting beam (Figure 72) is required for lifting the Algol rocket motors in a horizontal position and for installing and removing the trailer top from the rocket-motor semitrailer. The beam consists of a spreader bar made of 5-in.-dia pipe with top and bottom lugs on each to hold the cable ends and rocket-motor lifting links. Two 204-in.-long cables, joined by clevises to a triangular crane link, support the rocket-motor lifting beam from each end. The welded lugs on the bottom of the spreader bar have holes drilled on centers 314 in. apart, the exact length of the centers of the handling rings (PN 360690-3); therefore, the rocket motor may be picked up from a single point without adding stress to the chamber.

The auxiliary control hoist (Figure 73) provides fine elevation control in increments as small as 0.001 in. in either direction over a range of 12 in.

IX, B, Description (cont.)

A dial indicator gage indicates the force applied to the control hoist in units of 200 lb up to the full capacity of the unit with an accuracy of $\pm 0.5\%$ of full-scale range. A gage indicates pressure in the accumulator in pounds of lifting force (plunger-return force). When not in use, the hoist is stored in a casted, upright storage stand and covered with a fabric cover.

3. Rocket-Motor Transport and Erector Trailer (PN 368549-9)

The rocket-motor transport and erector trailer (Figure 74) is a three-axle pull trailer designed to transport Algol rocket motors from the assembly or storage areas to the missile assembly site, and to support the motor during the vertical-erection operation.

Principal dimensions are shown in Figure 75. Cradles, located at the fore and aft ends of the trailer, support the rocket motor in the horizontal position. In addition, the aft cradle pivots to provide lower support as the rocket motor is erected. A lock is provided to secure the aft cradle when in either the horizontal or vertical position. The front of the rocket is secured to the trailer by turnbuckles attached to the forward handling ring. The rear of the motor is secured to the trailer at the aft cradle by a strap.

A tool box is located inside the left side of the frame to store the electrostatic dischargers, the rocket-motor cover, and miscellaneous tools. Parking brakes are provided on the rear wheels.

4. Rocket-Motor Handling-Ring Set (PN 368767-9)

The rocket-motor handling-ring set (Figure 75) attaches to the fore and aft flanges of the rocket motor. The forward erecting ring serves as an attach point for the beam-type rocket motor sling, and the aft ring serves as the lower support during erection, rotating with the aft cradle on the transport erector trailer.

TX, B, Description (cont.)

5. Rocket-Motor Beam-Type Sling (PN 368556-9)

The beam-type rocket-motor sling (Figure 75) consists of two cable slings joined to a lifting link, a spreader bar, and two shackles that attach to the lifting lugs of the forward erecting ring.

6. Rocket-Motor Storage Dolly (PN 368550-9)

The rocket-motor storage dolly (Figure 76) serves as a work stand for rocket-motor assembly and inspection, and as a magazine storage dolly for Algol rocket motors. The dolly consists of a welded pipe X-frame dolly with a neoprene-padded cradle at each end. Four casters provide mobility of the stand, and a tongue that may be attached to either end of the frame provides hookup to a tug. Footbrakes at each caster assembly prevent the caster wheels from rolling.

7. Rocket Motor Borescope (PN 368554-9)

The rocket motor borescope (Figure 77) is an optical instrument used to inspect the propellant bore surfaces of Algol rocket motors to detect any propellant defects that might adversely affect motor performance. Principal dimensions are shown in Figure 78.

The propellant surfaces are inspected by a probe inserted into the propellant bore. The probe contains a mirror that travels the length of the probe slot and rotates 360 degrees to enable inspection of the complete core area. A roller unit with retractable rollers supports the bore end of the probe. The probe is removed when the borescope is not in use.

The power and optical assembly houses the optical and control elements of the borescope. A trinocular device and a camera enable the operator to view the propellant grain surface and record any view desired.

The probe and power and optical unit is supported by an adjustable-height stand.

IX, B, Description (cont.)

8. Rocket-Motor-Igniter Installing Tool (PN 368720-9)

The igniter installation tool is used to install or remove the igniter with the motor either in the horizontal or vertical position and to remove or install the forward shipping plug in the motor.

9. Handling Ring (PN 360690-3)

The handling rings are used during the final stages of motor preparation for shipment. The rings are used for lifting the motor horizontally and act as chocks to keep the motor from shifting fore and aft in the motor cradles during shipment.

10. Rocket-Motor Nozzle Plug (PN 368807-9)

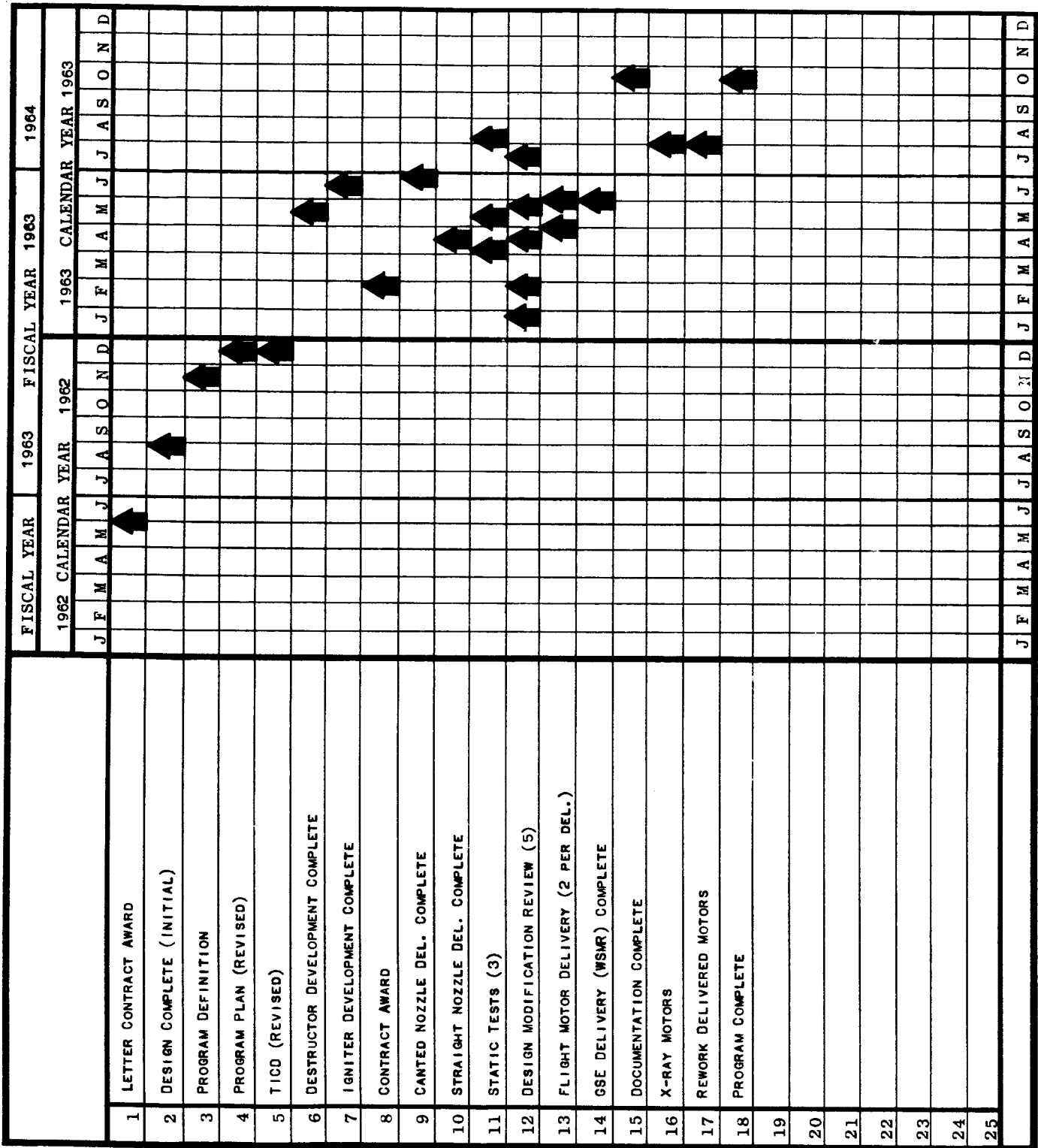
The nozzle plug is used during a motor-pressurization (leak) check after final assembly and just prior to installation into the vehicle.

C. MANUALS

Two manuals were required to support the GSE delivered to NASA.

The Operations Handling and Maintenance Manual, STM 170, includes step by step instructions for processing the Algol rocket motor from the Aerojet manufacturing facility to assembly into the vehicle at the launch site.

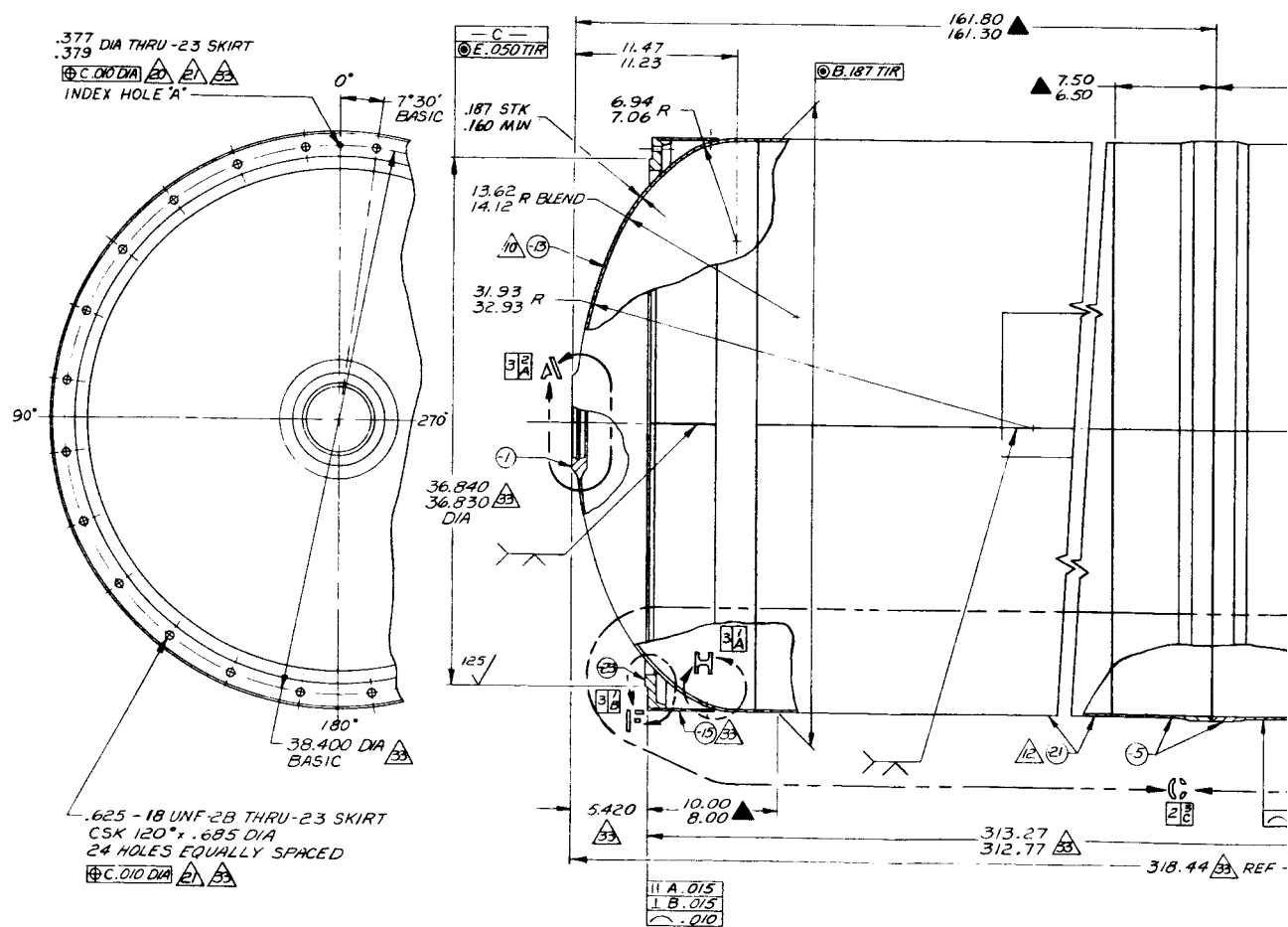
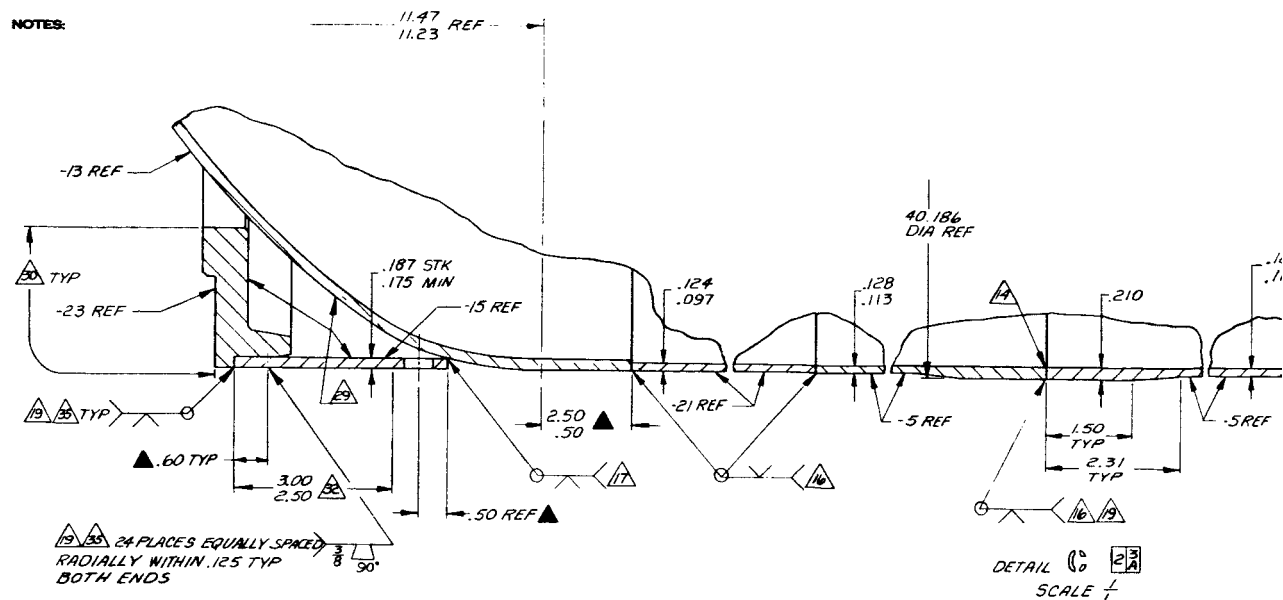
The maintenance instructions for Little Joe ground support equipment, STM 171, provides maintenance instructions for the five groups of GSE supplied.

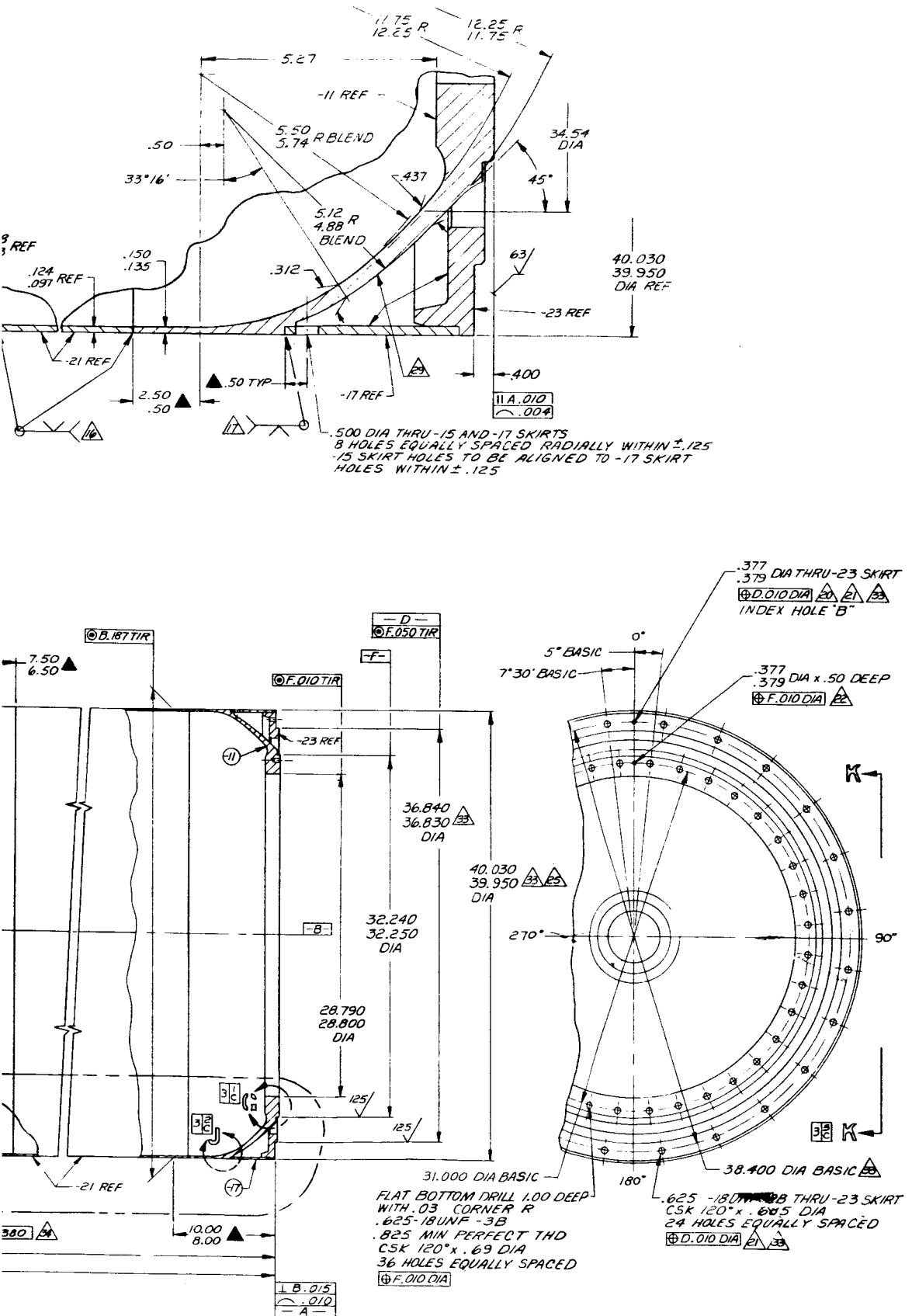


Little Joe II Program Milestone Completion Schedule

Figure 1

NOTES:





Little Joe II Motor Chamber

Figure 2, Sheet 1 of 2

2

NOTES:

2.50 ARC DIM ON
2.00
OUTSIDE SURFACE
OF CHAMBER

90°

8.50 ARC DIM ON
8.00
OUTSIDE SURFACE
OF CHAMBER

FUNCTION OF SPACES
ON 375° SIDE

2.50 5 PLACES

2.50

18.25
17.25

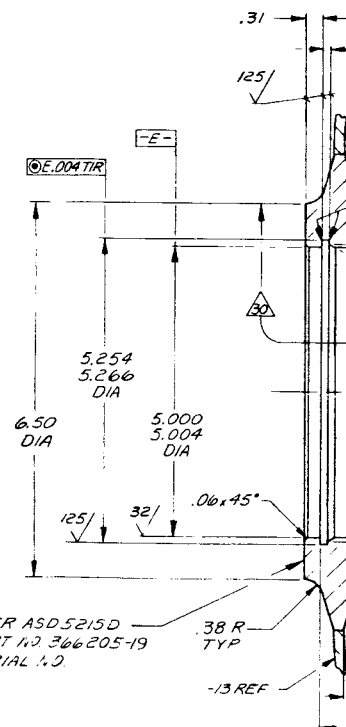
6 PLACES

18.50
17.50
3 PLACES

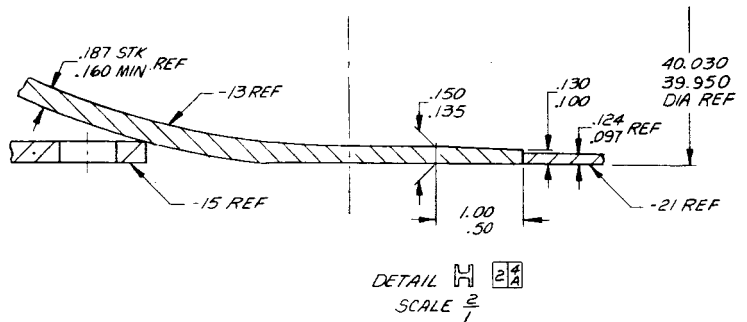
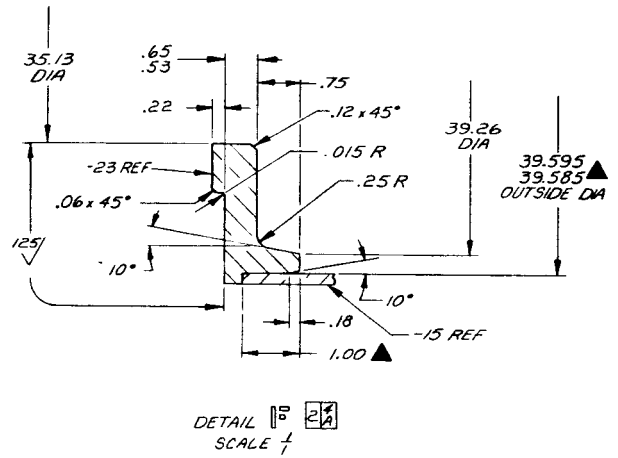
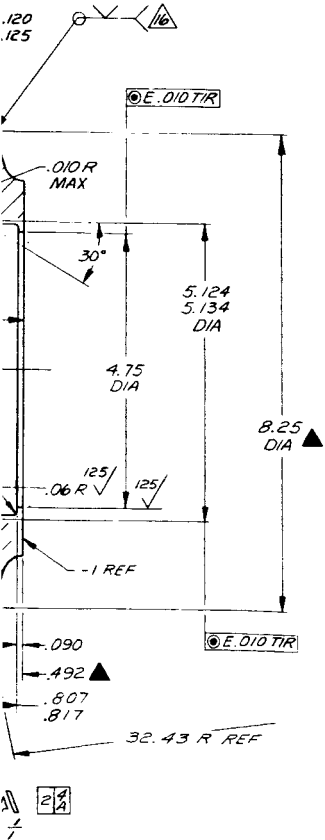
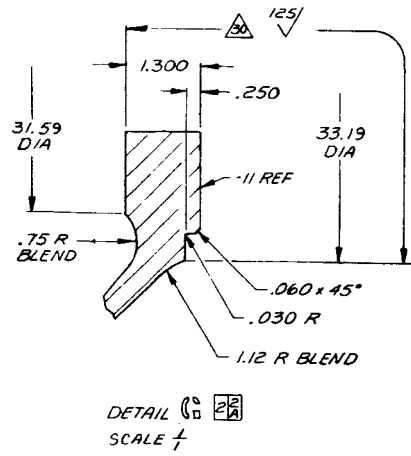
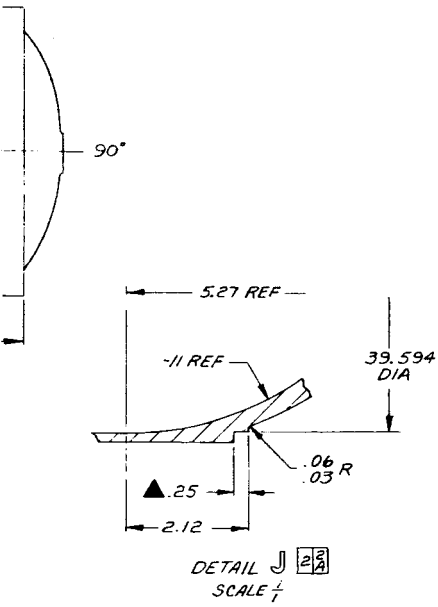
20.00
19.00

29.00
28.00

VIEW K-K 2A
SCALE $\frac{1}{8}$
2 PLACES 180° APART

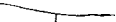
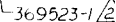
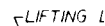
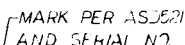
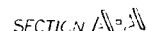


DETAIL
SCALE



2

Little Joe II Motor Chamber



DETAIL 13
SCALE $\frac{2}{1}$

-369523-1 REF

366222-9.




MS-R (90) 65 Δ^8

- 36,6300 - 1 $\triangle 4$
M. 246 r. 6 - 370

36€

4 ①



356220-1  
MS20995C 47 

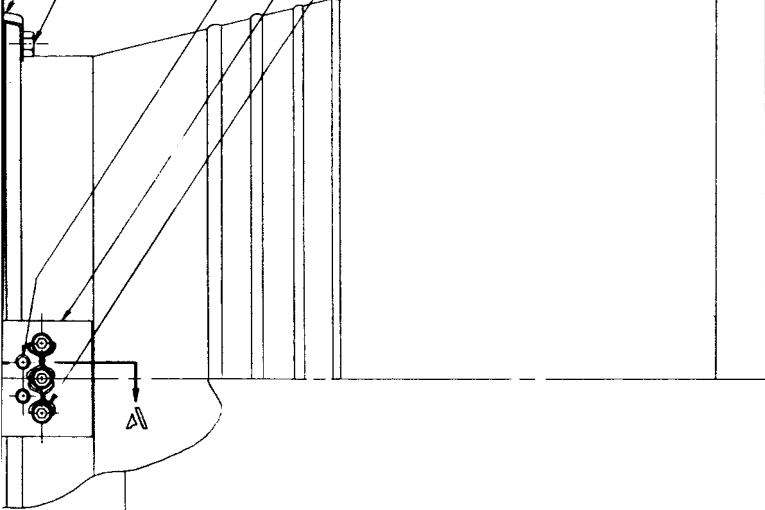

-ANIZETTE 15
-994 DIA x 1.88 LF
-994
2 HOLED PLACES LOCATED FROM
FADING .375 DIA HOLES IN 365223-1

UG

-366223-1

- COML PROD
HI PS. E NB 22-8H-14 9
MS20995C47 11

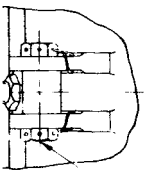
-366218-1 20






-AN8-6A 6215-1 $\triangle 2$

$-7/2$

C1032H6

366210-5 REF		
GLASS FABRIC REF		
ROVING REF		
366217-1 REF		
366217-3 REF		
366207-1 REF	366208-19 REF	366213-19
TAPE REF		
366209-19 REF		

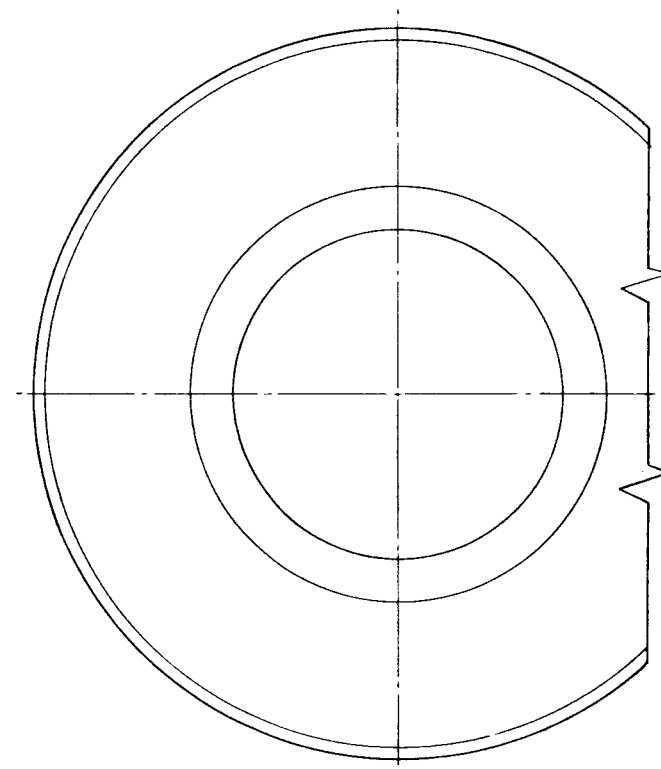
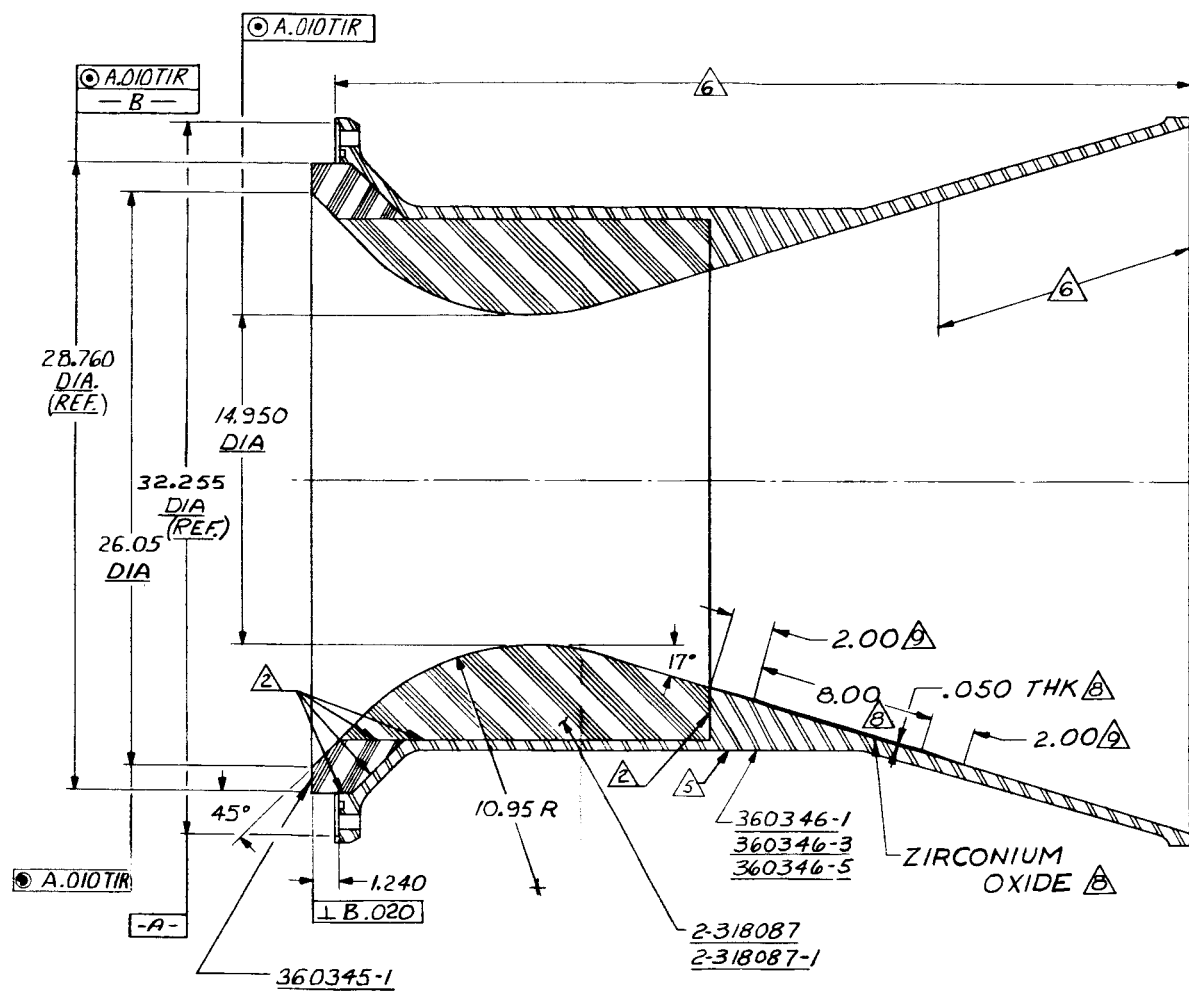


5-9   -366219-1  
MS20995C47 

Cantable Nozzle

Figure 4

2

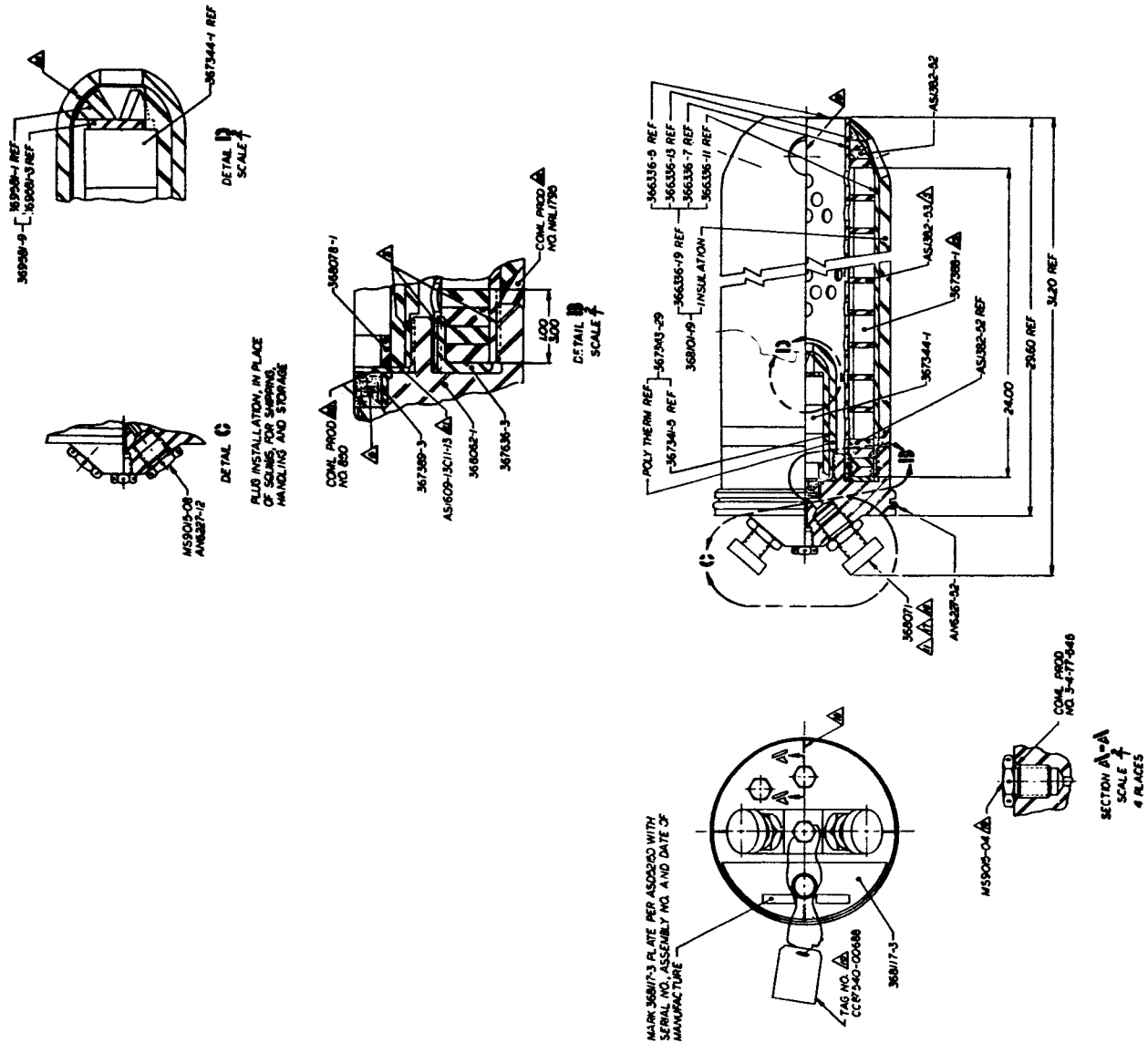


Straight Nozzle

Figure 3

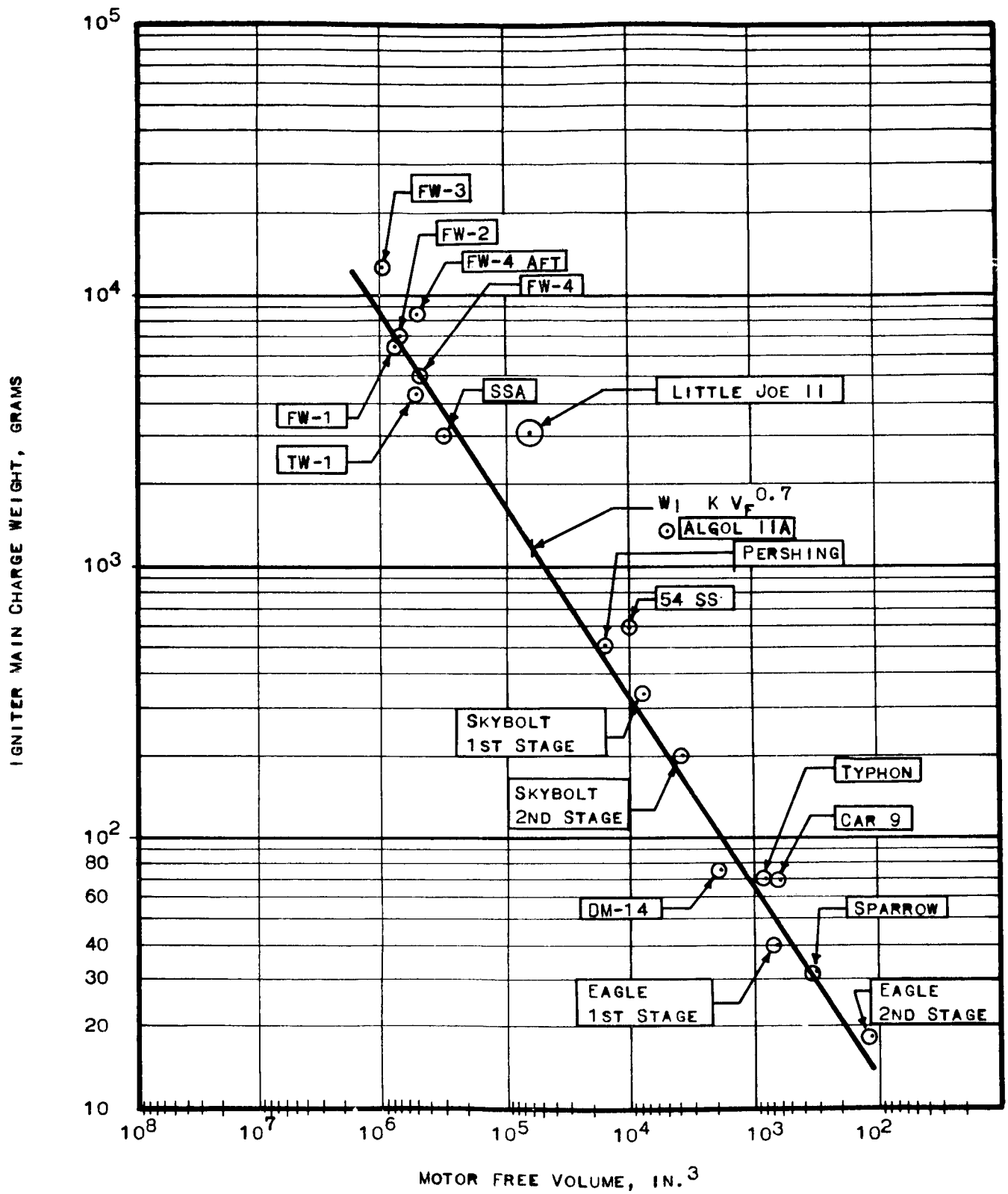
3①

②



High-Altitude Igniter

Figure 5



Comparison of Igniter Charge Weights vs Motor Free Volumes

Figure 6

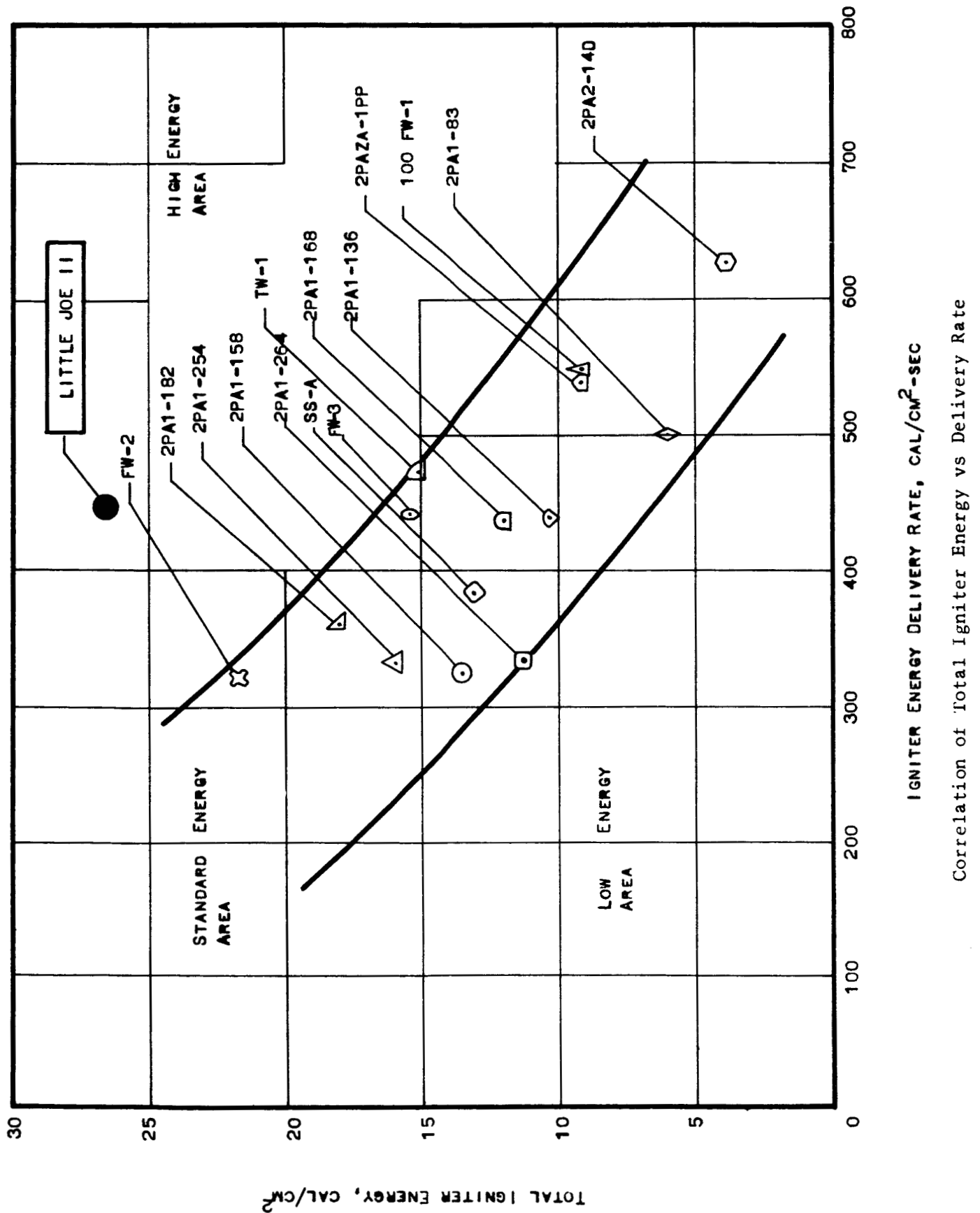


Figure 7

	NUMBER OF TESTS OR UNITS	PELLET TYPE	MAIN CHARGE WEIGHT GRAMS	THROAT AREA SQ. IN.	BOOSTER CONFIGURATION	NUMBER OF SQUIBS
Phase A To Investigate Pyrotechnic Formulations	6	3 Units- ACC-32014 3 Units- ACC-14046	1950	3.76	3 Holes	3 Units- 2 Each 3 Units- 1 Each
Phase B To Investigate Charge Weight & Port Size	10	All Units- ACC-14046	6 Units- 1950 4 Units- 3000	6 Units- 3.76 2 Units- 5.51 2 Units- 6.90	6 Units- 1 Hole 4 Units- 1 Hole & Retainer	2 Each
Phase C To Evaluate Repeatability	14	ACC-14046	3000	5.51	1 Hole & Retainer	12 Units- 2 Each 2 Units- 1 Each
Phase D Full Scale Motor Test	3	ACC-14046	3000	5.51	1 Hole & Retainer	2
Phase E Delivery	6	ACC-14046	3000	5.51	1 Hole & Retainer	2

Figure 8

NO-FIRE DESIGN CAPABILITY

1. No-fire current each bridgewire circuit, 1.0 amp minimum for 5 min minimum.
2. No-fire wattage each bridgewire circuit, 1.0 watt minimum for 5 min minimum.
3. No-fire voltage, pin to case 1000 V RMS minimum.
4. Static discharge of 0.01 joule from a 0.04 micro farad capacitor applied from shunted leads to case.

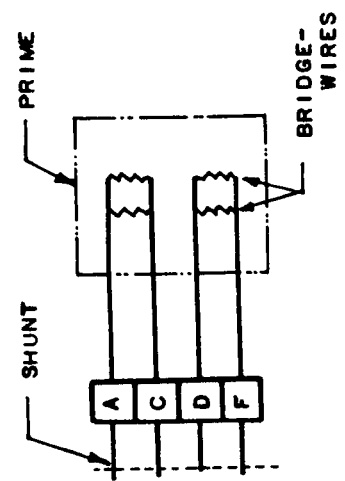
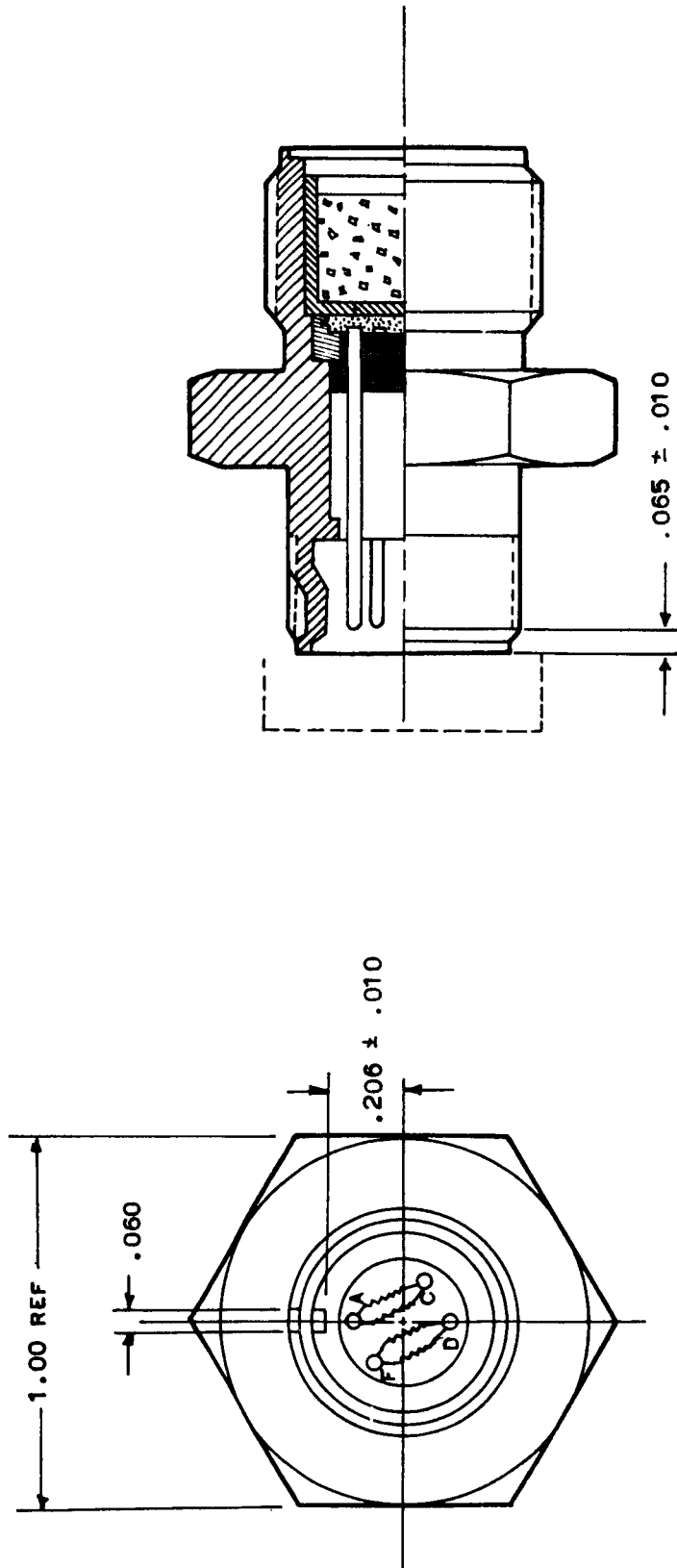
FUNCTIONAL DESIGN CAPABILITY

1. 100% firing current each bridgewire circuit, 4.5 amps.
2. Resistance each bridgewire circuit, 0.5 ohms minimum.
3. Altitude capability, sea level to 200,000 ft.
4. Minimum autoignition temp, 350°F for 8 hr.

PHYSICAL DATA

1. Squib seal shall be glass or ceramic to metal.
2. Initiator charge to consist of 0.600 \pm 0.01 gr of equal parts by weight of ignition powder per Specification AGC-34154 and pyrotechnic powder a 35 mi, per Specification AGC-32014.
3. Dual bridgewire circuits.
4. Closure to be resistance welded per MIL-W-6858 Class B or soft soldered per MIL-S-6872.
5. Connector end mates with Bendix PC 06-10-6S straight plug.
6. Squib case to be B-113/C-1213 per QQ-S-633, CD Hex., cadmium plated per QQ-P-416, Type 1, Class 1.
7. Pressure test glass to metal seal with dry N₂ for 10 sec at 10,000 psig prior to plating. Test for leaks with leak test compound, Type 1 per MIL-L-25567. No leakage permitted. Units will be accepted on an individual basis.

Initiator Design Data



Schematic Drawing of Initiator

Figure 10

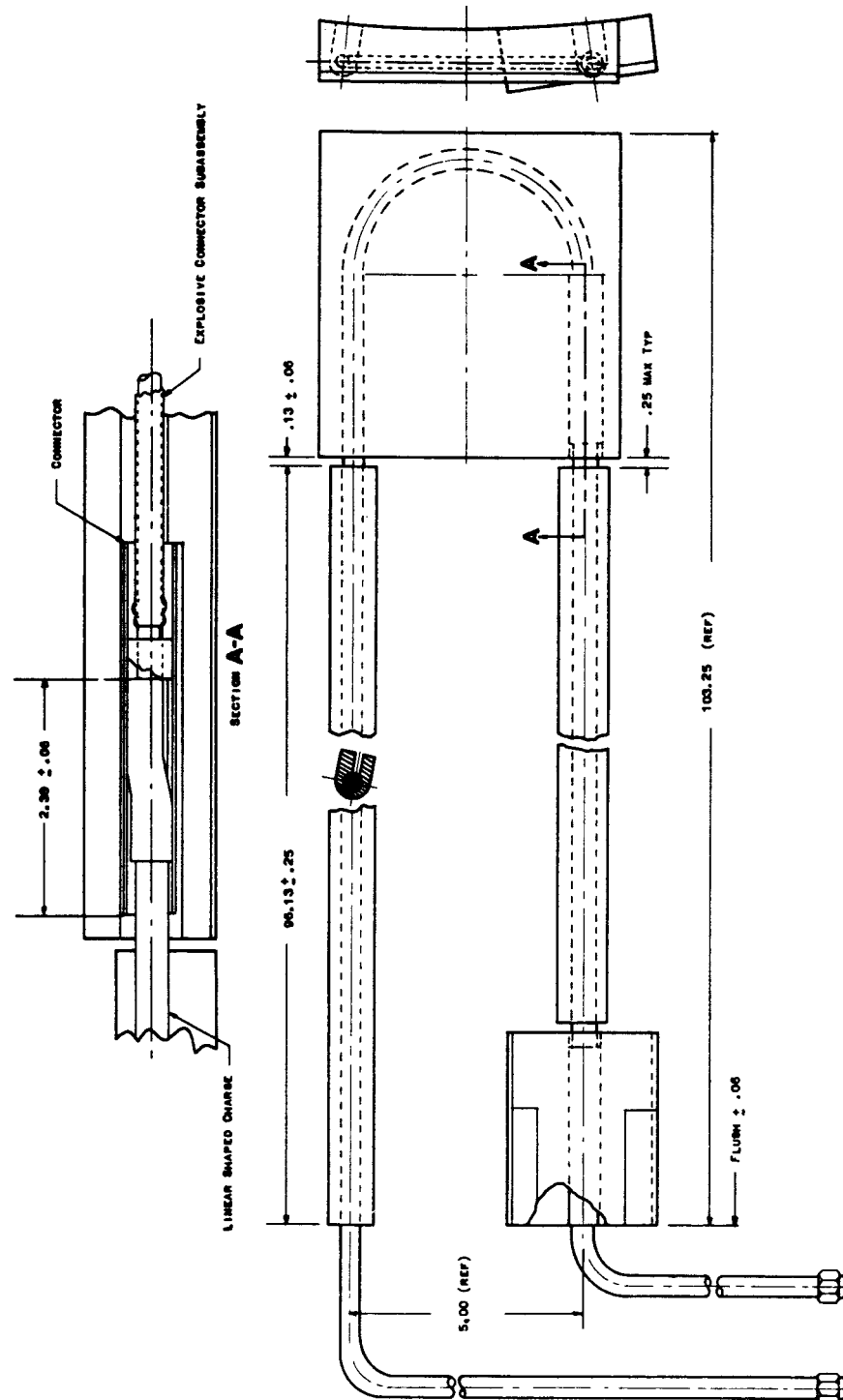


Figure 11

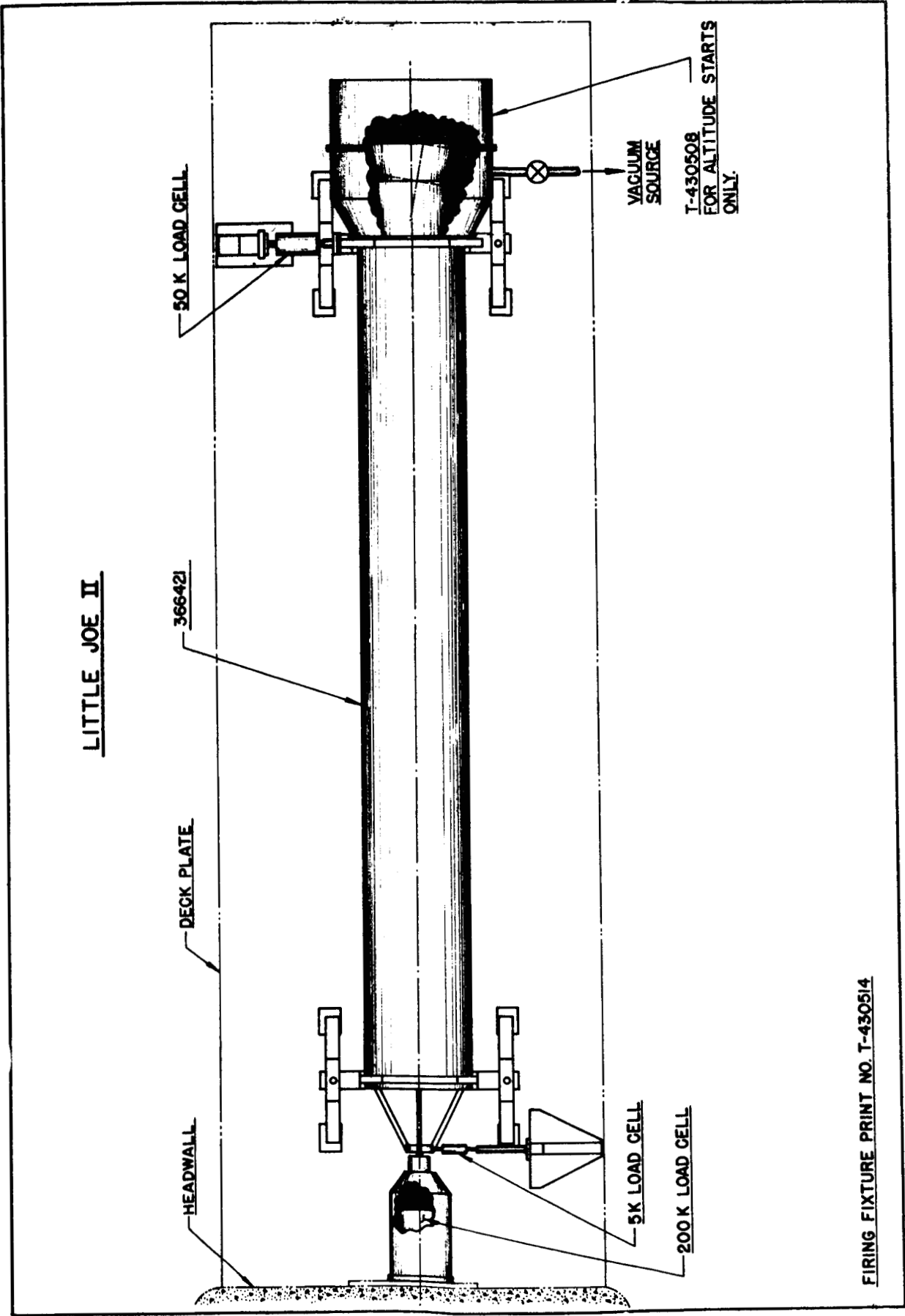
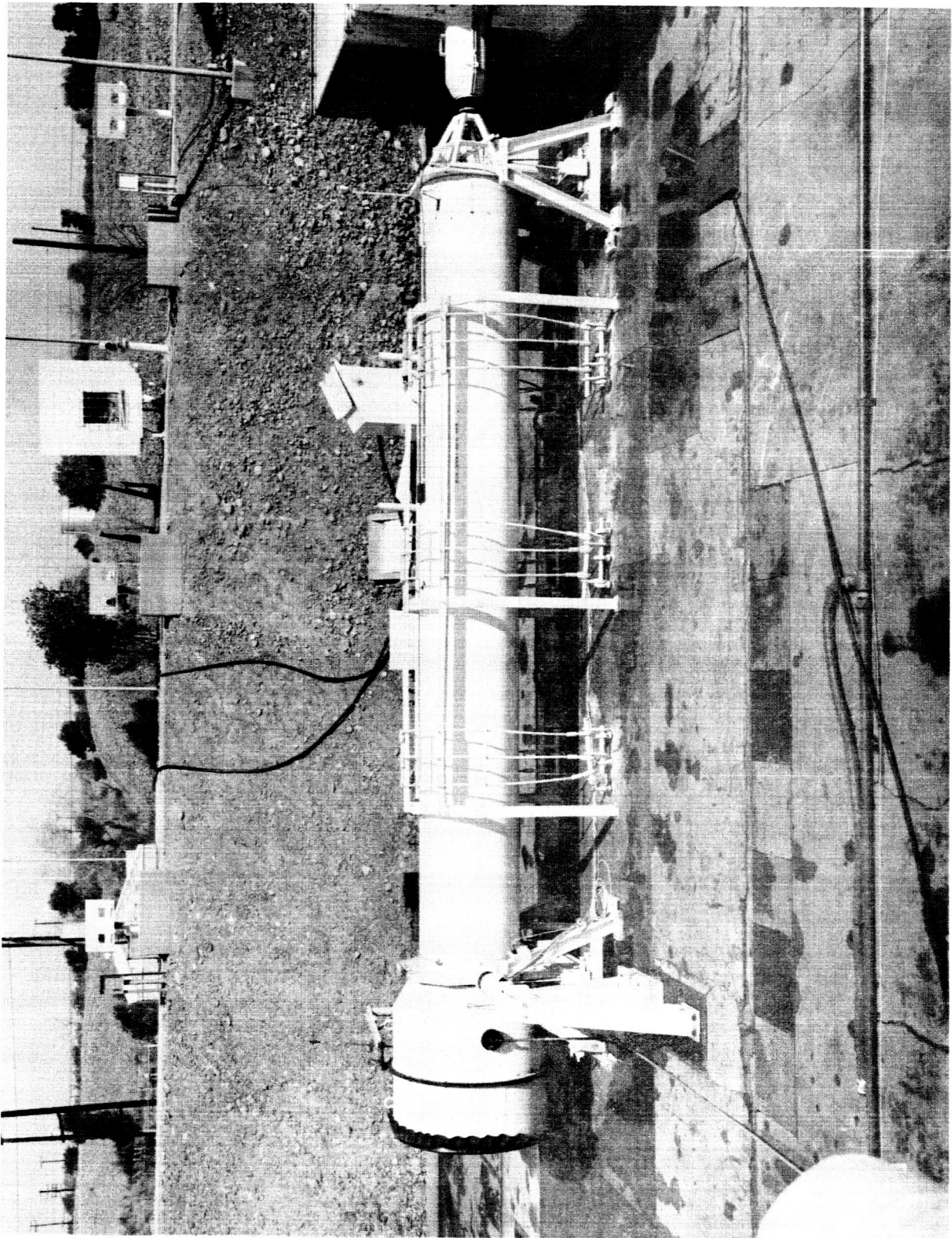


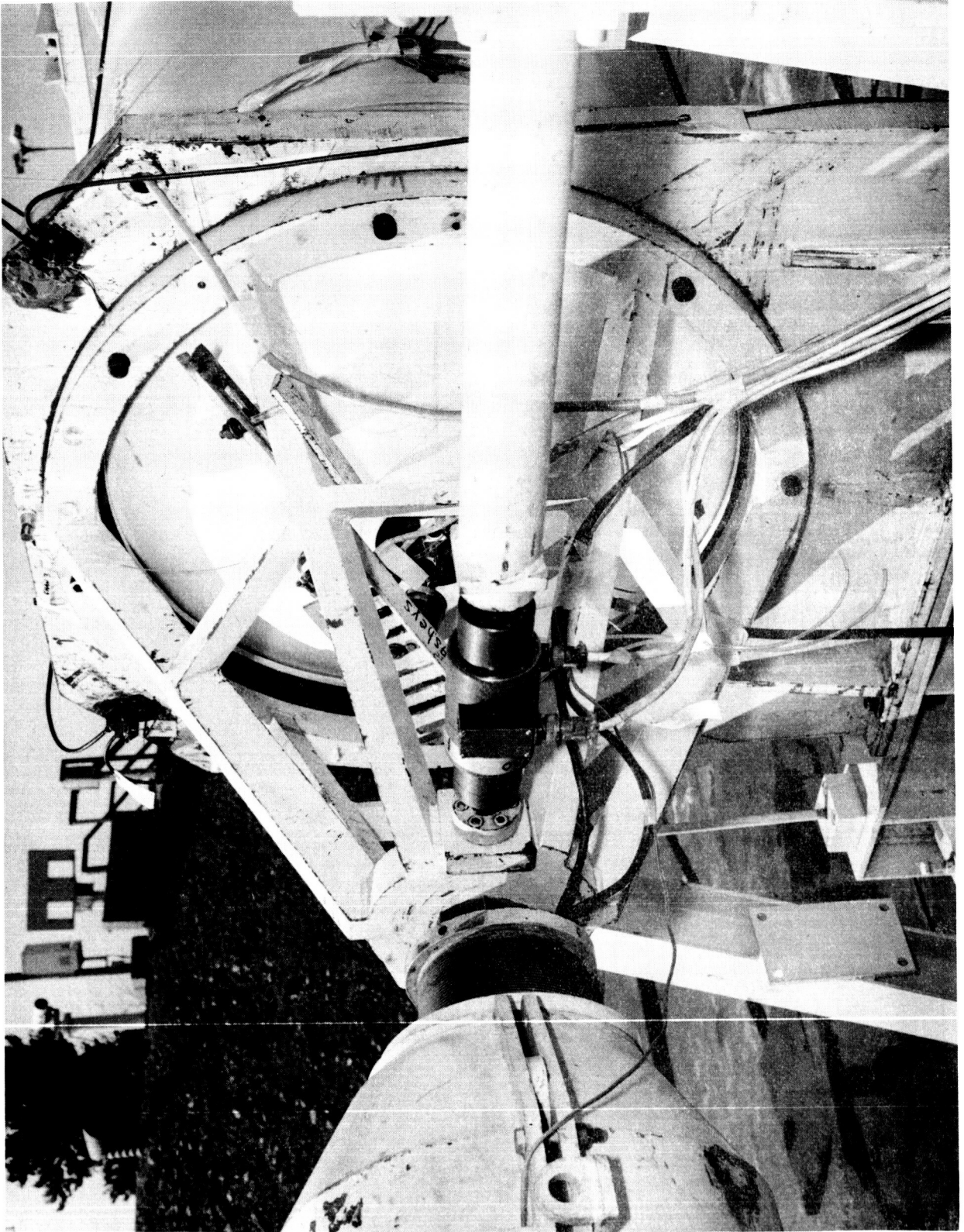
Figure 12

Schematic Drawing of Motor Test Installation With Altitude Facility



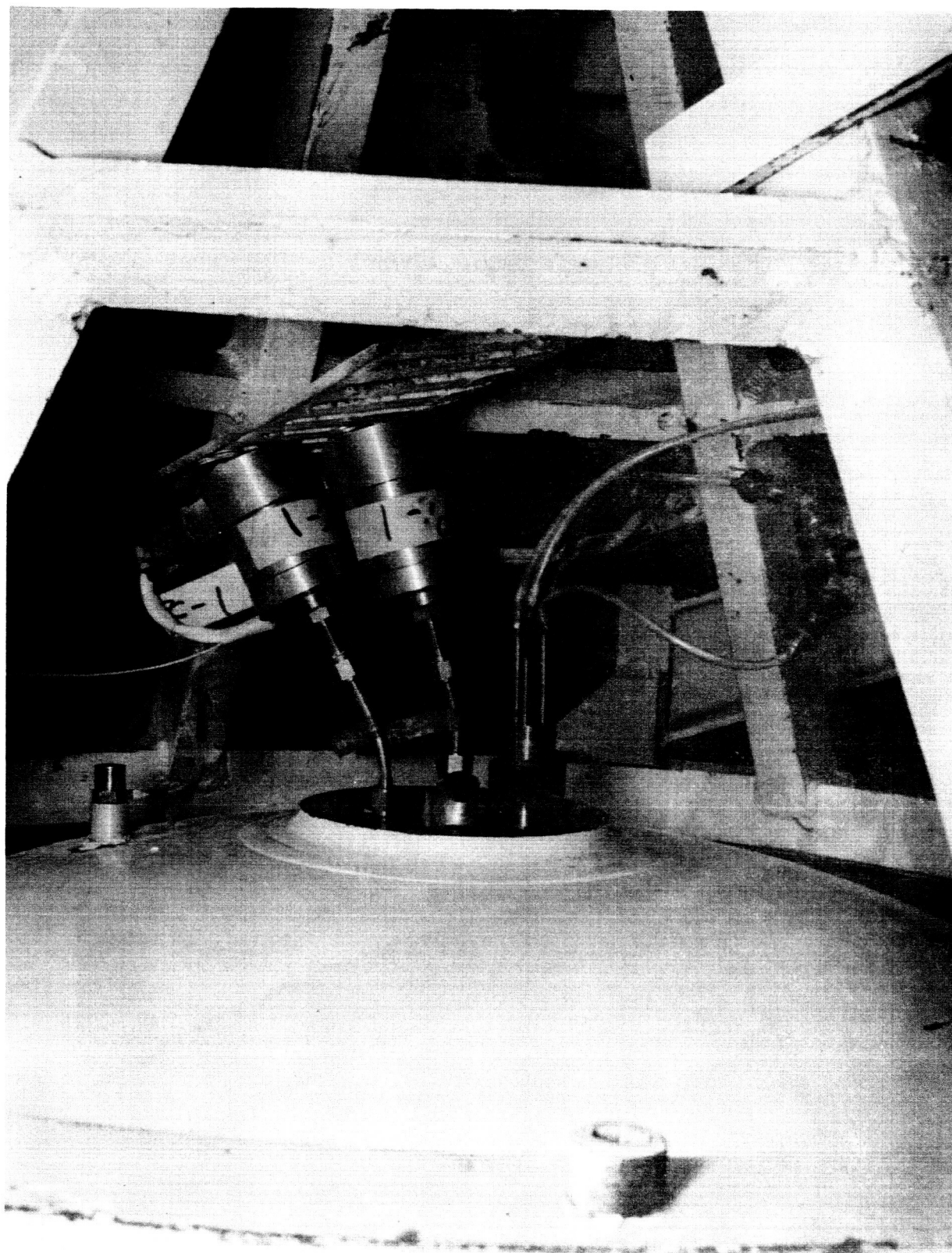
Motor LJ-7, Prefiring Side View (Photo 8-63 SP 221)

Figure 13



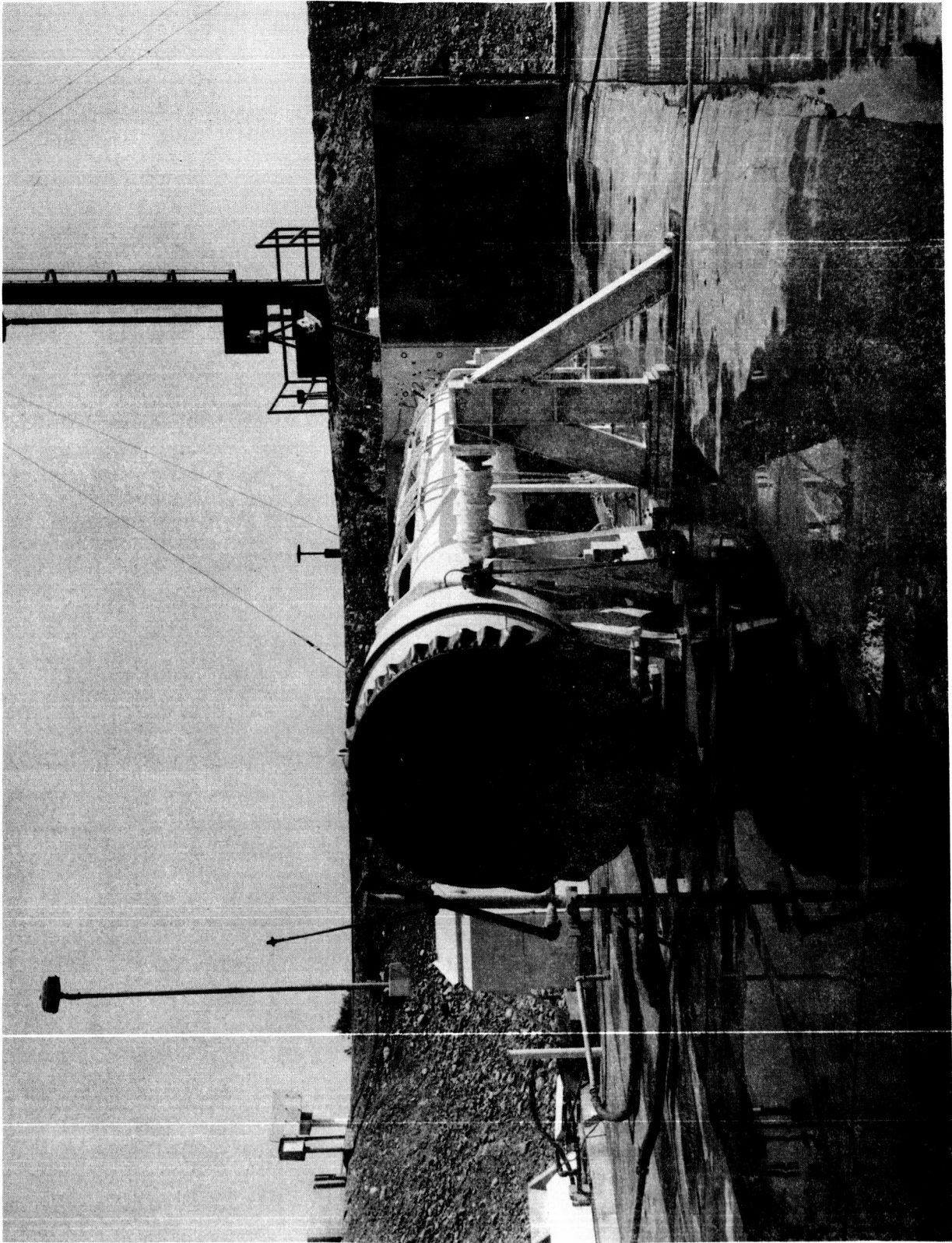
Motor LJ-7, Prefiring Front View (Photo 8-63 SP 225)

Figure 14



Motor LJ-7, Prefiring View of Igniter and Transducers (Photo 8-63 SP 226)

Figure 15



Motor LJ-7, Prefiring Aft View (Photo 8-63 SP 219)

Figure 16

PC-1 - CHAMBER PRESSURE 750 PSI
 PC-2 - CHAMBER PRESSURE (HIGH FREQ) 750 PSI
 PI-1 - IGNITER PRESSURE 10K
 FE1 - AFTSIDE FORCE 50K
 FE2 - FWD SIDE FORCE 5K
 GCFY - ACCELEROMETER - FWD CASE
 GFRY - ACCELEROMETER - FWD FIRING RING
 GCAY - ACCELEROMETER - AFT CASE
 GAFT - ACCELEROMETER - AFT FIRING RING

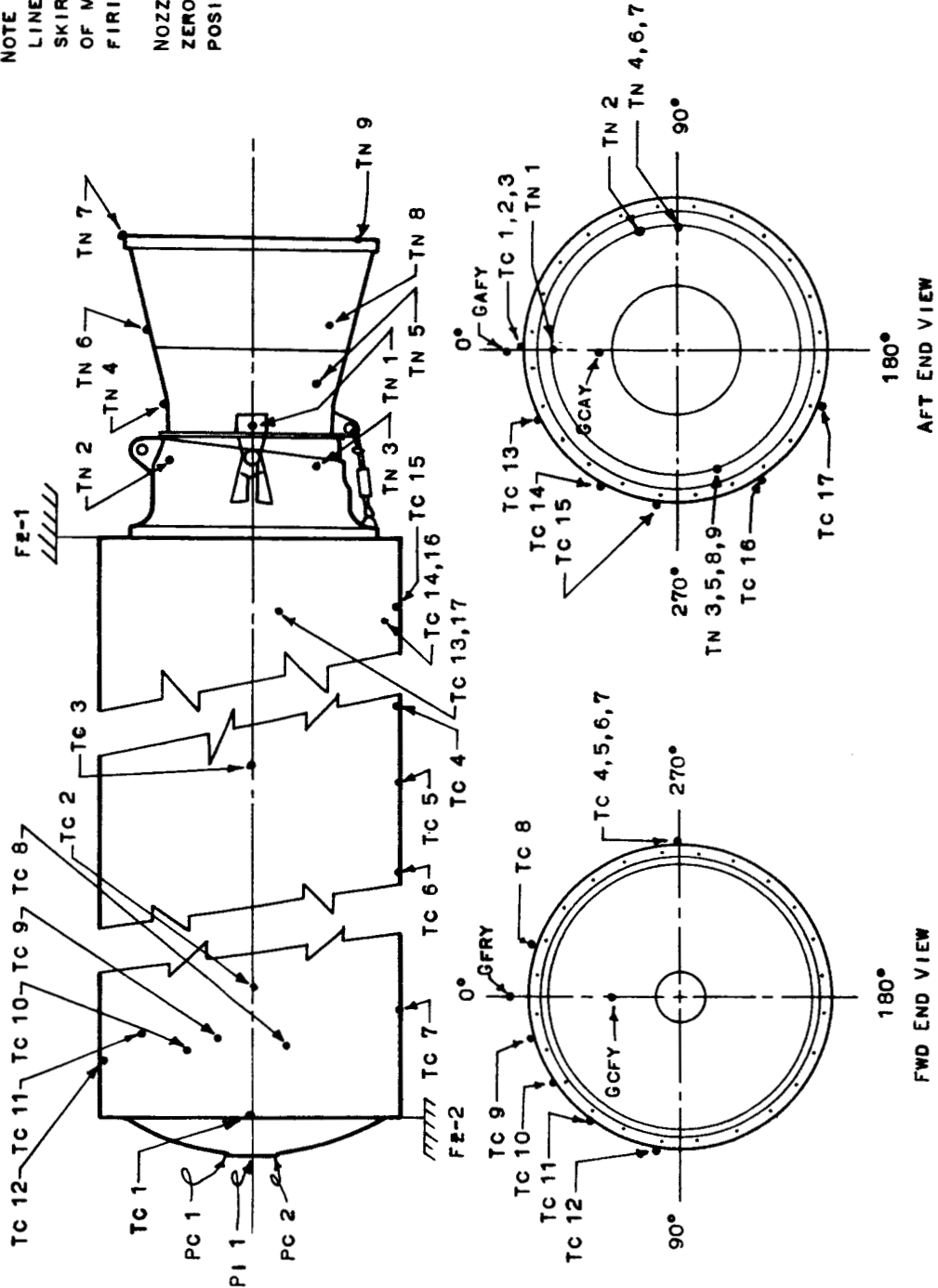
TN 1 - 0°-14
 TN 2 - 80°-9
 TN 3 - 260°-9
 TN 4 - 90°-15
 TN 5 - 260°-15
 TN 6 - 90°-27
 TN 7 - 90°-39
 TN 8 - 260°-27
 TN 9 - 260°-39

TC 1 - 0°-312.5
 TC 2 - 0°-185
 TC 3 - 0°-60
 TC 4 - 270°-80
 TC 5 - 270°-131
 TC 6 - 270°-181
 TC 7 - 270°-233
 TC 8 - 352°-298
 TC 9 - 14°-296
 TC 10 - 37°-297

TC 11 - 59°-296
 TC 12 - 82°-298
 TC 13 - 330°-10
 TC 14 - 302°-12
 TC 15 - 274°-11
 TC 16 - 246°-12
 TC 17 - 218°-10

NOTE - DATUM
 LINE IS AFT MOTOR
 SKIRT. 0° IS TOP
 OF MOTOR CASE IN
 FIRING HARNESS.

NOZZLE SHOWN IN
 ZERO DEGREE
 POSITION



Instrumentation Locations, Motor LJ-7

Figure 17

MOTOR		LJ-1	LJ-4	LJ-7
AVERAGE CHAMBER PRESSURE, WEB-	PSIA	447	463	451
AVERAGE THRUST, WEB-	LBF	109,349	109,148	109,294
BURNING TIME, WEB-	SEC	33.9	33.5	33.3
IMPULSE, WEB-	LBFS	3,714,682	3,660,613	3,641,024
TOTAL IMPULSE,	LBFS	4,107,314	3,999,896	4,085,378
AVERAGE WEIGHT FLOW, WEB-	LB/SEC	506	515	507
PROPELLANT WEIGHT,	LB	18,972	18,933	18,919
TEST DATE		4 APR 1963	6 MAY 1963	1 AUG 1963
GRAIN TEMPERATURE,	°F	70	70	78

Figure 18

Performance Characteristics, Motor LJ-1, -4, and -7

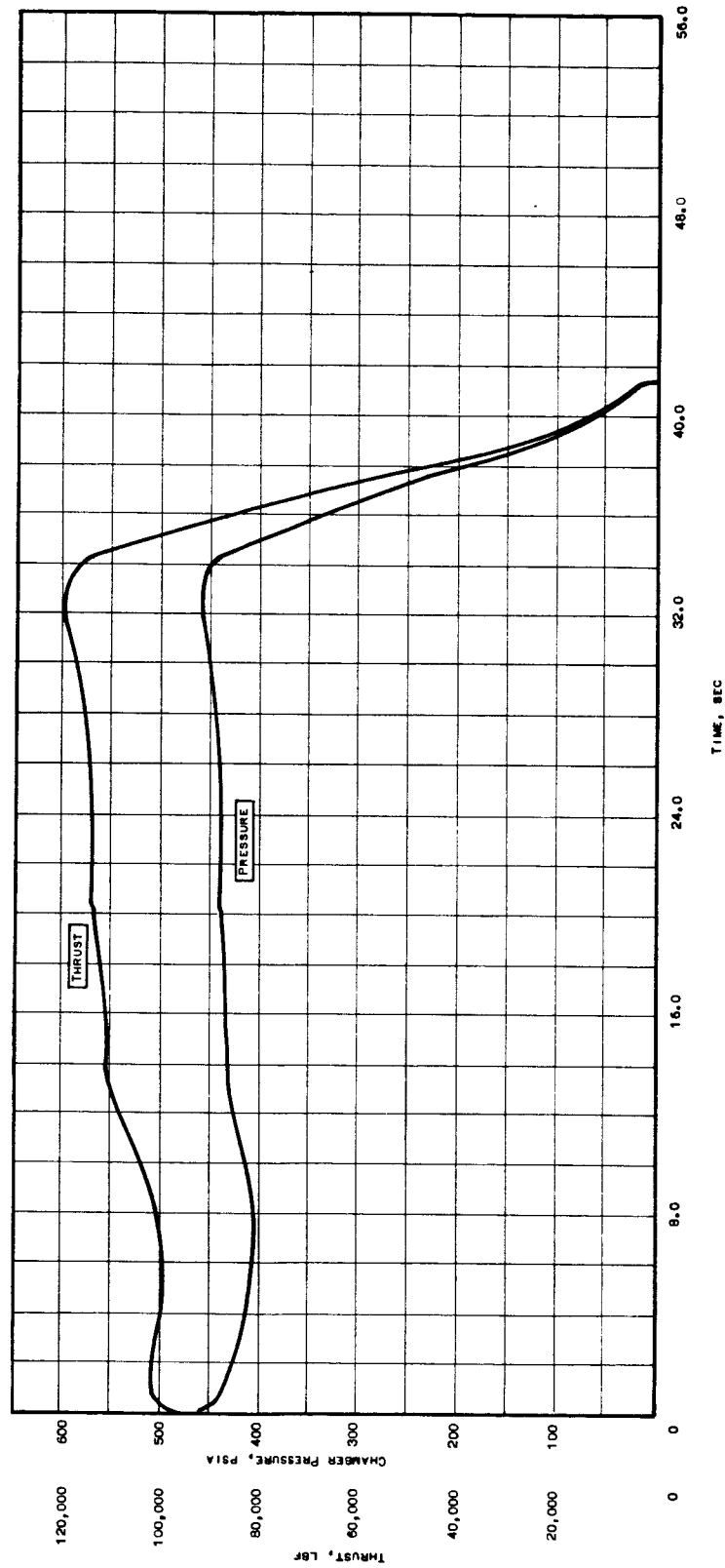


Figure 19

Thrust and Pressure vs Time, Motor LJ-1

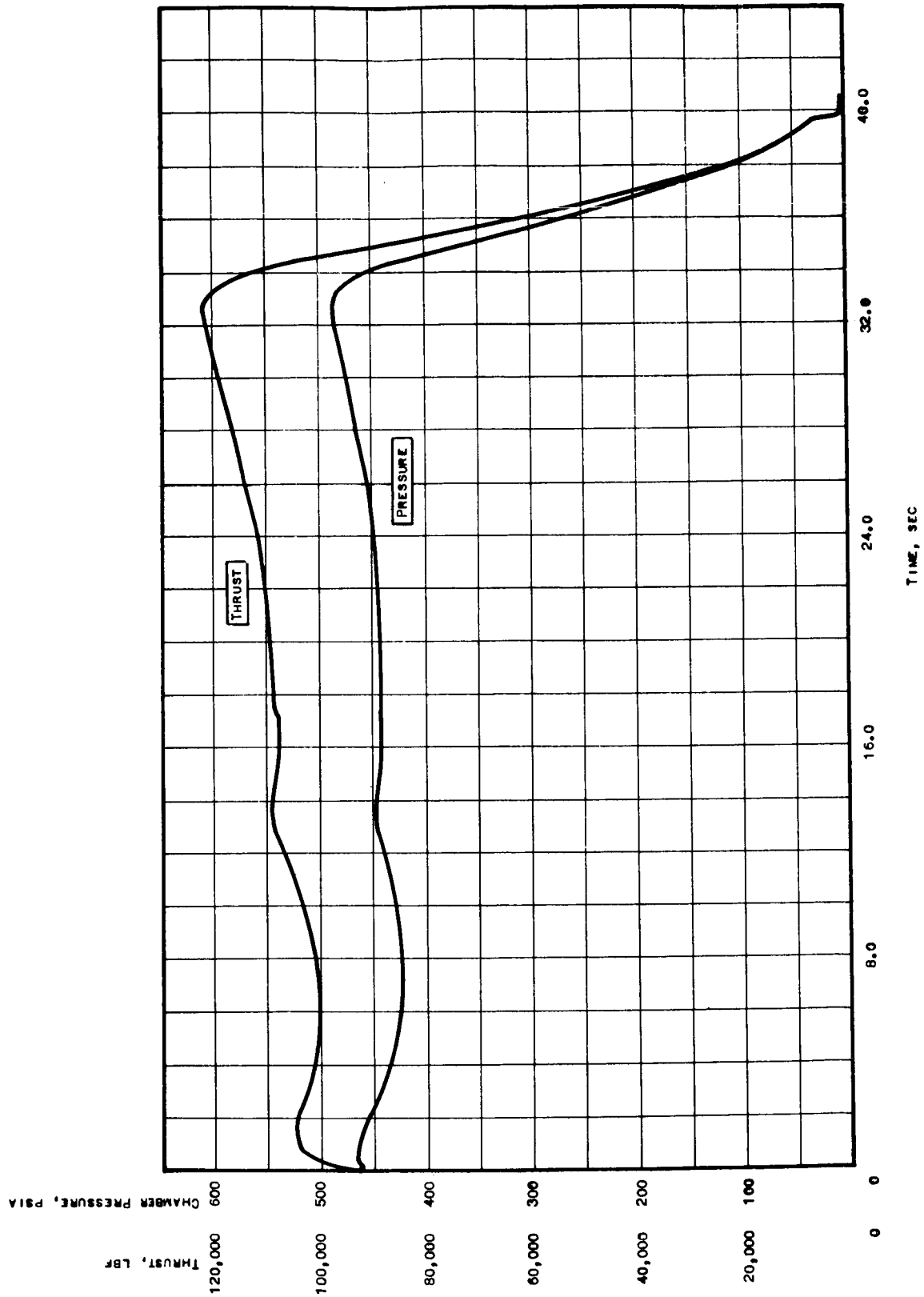
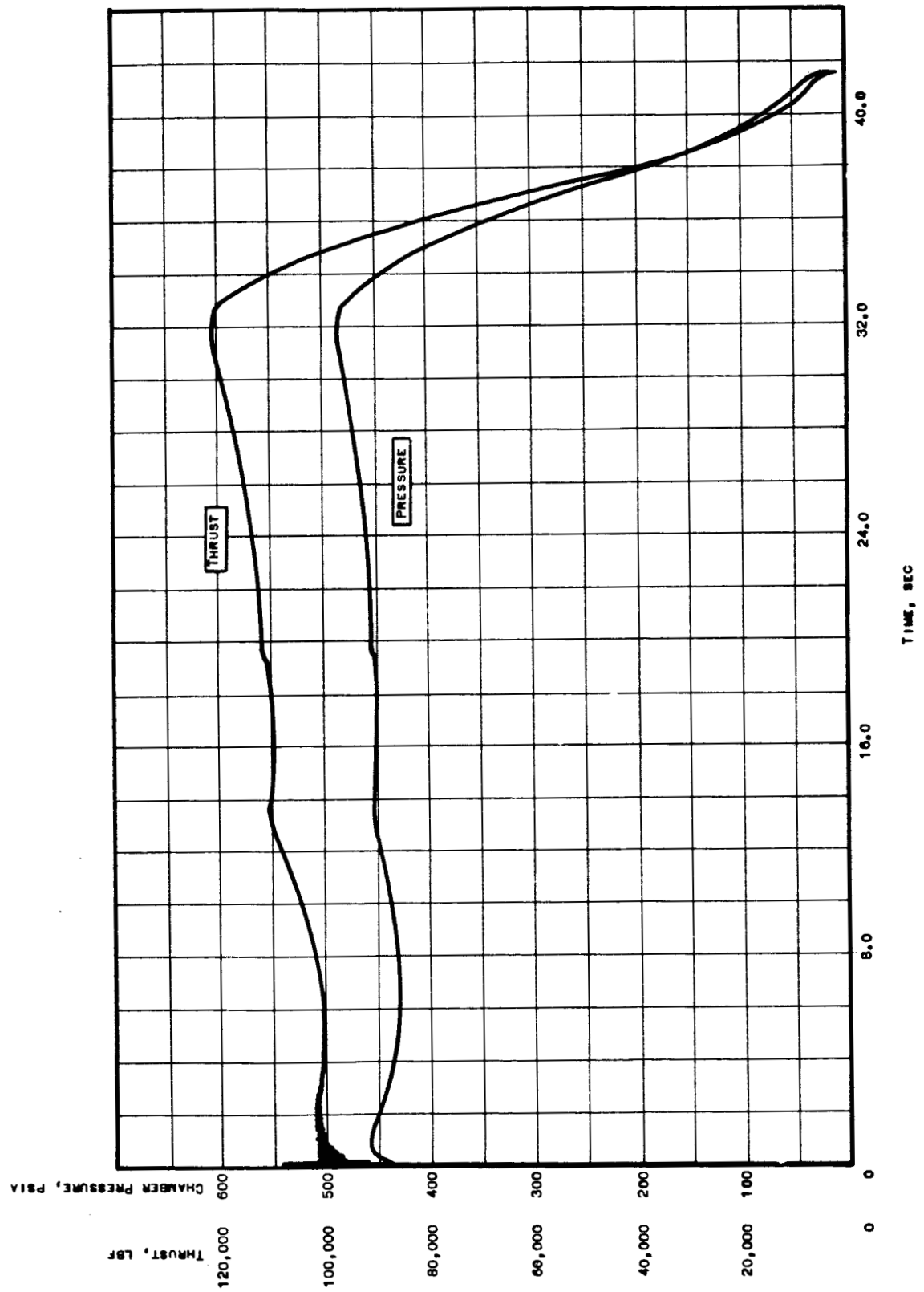


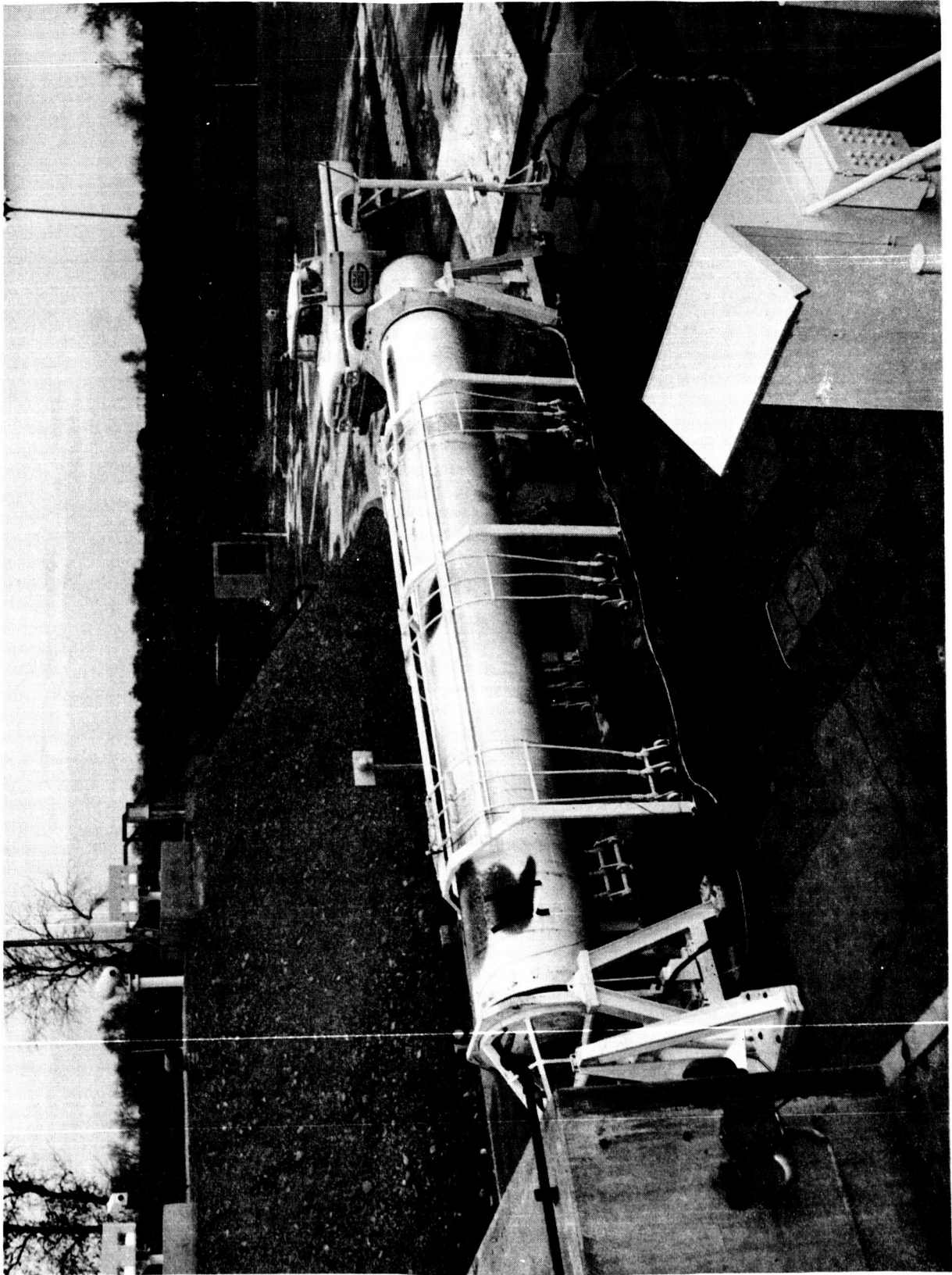
Figure 20

Thrust and Pressure vs Time, Motor LJ-4



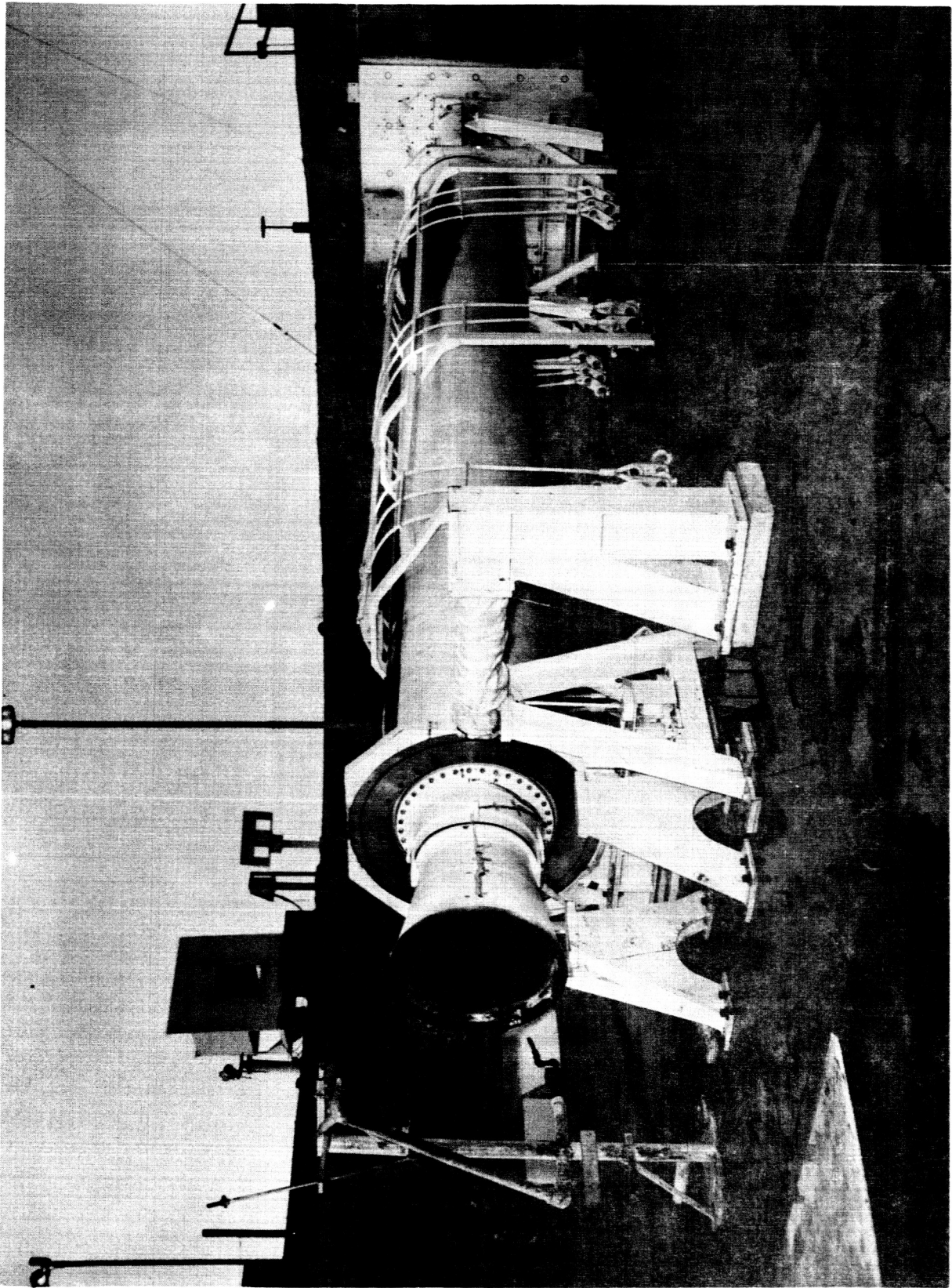
Thrust and Pressure vs Time, Motor LJ-7

Figure 21



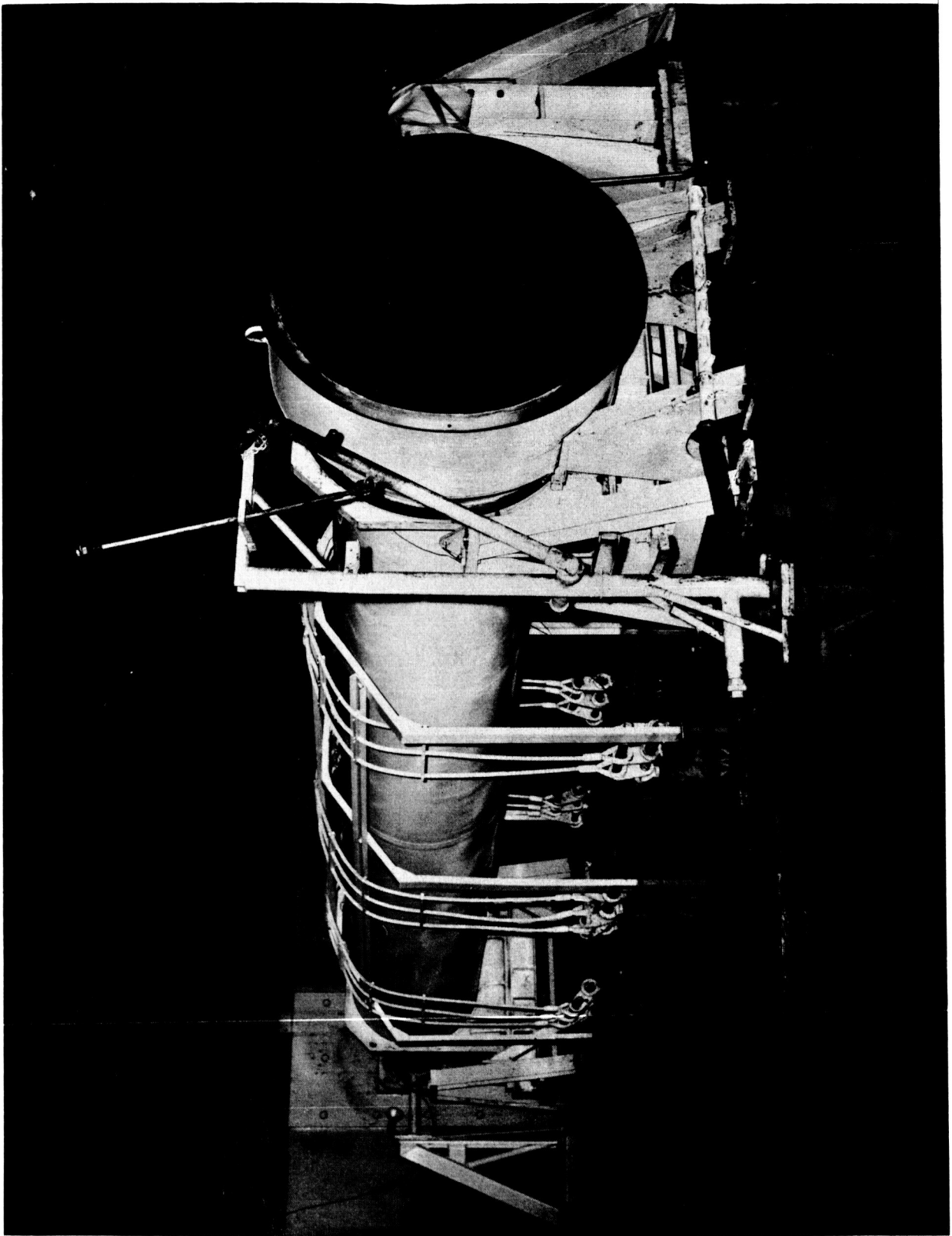
Postfiring Side View, Motor LJ-1 (Photo 4-63S 06593)

Figure 22



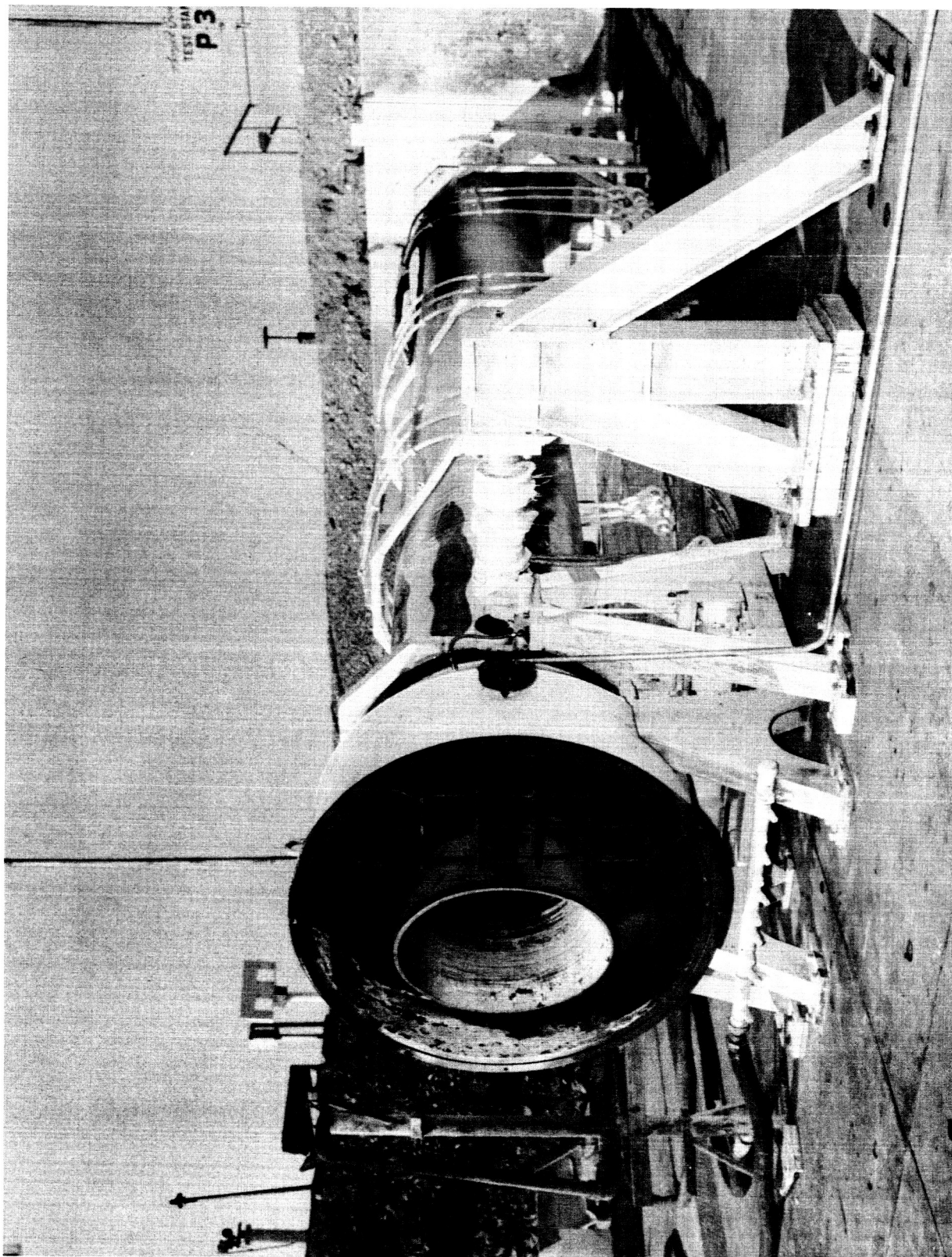
Postfiring Side View, Motor LJ-1 (Photo 4-63S 06592)

Figure 23



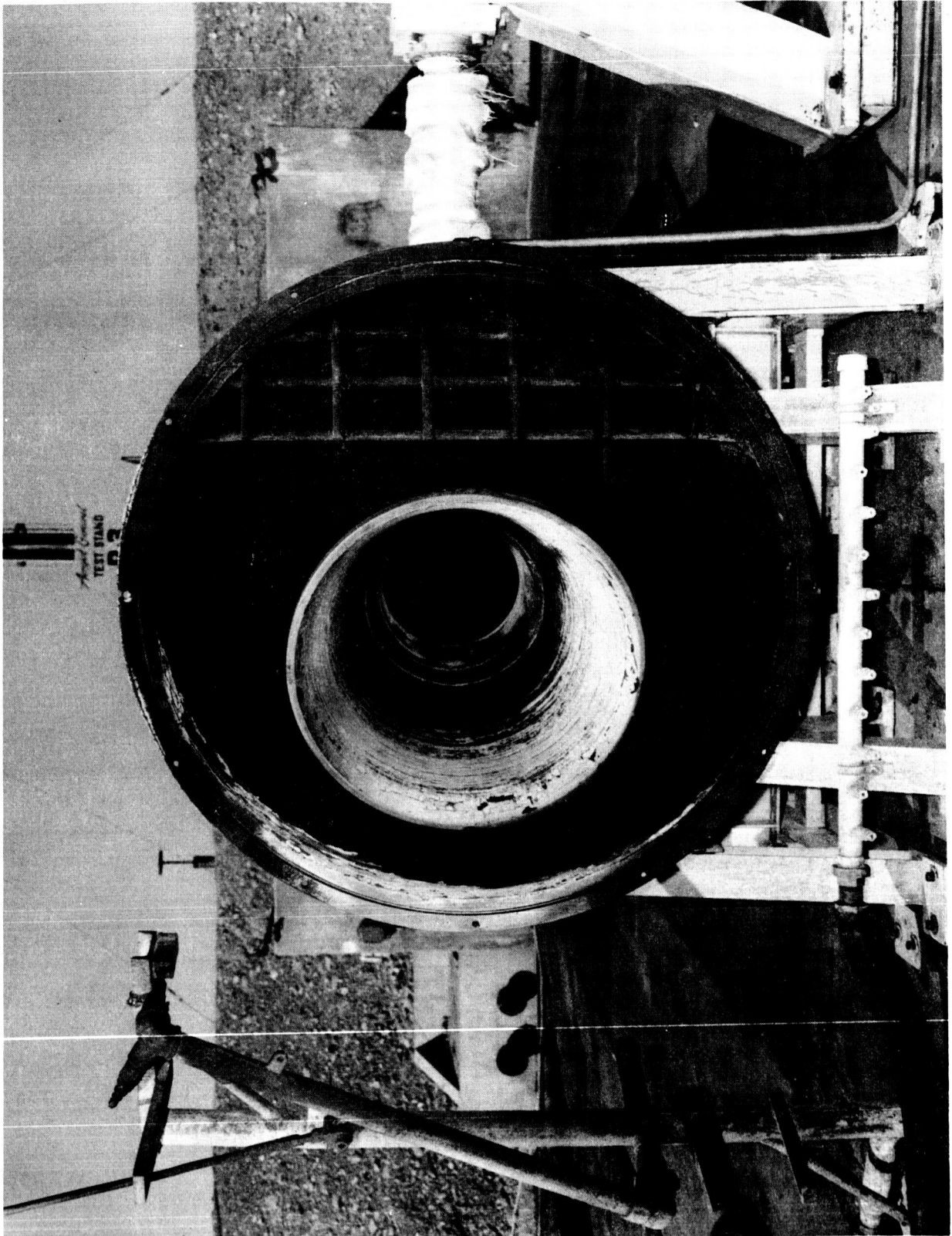
Postfiring Aft View, Motor LJ-4 (Photo 5-63S 08474)

Figure 24



Postfiring Aft View, Motor LJ-7 (Photo 8-63 SP 453)

Figure 25



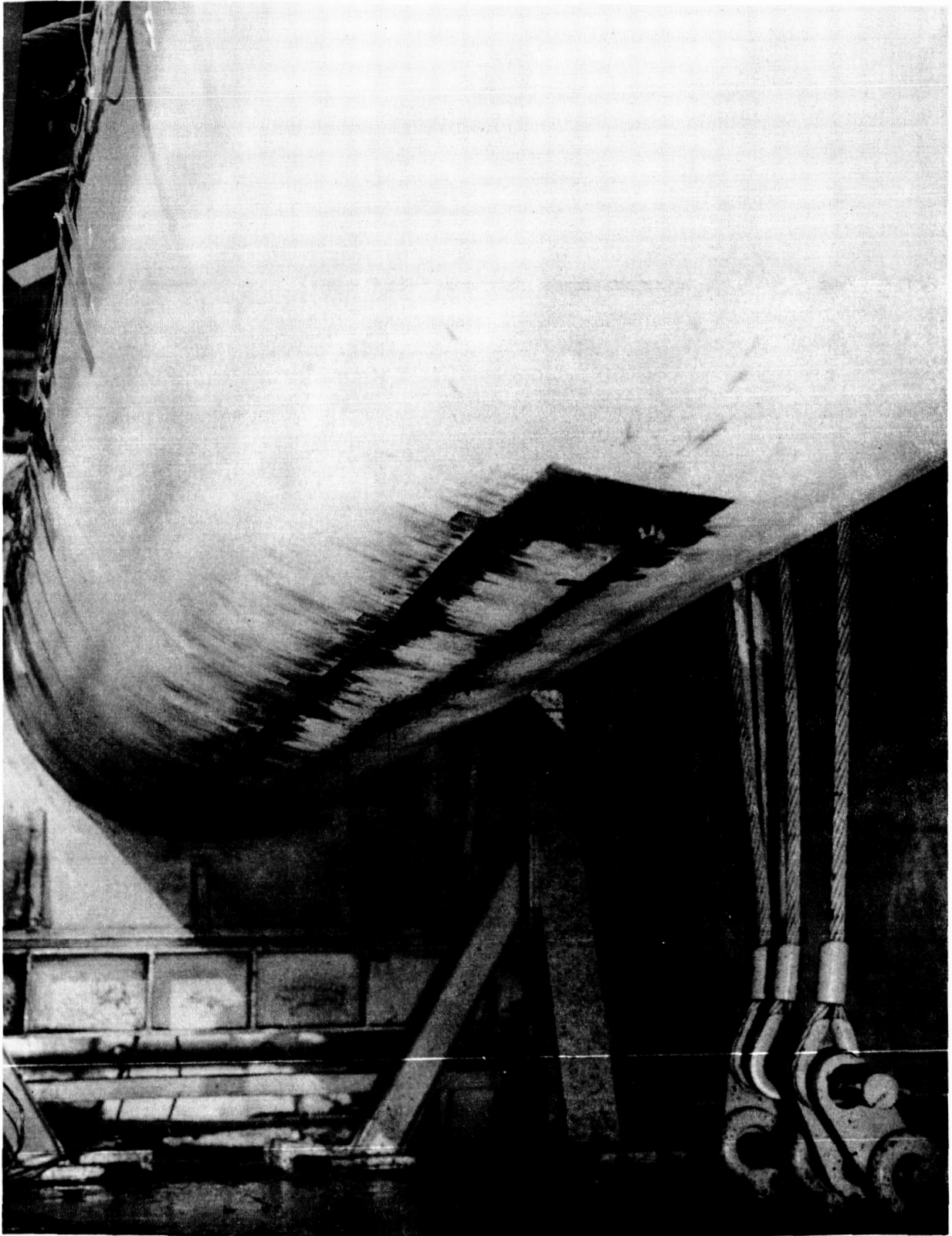
Postfiring View of Nozzle, Motor LJ-7 (Photo 8-63 SP 456)

Figure 26



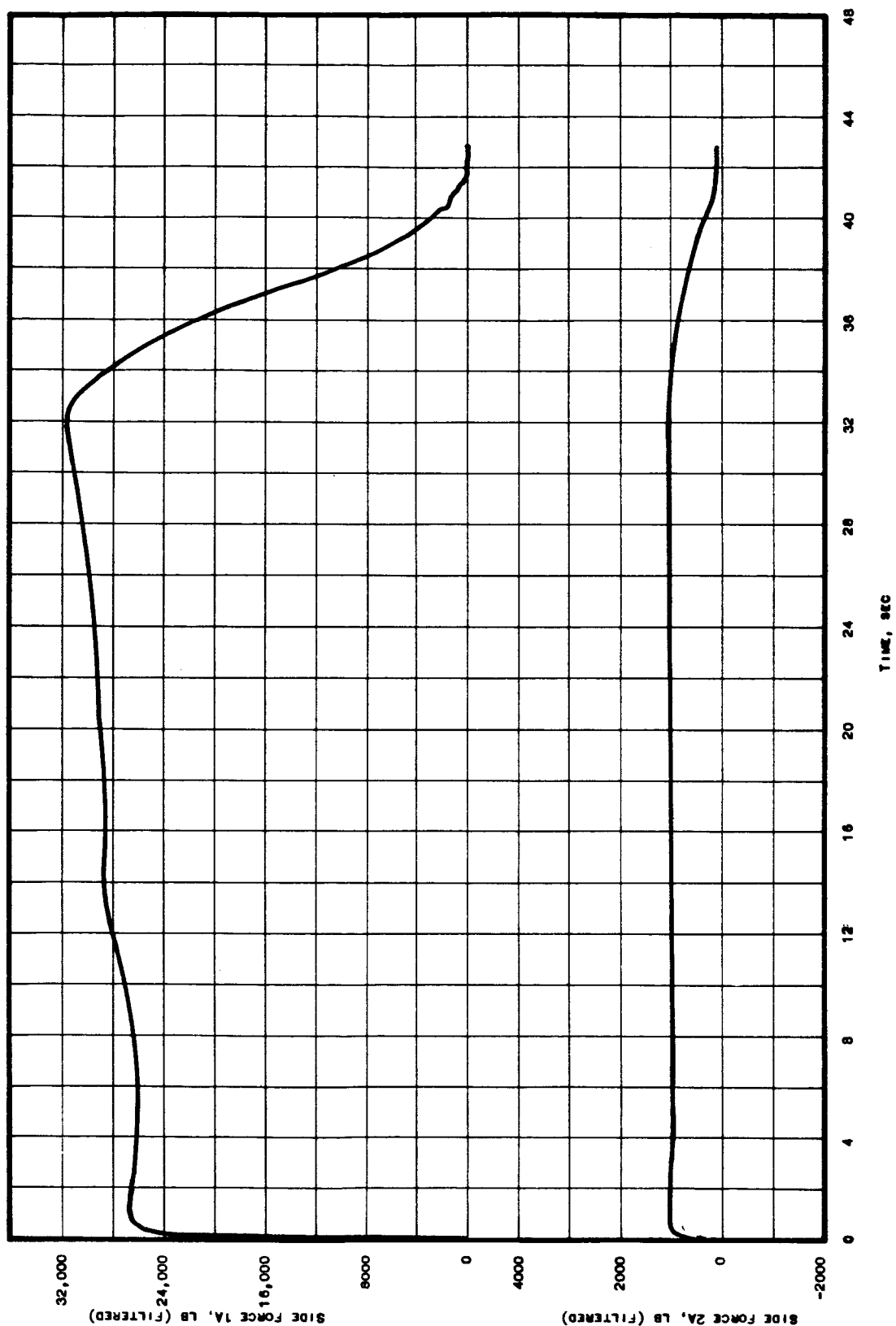
Postfiring View of Top Destruct Cut, Motor LJ-7 (Photo 8-63 SP 455)

Figure 27



Postfiring View of Bottom Destruct Cut, Motor LJ-7

Figure 28



Side-Force Data, Motor LJ-7

Figure 29

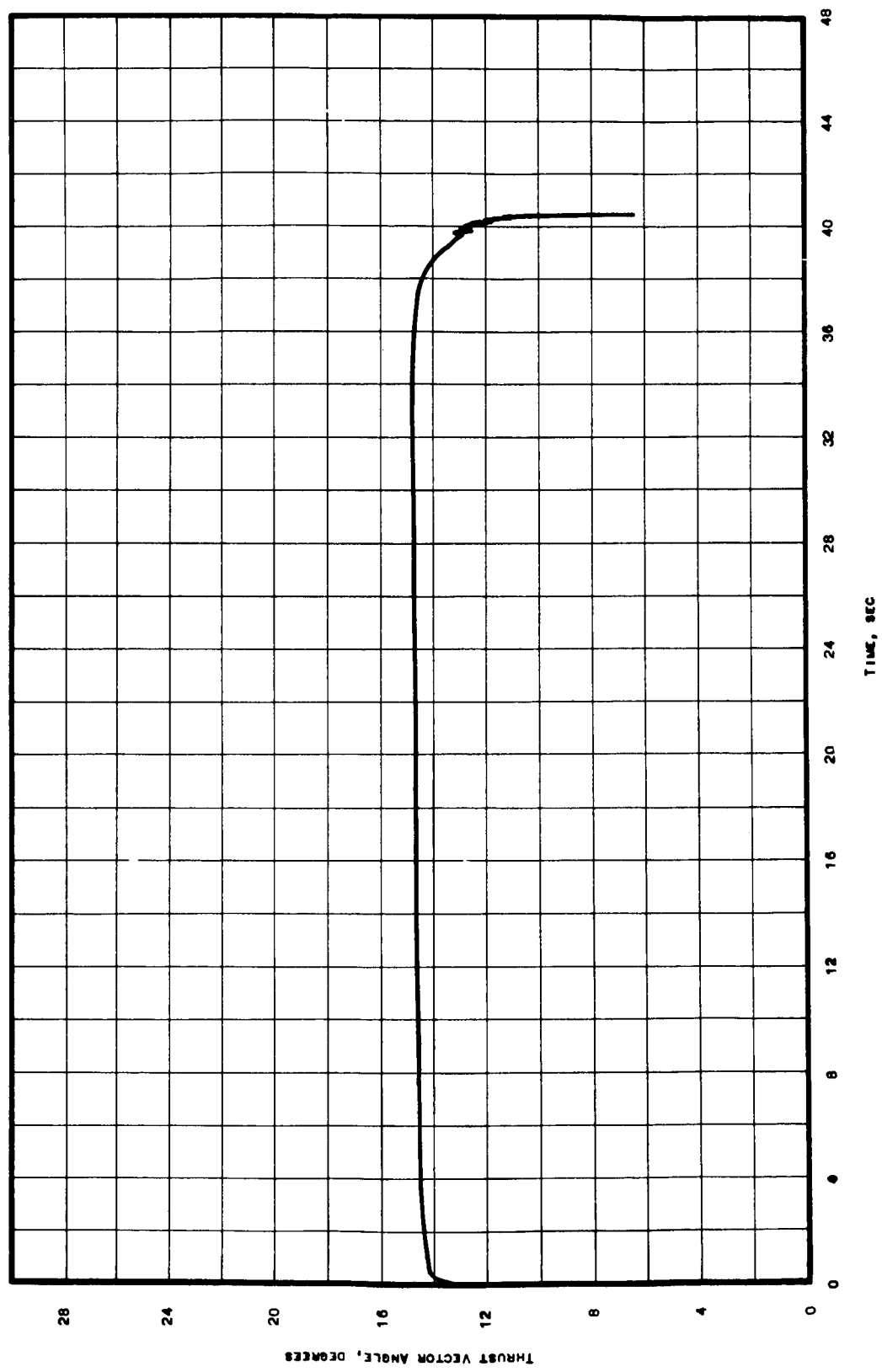


Figure 30

Jet-Deflection-Angle Data, Motor LJ-7

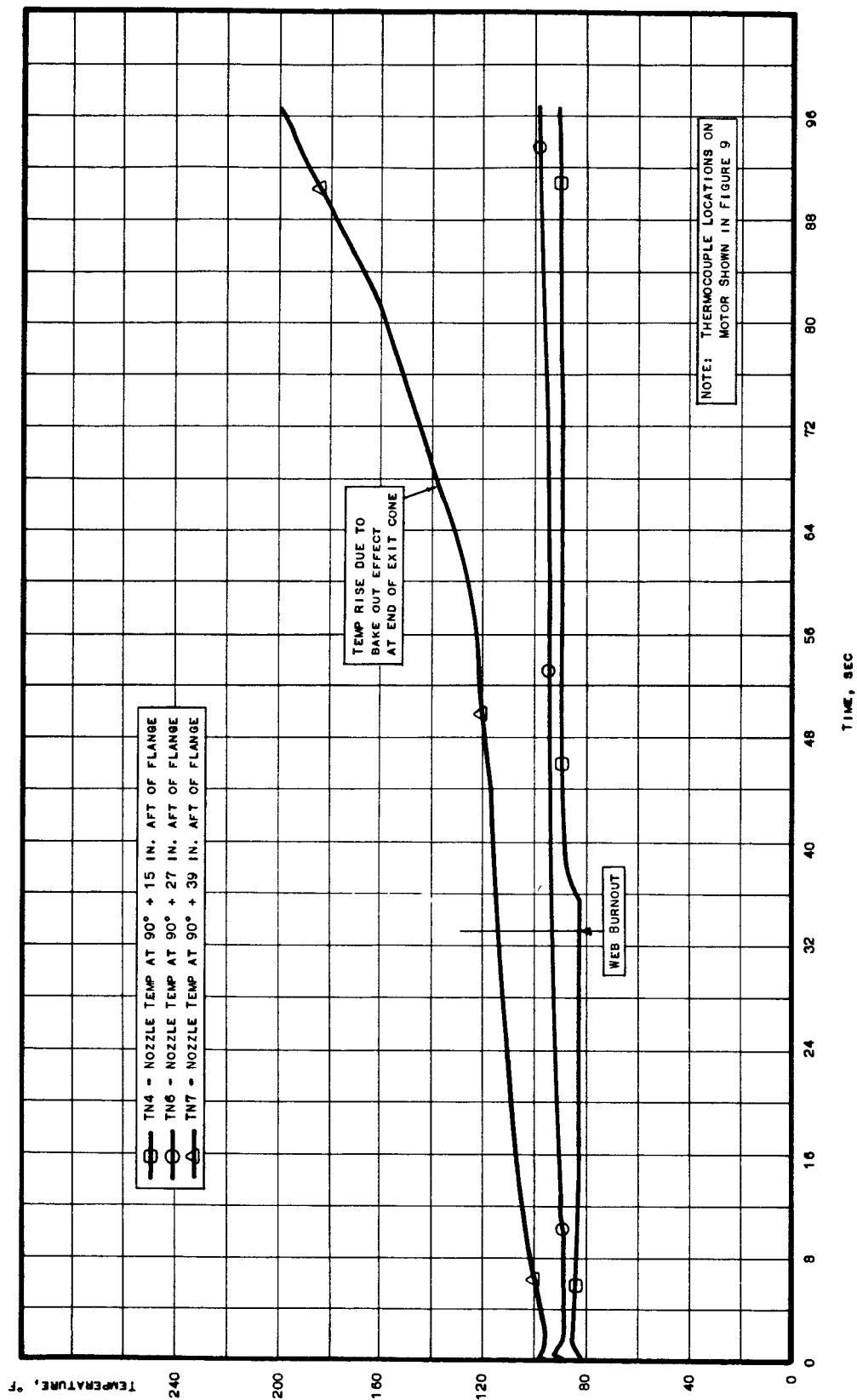


Figure 31

Nozzle Temperature at Locations TN4, TN6, and TN7; Motor LJ-7

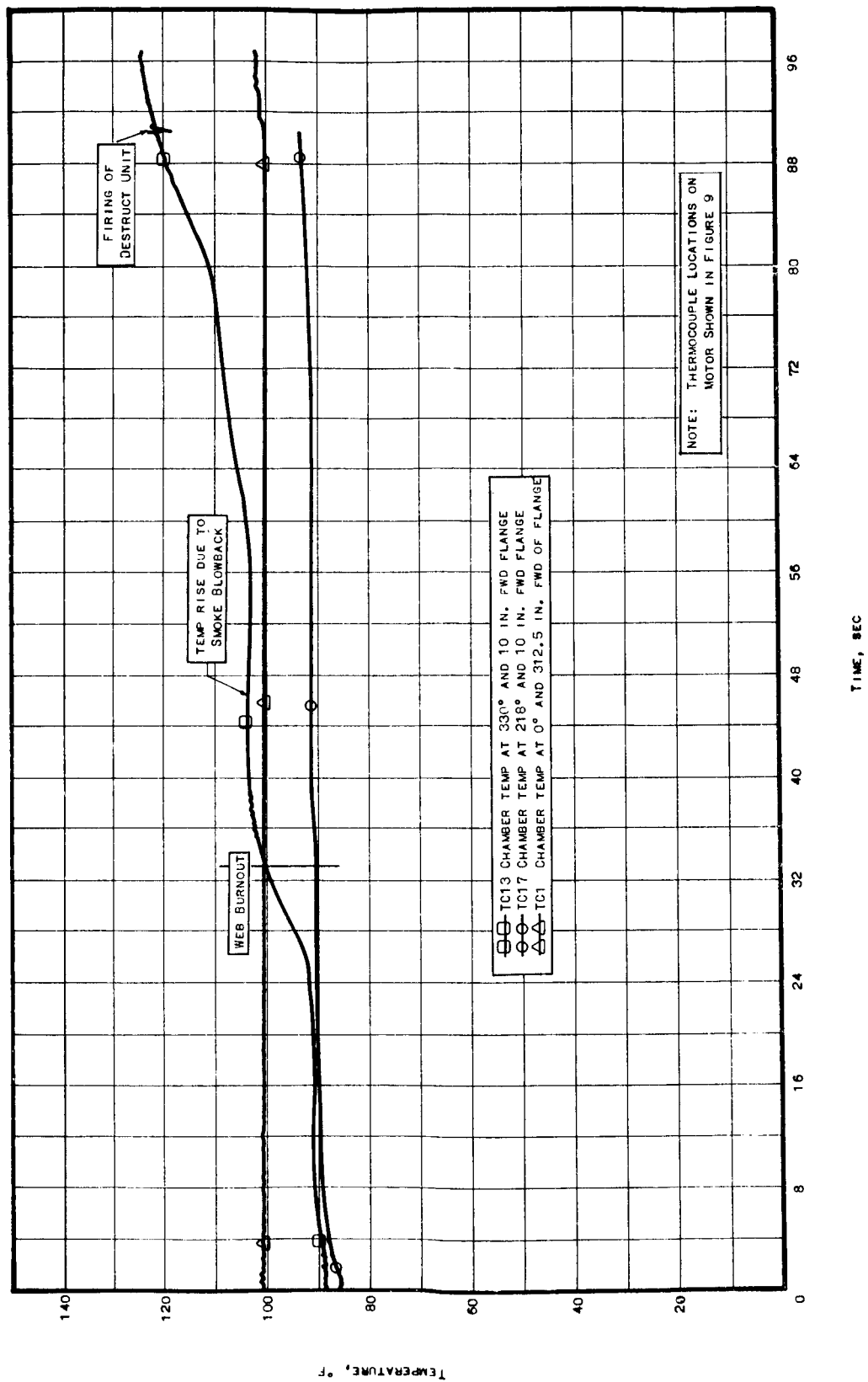


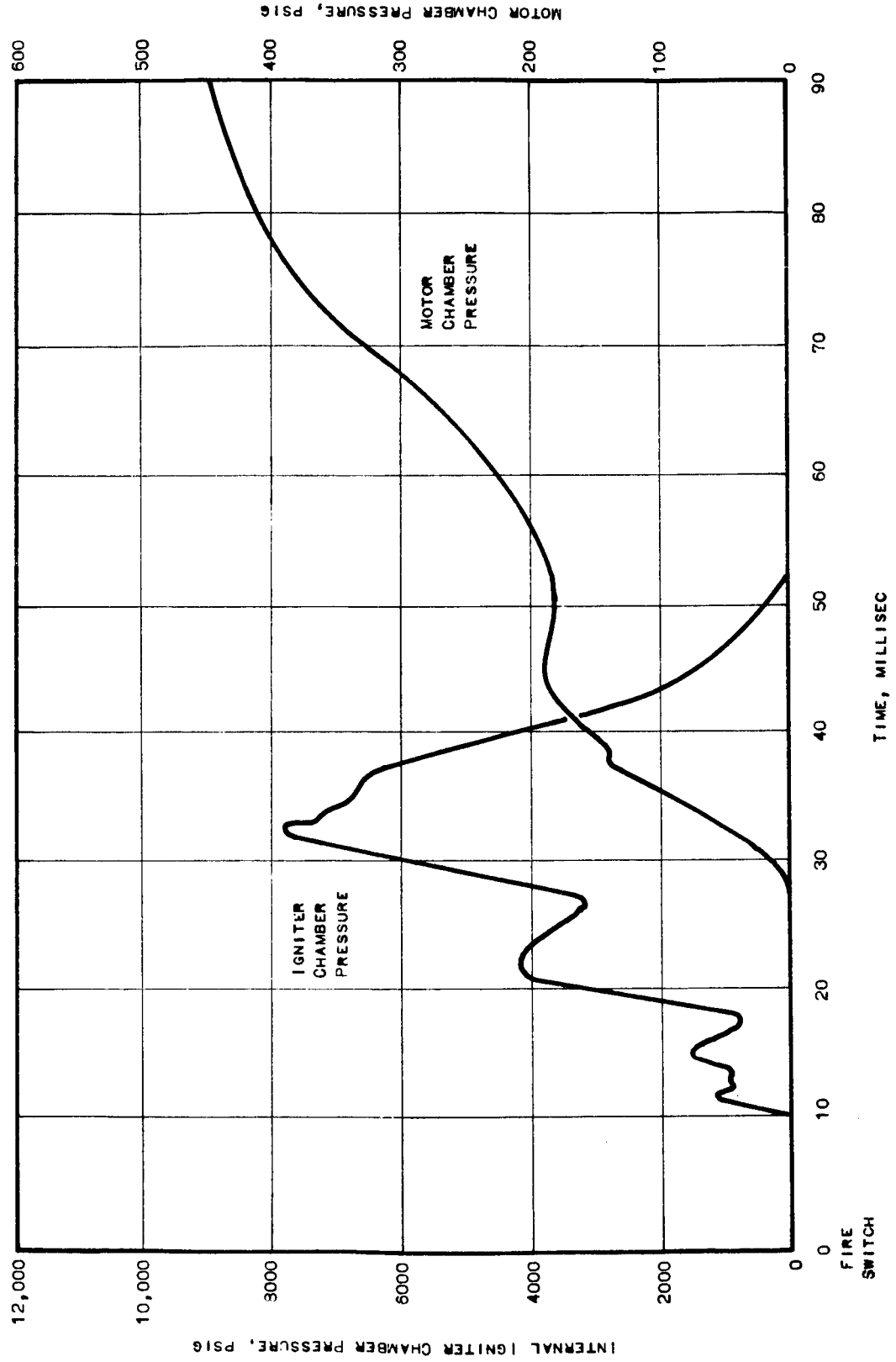
Figure 32

Chamber Temperatures at Locations TC13, TC17, and TC1; Motor LJ-7

IGNITER SERIAL NO.	TEST TEMPERATURE OF	ELEVATION	NUMBER OF SQUIBS	TIME TO MAJOR EVENTS - MILLISECONDS						MAXIMUM PRESSURES			COMMENTS	
				FIRST PRESSURE	PEAK SQUIB PRESSURE	FIRST BOOSTER PRESSURE	BOOSTER MAX. PRESSURE	MAIN CHARGE IGNITION	MAX. PRESSURE	DURATION MILLISECONDS	SQUIB PSIA	BOOSTER PSIA		MAIN CHARGE PSIA
14	80	ALT	2	13	15	18	25	31	38	54	1290	4700	7100	Vibrated From 40 to 4,000 CPS to 10 g's Before Firing Vibrated From 40 to 4,000 CPS to 10 g's before Firing One Squib Poorest Environmental Conditions for Ignition Best Environmental Conditions For Ignition One Squib Fired on Motor LJ-1 4-4-63 Fired on Motor LJ-4 5-6-63 Fired on Motor LJ-7 8-1-63
15	80	ALT	2	13	15	16	22	29	35	49	1510	4800	7100	
16	80	ALT	2	12	15	18	22	28	33	48	1670	4330	5960	
17	80	ALT	2	13	14	17	22	28	36	49	1400	4660	5970	
18	80	SL	2	12	14	15	20	26	35	49	1150	4560	7100	
23	80	ALT	2	13	14	15	21	26	32	47	2070	4590	7120	
24	80	ALT	2	12	14	17	22	31	38	52	1070	4060	7380	
25	80	SL	2	11	13	18	22	26	32	47	1070	4530	7150	
26	80	SL	2	12	13	17	22	26	31	46	1430	4390	7420	
27	80	SL	2	11	14	18	23	27	32	49	890	4550	7150	
28	100	ALT	2	11	14	16	21	32	38	53	1000	4200	7140	
29	80	ALT	2	13	15	17	21	28	35	47	1370	4290	7590	
30	80	ALT	2	11	14	17	21	26	32	46	610	4450	6850	
31	80	ALT	2	12	14	16	21	26	32	46	1340	4450	7150	
32	80	ALT	1	12	13	17	22	27	33	47	1360	4400	7100	
33	40	ALT	2	10	14	17	21	25	31	45	1360	4200	7180	
34	100	SL	2	10	13	15	20	24	30	43	1310	4150	7400	
35	40	SL	1	11	13	21	25	30	36	51	470	4160	6850	
HIGH	100	-	-	13	15	21	25	32	38	54	2070	4800	7590	
LOW	40	-	-	10	13	15	20	24	30	43	470	4060	5960	
AVERAGE	-	-	-	11.8	13.9	16.9	21.8	27.6	33.7	48.2	1220	4420	6960	
10	70	SL	2	14	16	18	24	28	34	47	1870	4400	6850	
22	70	ALT	2	12	15	18	22	27	34	52	1640	4260	7960	
21	78	ALT	2	11	15	18	25	30	39	53	1190	4350	7180	

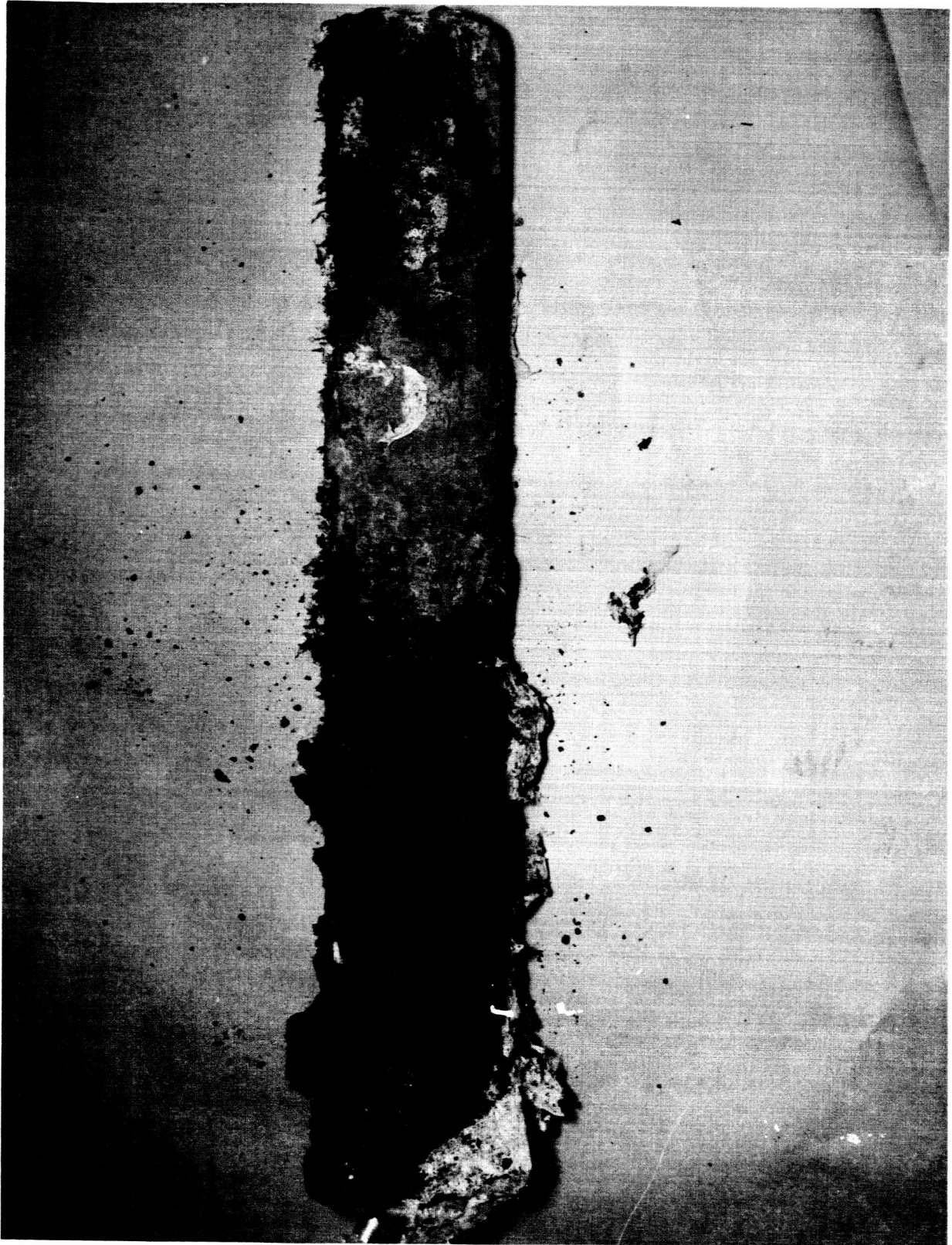
Igniter Qualification-Test Results

Figure 33

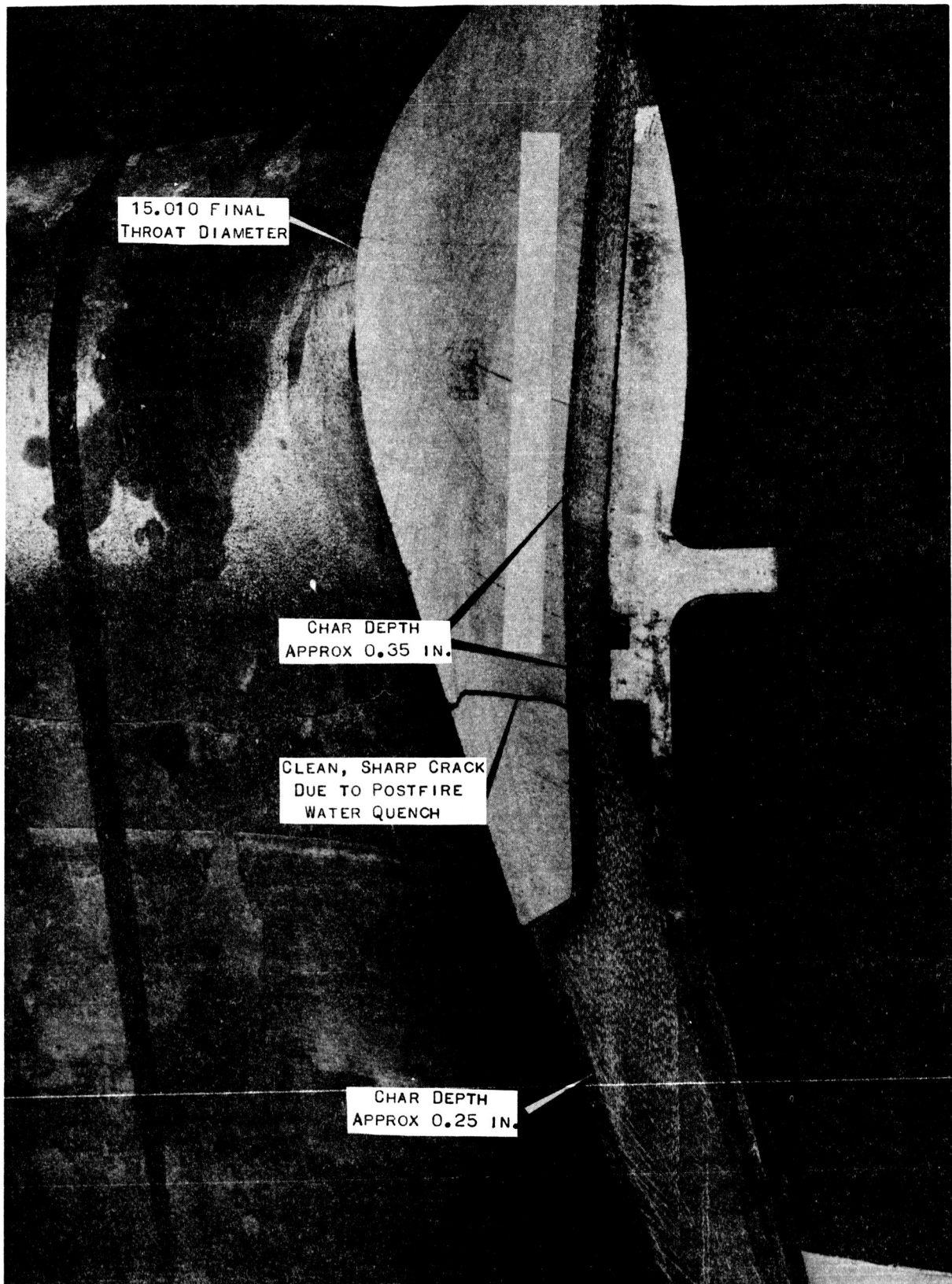


Motor LJ-4 Ignition-Performance Data

Figure 34

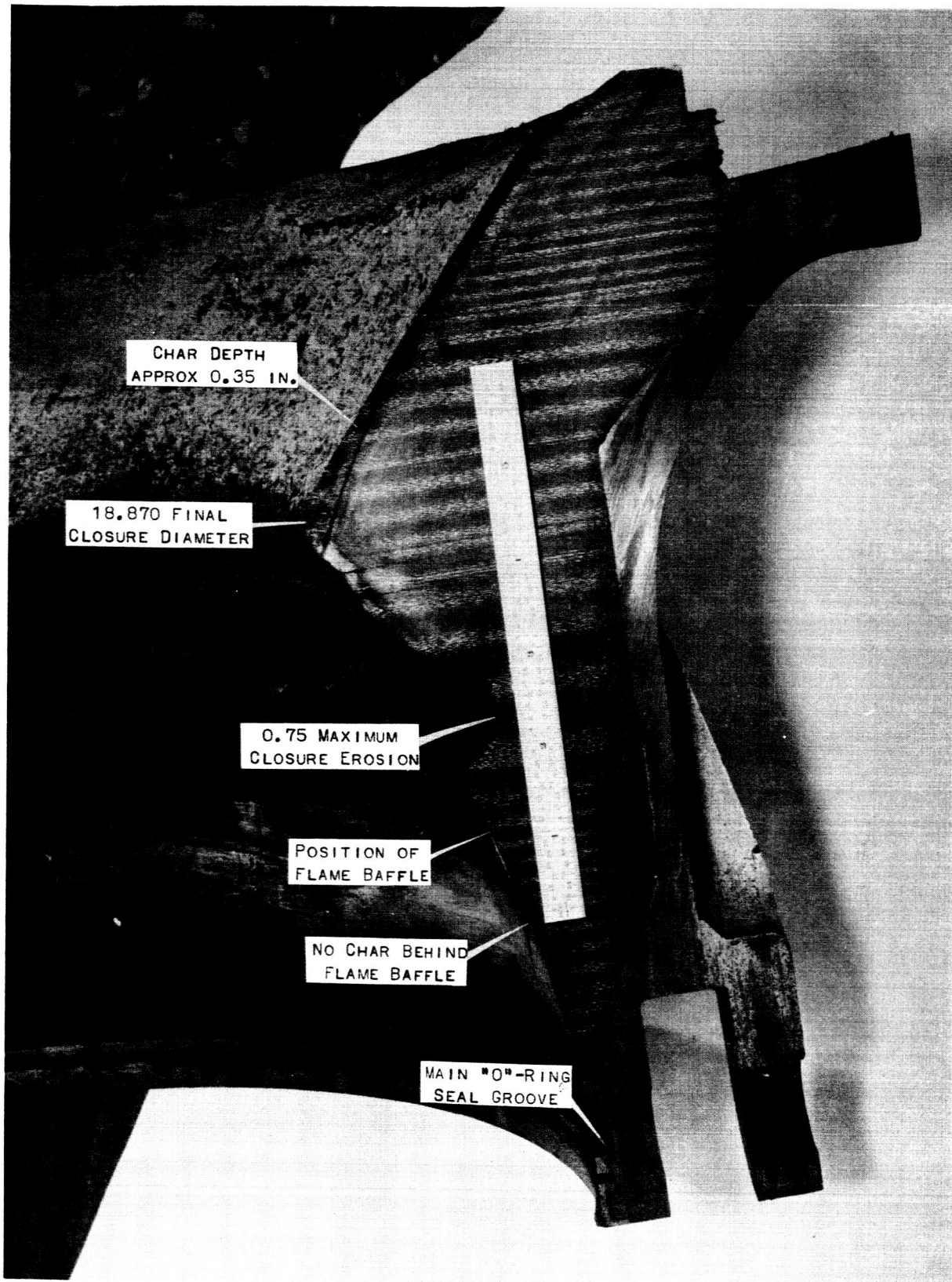


Postfiring View, Motor LJ-4 Igniter (Photo 4-63 SP 6921)



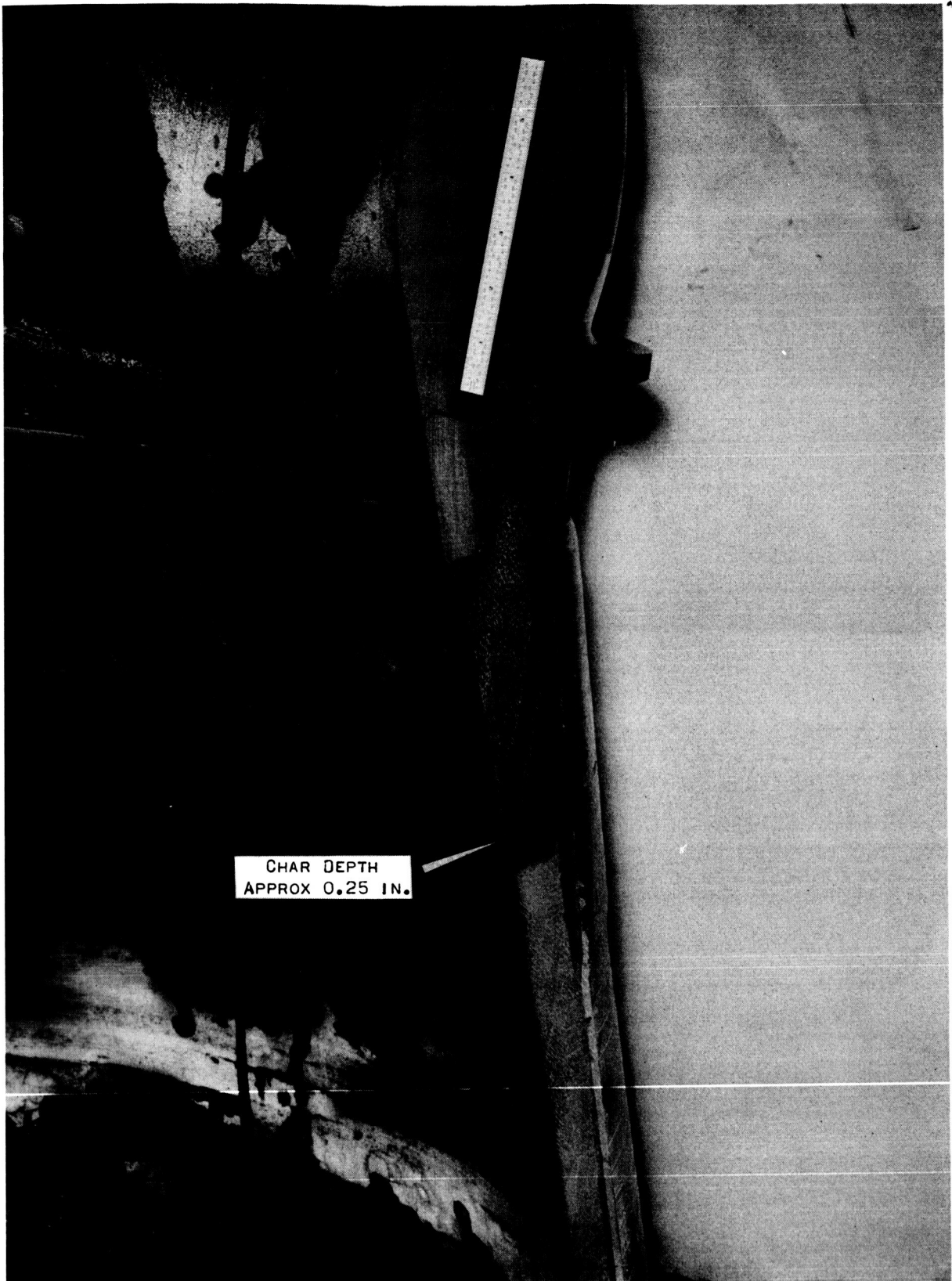
Postfiring View of Nozzle Throat Section, Motor LJ-1 (Photo 5-63S 08762)

Figure 36



Postfiring View of Aft-Closure Section, Motor LJ-1 (Photo 5-63S 08758)

Figure 37



Postfiring View of Nozzle Exit-Cone Section, Motor LJ-1 (Photo 5-63S 08757)

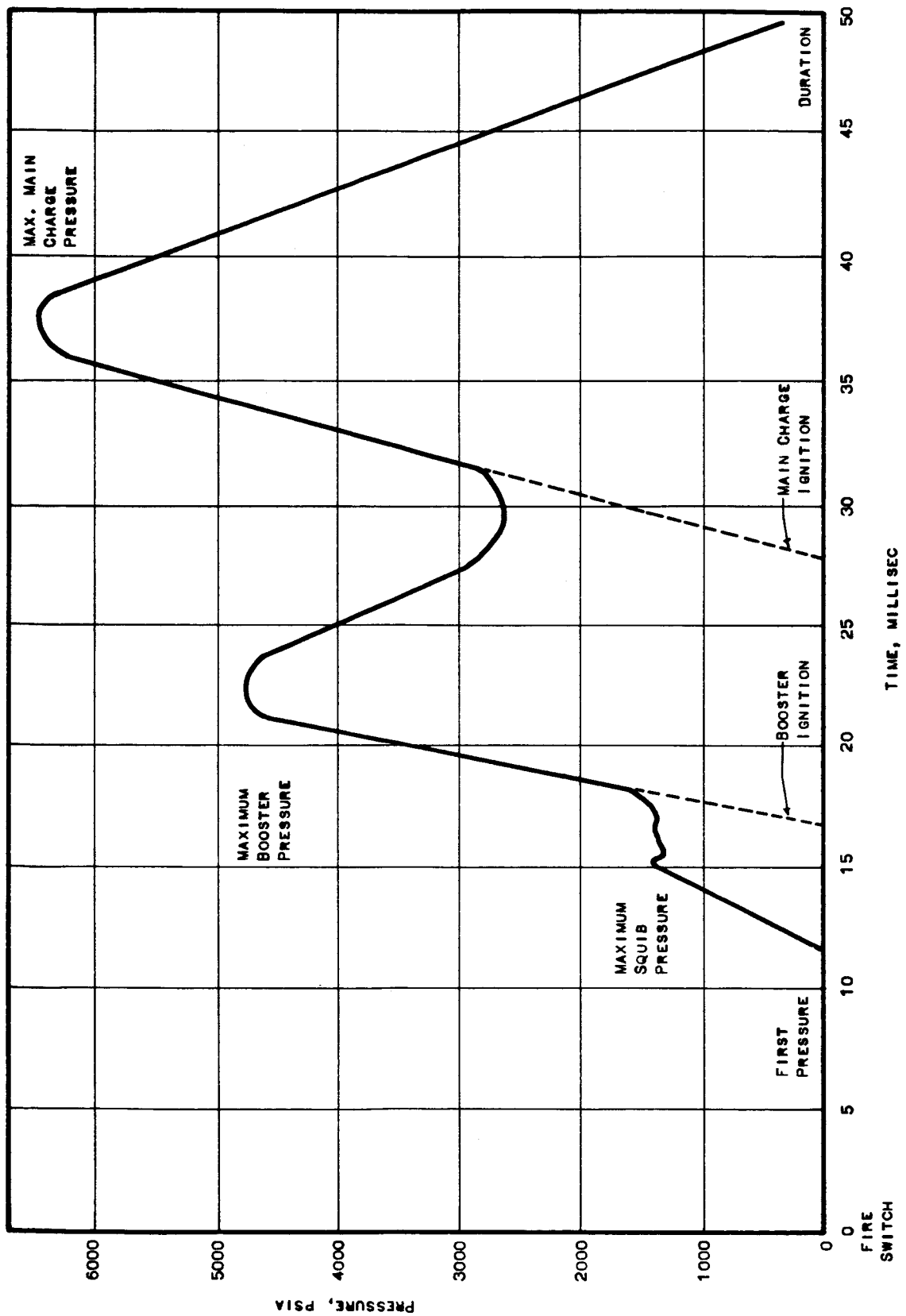
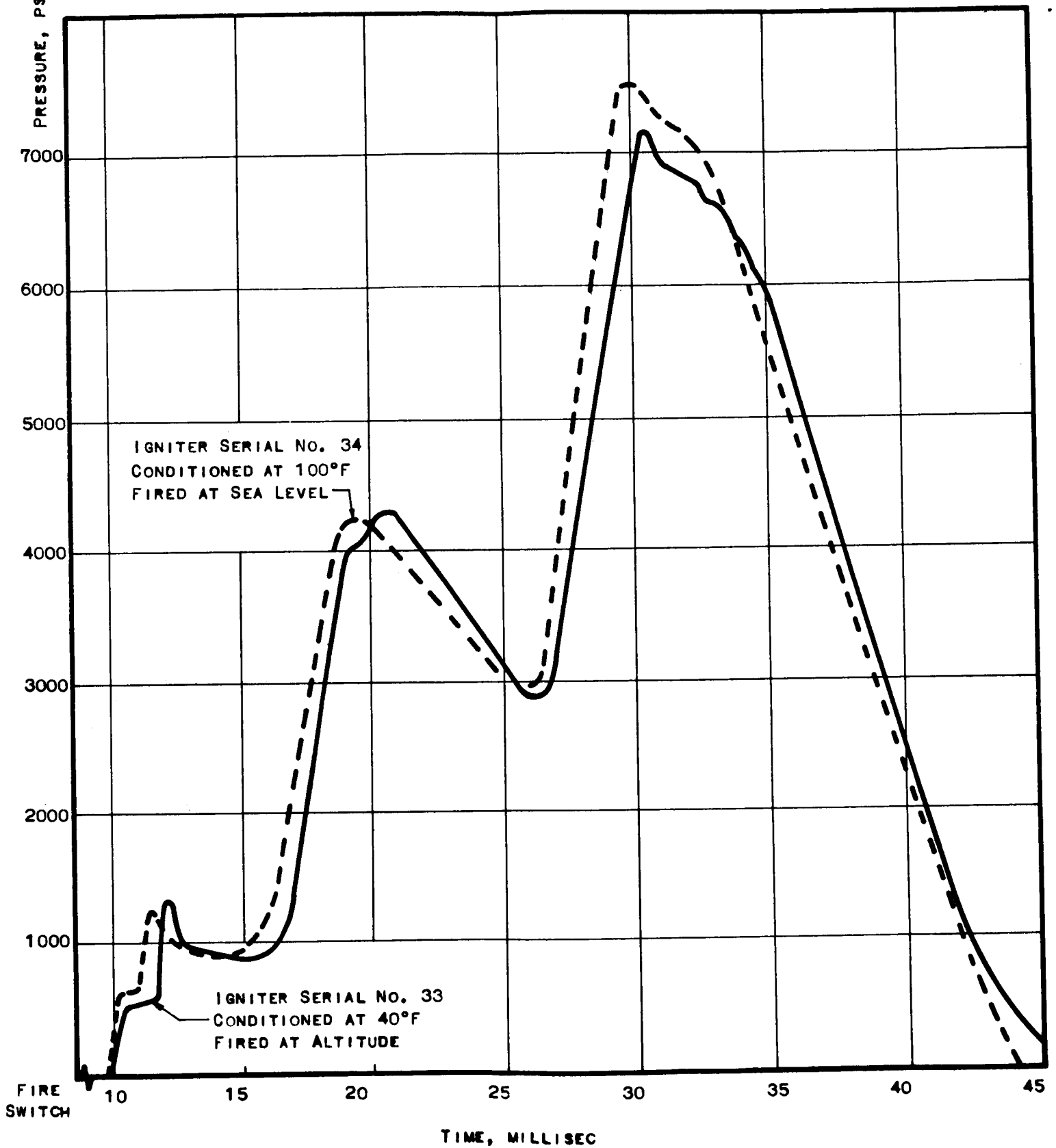


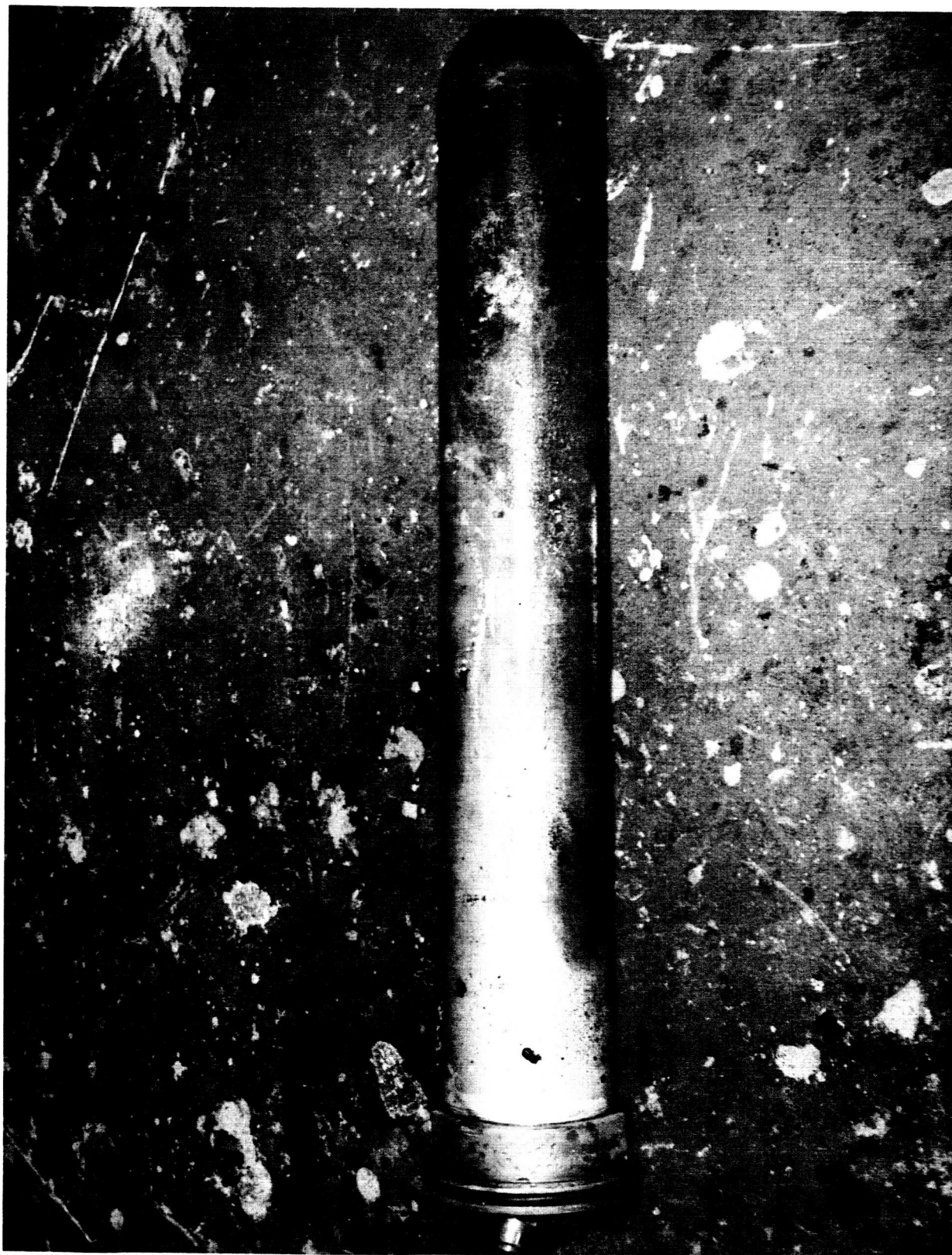
Figure 39

Sequence of Igniter Performance



Igniter Performance After Exposure to Extremes of Environmental Conditioning

Figure 40



Postfiring View of Altitude Igniter (Photo 6-63 SP 7502)

Figure 41

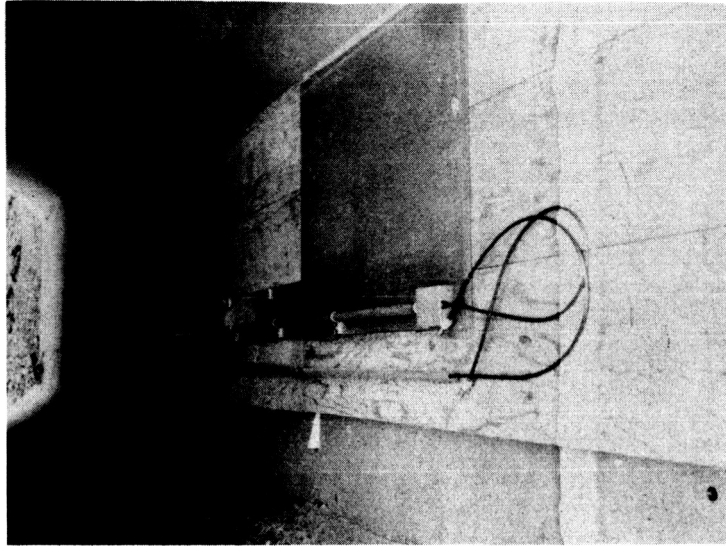


Figure 42. Destruct-Unit Test Assembly

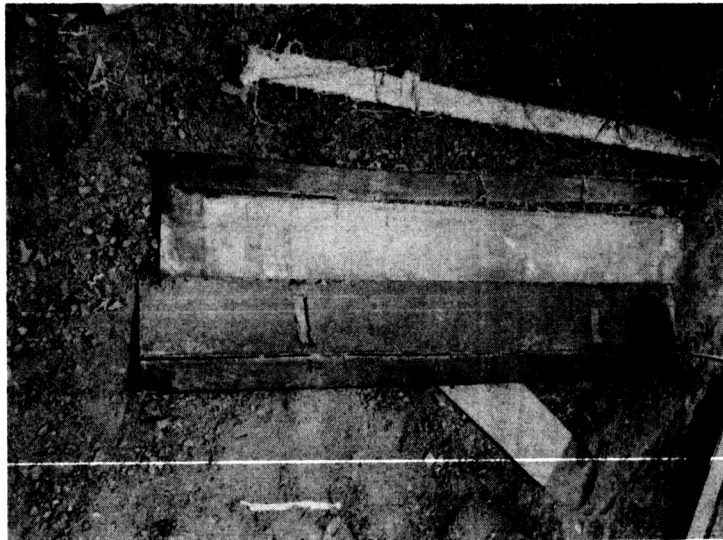
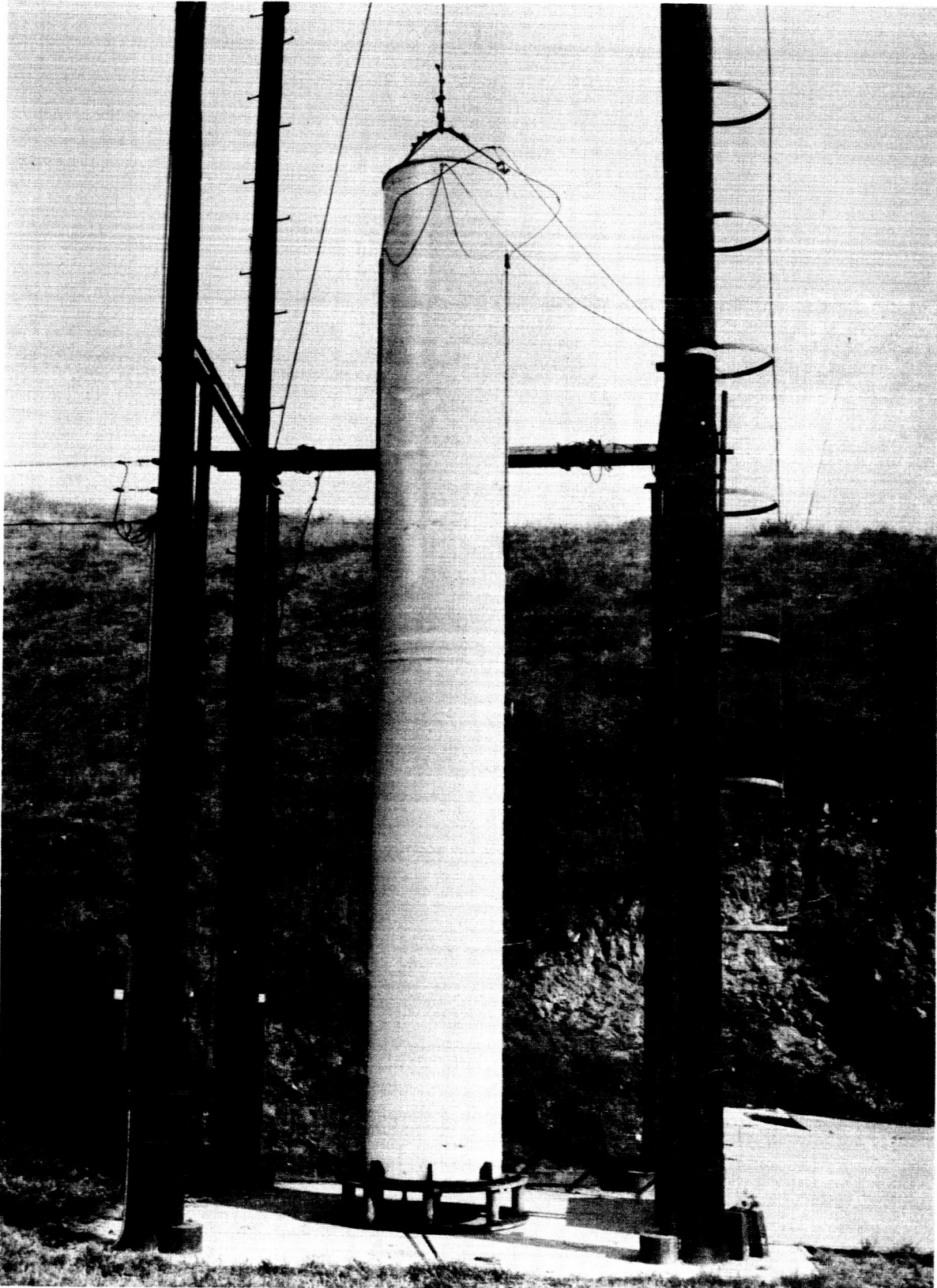
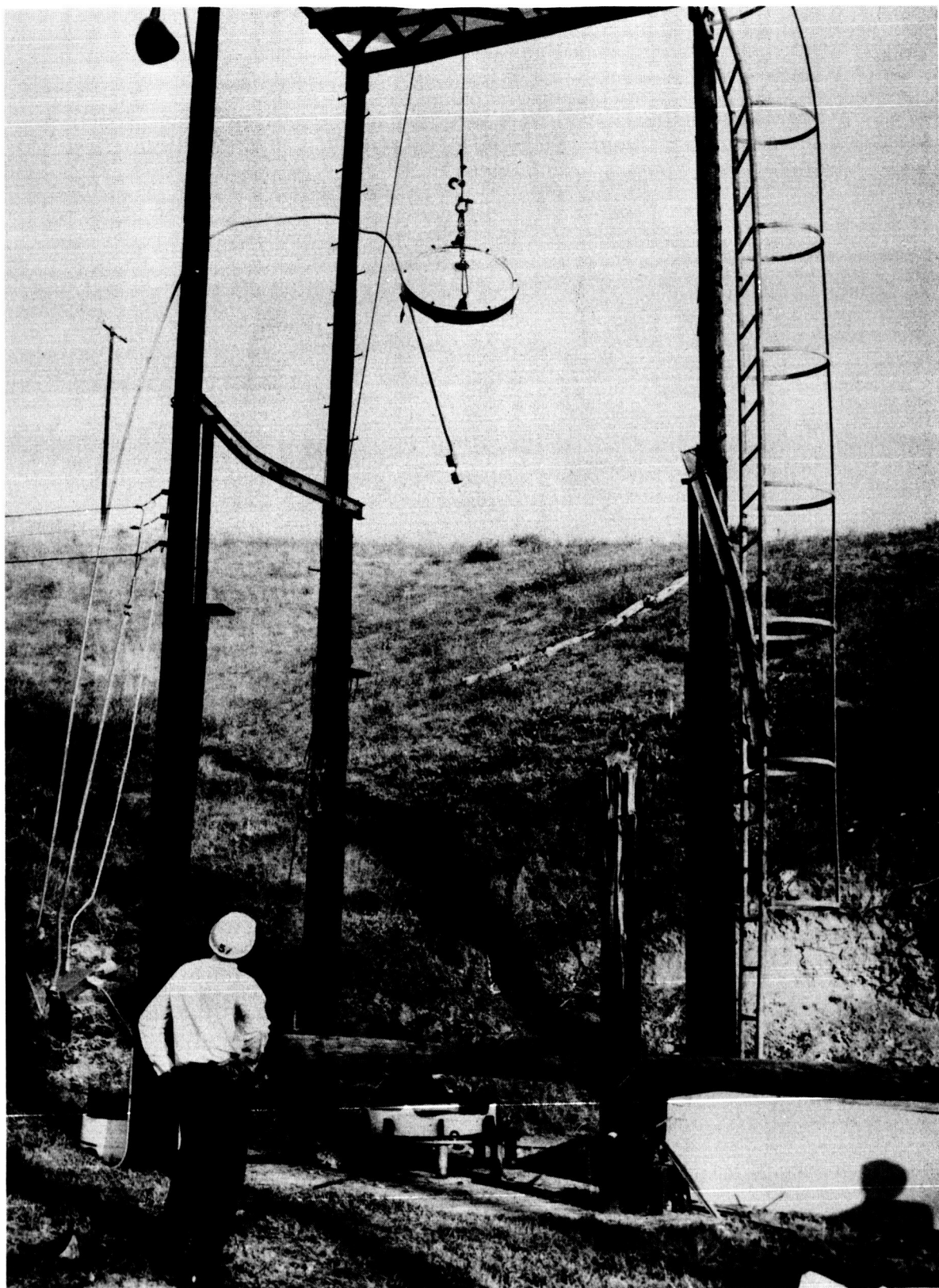


Figure 43. Witness Plates Cut During Destruct Test



Prefiring View of Motor Destruct-Test Setup (Photo 7-63 SP 708)

Figure 44



Postfiring View of Test Stand (Photo 7-63 SP 707)

Figure 45

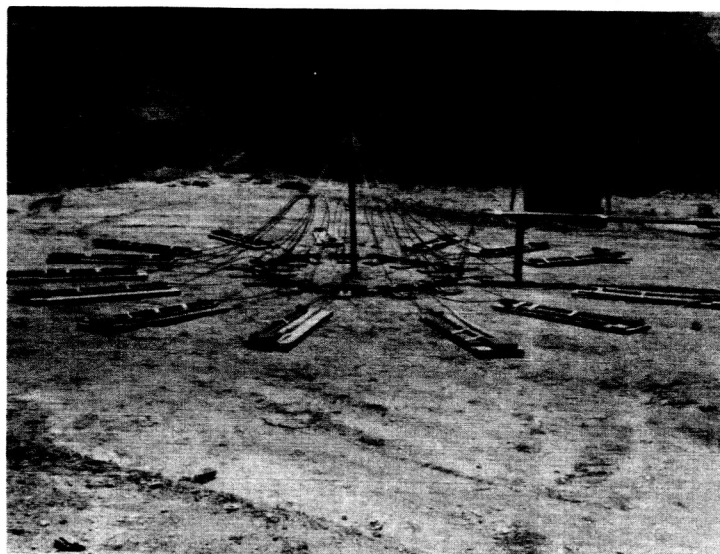


Figure 46. Primacord Harness Assembly and Test Plates,
Seven-Motor-Configuration Destruct Test

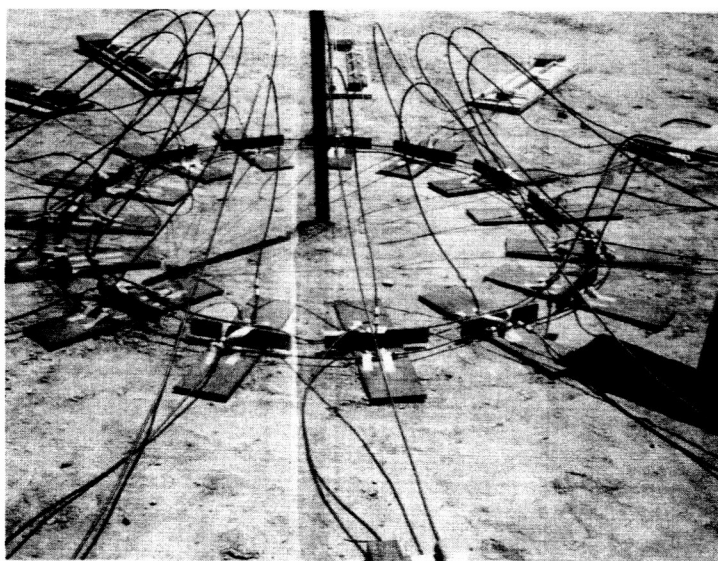
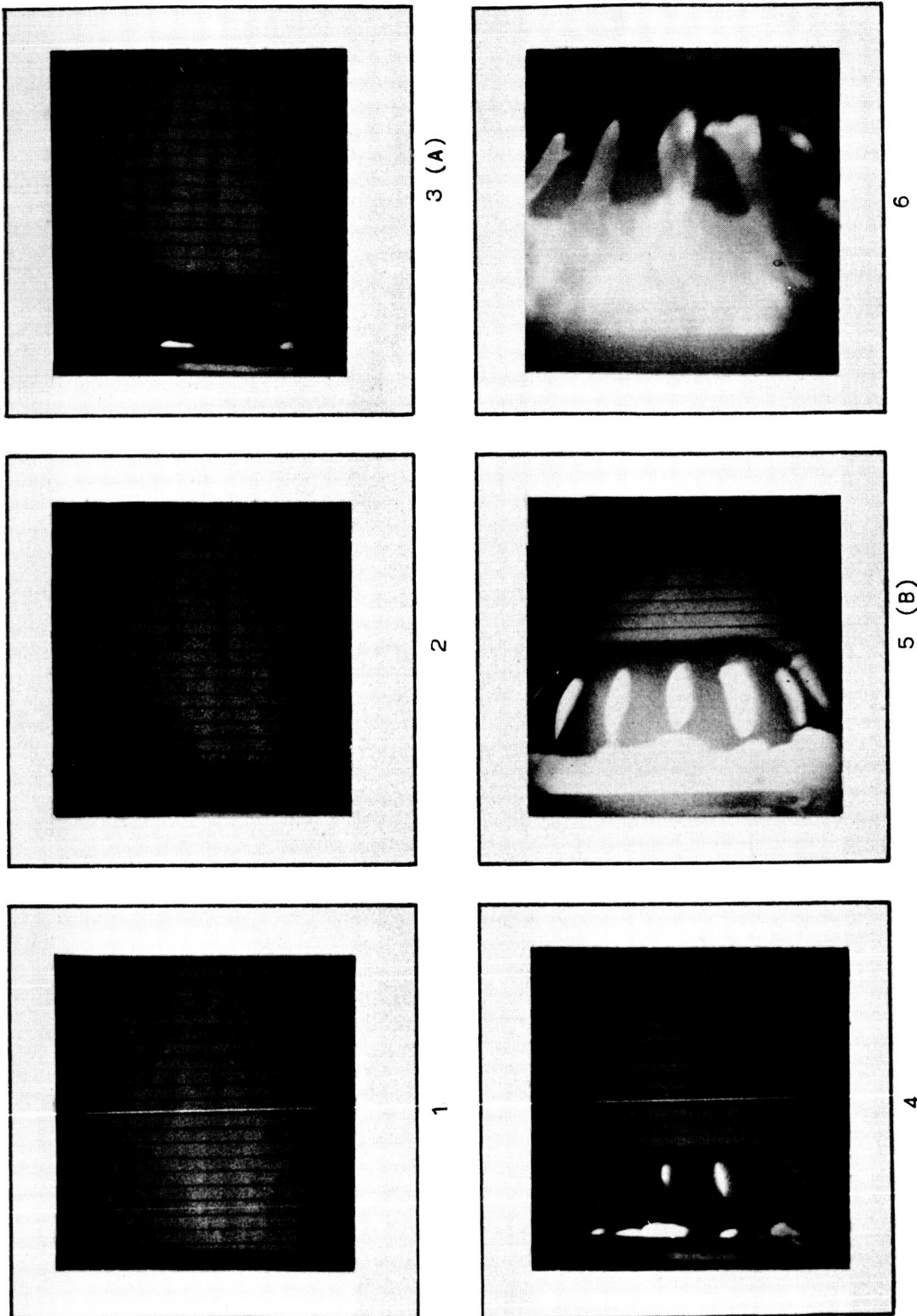


Figure 47. Close-Up of Seven-Motor-Configuration Test

Figure 46 and Figure 47



(A) FIRST APPEARANCE OF FLAME AT 0.015 SEC
 (B) COMPLETE SEPARATION OF SEAL AT 0.025 SEC

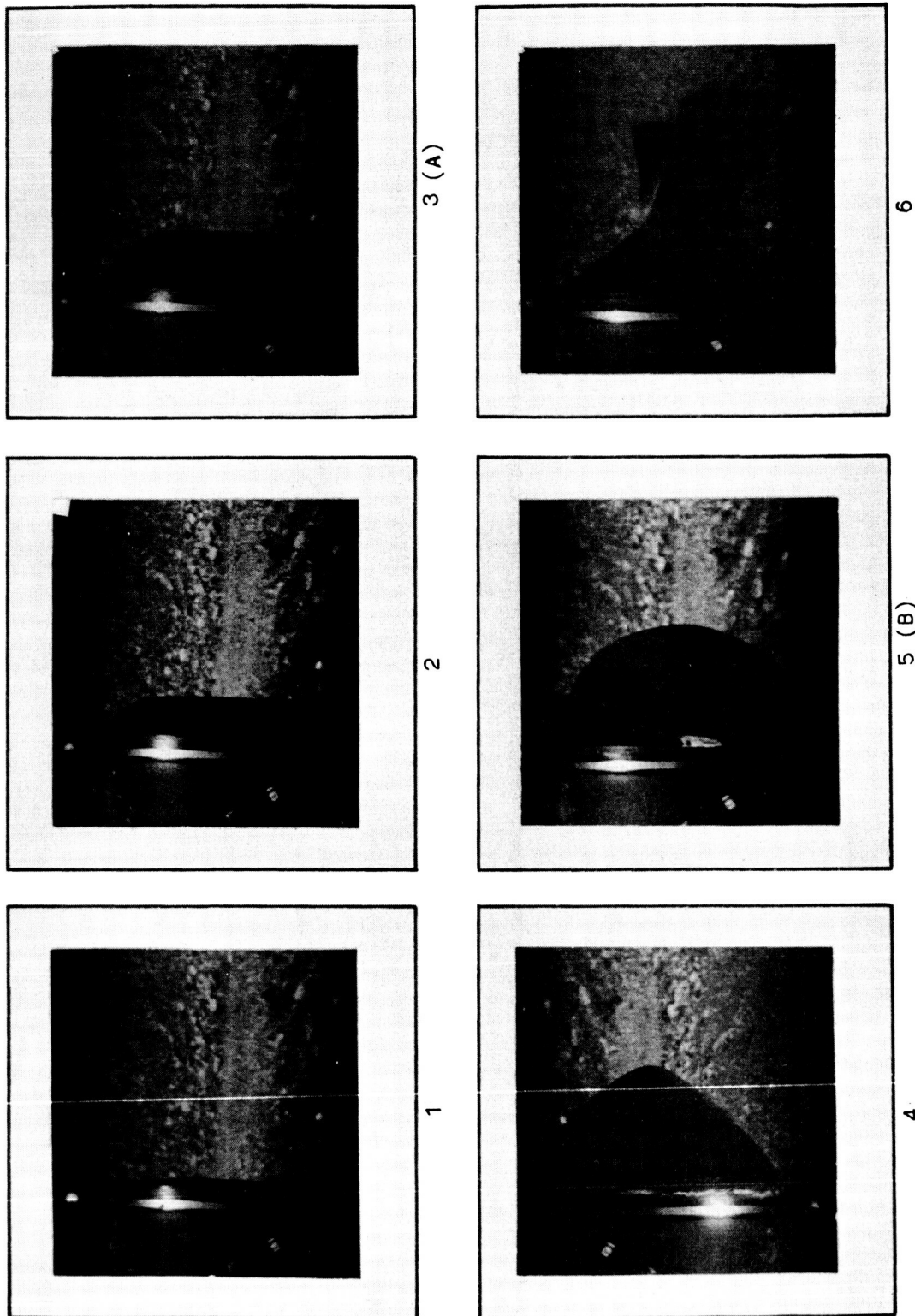
Excerpts From Film of Weather-Seal Break Test,
 Full Igniter Charge Pressurization

Figure 48



Weather Seal Broken by Igniter Charge (Photo 4-63 S 07882)

Figure 49



(A) SEAL AT 0.020 SEC
(B) FAILURE AT 0.030 SEC

Excerpts From Film of Weather-Seal Break Test,
Igniter Booster-Charge Pressurization

Figure 50

MOTOR SERIAL NO.		LITTLE JOE II MOTOR FABRICATION - PROCESSING SCHEDULE																			
MOTOR NO.	SERIAL NO.	MATERIALS		WELDING		WELDING		WELDING		WELDING		WELDING		WELDING		WELDING		WELDING		WELDING	
		WELDING	WELDING	WELDING	WELDING	WELDING	WELDING	WELDING	WELDING	WELDING	WELDING	WELDING	WELDING	WELDING	WELDING	WELDING	WELDING	WELDING	WELDING	WELDING	WELDING
LJ-1	806659	10.00	10.00	10.00	10.00	10.00	10.00	10.00	10.00	10.00	10.00	10.00	10.00	10.00	10.00	10.00	10.00	10.00	10.00	10.00	10.00
LJ-2	806660	10.00	10.00	10.00	10.00	10.00	10.00	10.00	10.00	10.00	10.00	10.00	10.00	10.00	10.00	10.00	10.00	10.00	10.00	10.00	10.00
LJ-3	806661	10.00	10.00	10.00	10.00	10.00	10.00	10.00	10.00	10.00	10.00	10.00	10.00	10.00	10.00	10.00	10.00	10.00	10.00	10.00	10.00
LJ-4	806663	10.00	10.00	10.00	10.00	10.00	10.00	10.00	10.00	10.00	10.00	10.00	10.00	10.00	10.00	10.00	10.00	10.00	10.00	10.00	10.00
LJ-5	806662	10.00	10.00	10.00	10.00	10.00	10.00	10.00	10.00	10.00	10.00	10.00	10.00	10.00	10.00	10.00	10.00	10.00	10.00	10.00	10.00
LJ-6	806665	10.00	10.00	10.00	10.00	10.00	10.00	10.00	10.00	10.00	10.00	10.00	10.00	10.00	10.00	10.00	10.00	10.00	10.00	10.00	10.00
LJ-7	806664	10.00	10.00	10.00	10.00	10.00	10.00	10.00	10.00	10.00	10.00	10.00	10.00	10.00	10.00	10.00	10.00	10.00	10.00	10.00	10.00
LJ-6A	806665	10.00	10.00	10.00	10.00	10.00	10.00	10.00	10.00	10.00	10.00	10.00	10.00	10.00	10.00	10.00	10.00	10.00	10.00	10.00	10.00

Figure 51

Little Joe II Motor Fabrication and Processing Schedule (Photo 9-63 SP 1711)

ALGOL ID MOD I MOTORS

	<u>Empty, lb</u>	<u>Propellant, lb</u>	<u>Nozzle, lb</u>	<u>Total, lb</u>
<u>DESIGN</u>	2098	19,000	802	22,000
LJ-1	2053	18,972	782	21,836 (A)
LJ-4	2045	18,933	776	21,740 (A)
LJ-7	2040	18,919	776	21,870 (B)
AVERAGE (3)	2046	18,941	778	21,815
STD. DEV.	6	27	4	-

ALGOL ID MOD 2 MOTORS

	<u>Empty, lb</u>	<u>Propellant, lb</u>	<u>Nozzle, lb</u>	<u>Total, lb</u>
<u>DESIGN</u>	2098	19,000	1005	22,152
LJ-2	2052	18,963	1038	22,046 (A)
LJ-3	2046	18,971	1031	22,052 (A)
LJ-5	2045	18,960	1025	22,062 (A)
LJ-6A	2119	18,918	1036	22,088 (A)
AVERAGE (4)	2065	18,953	1032	22,062
STD. DEV.	32	24	6	19

(A) Incomplete motor - less igniter and destruct unit

(B) Complete motor

Little Joe II Motor Weight Summary

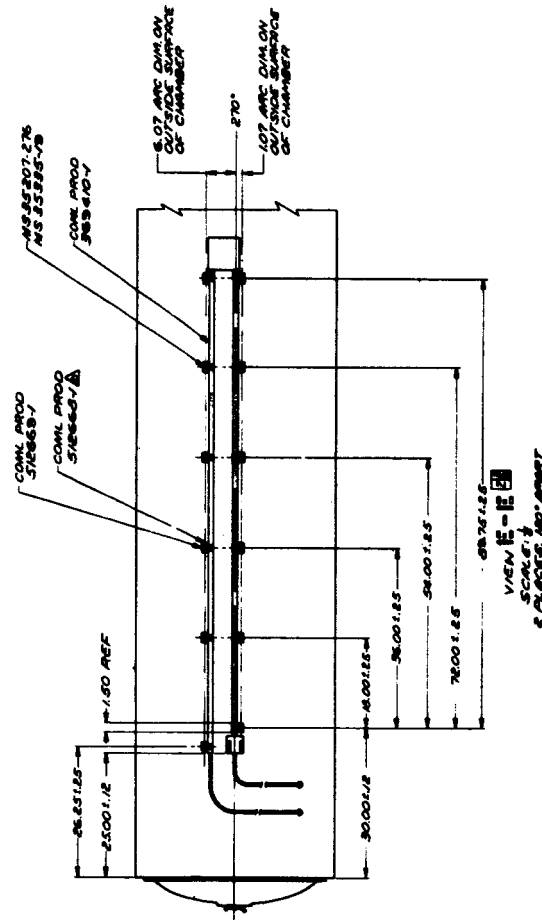
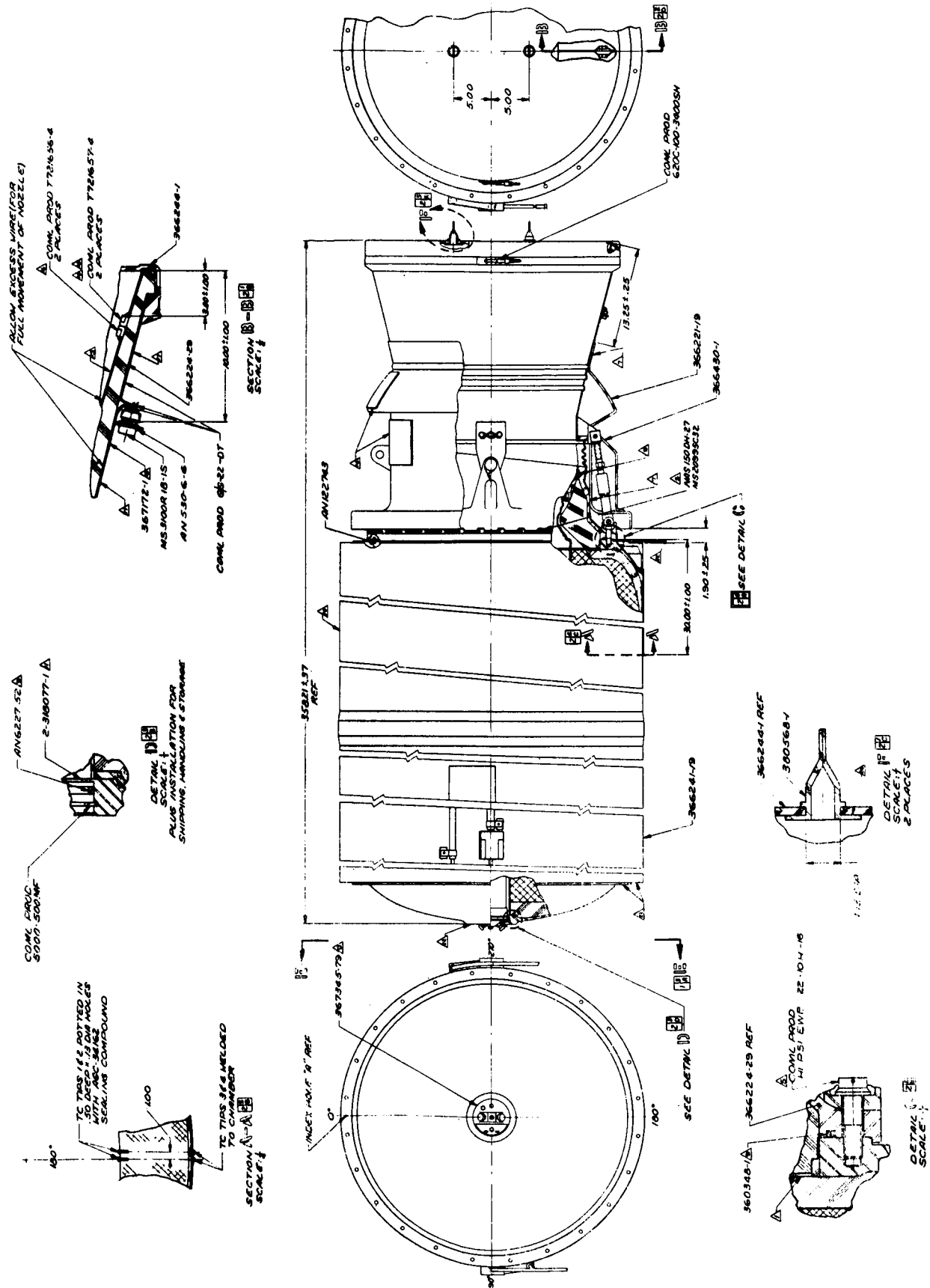
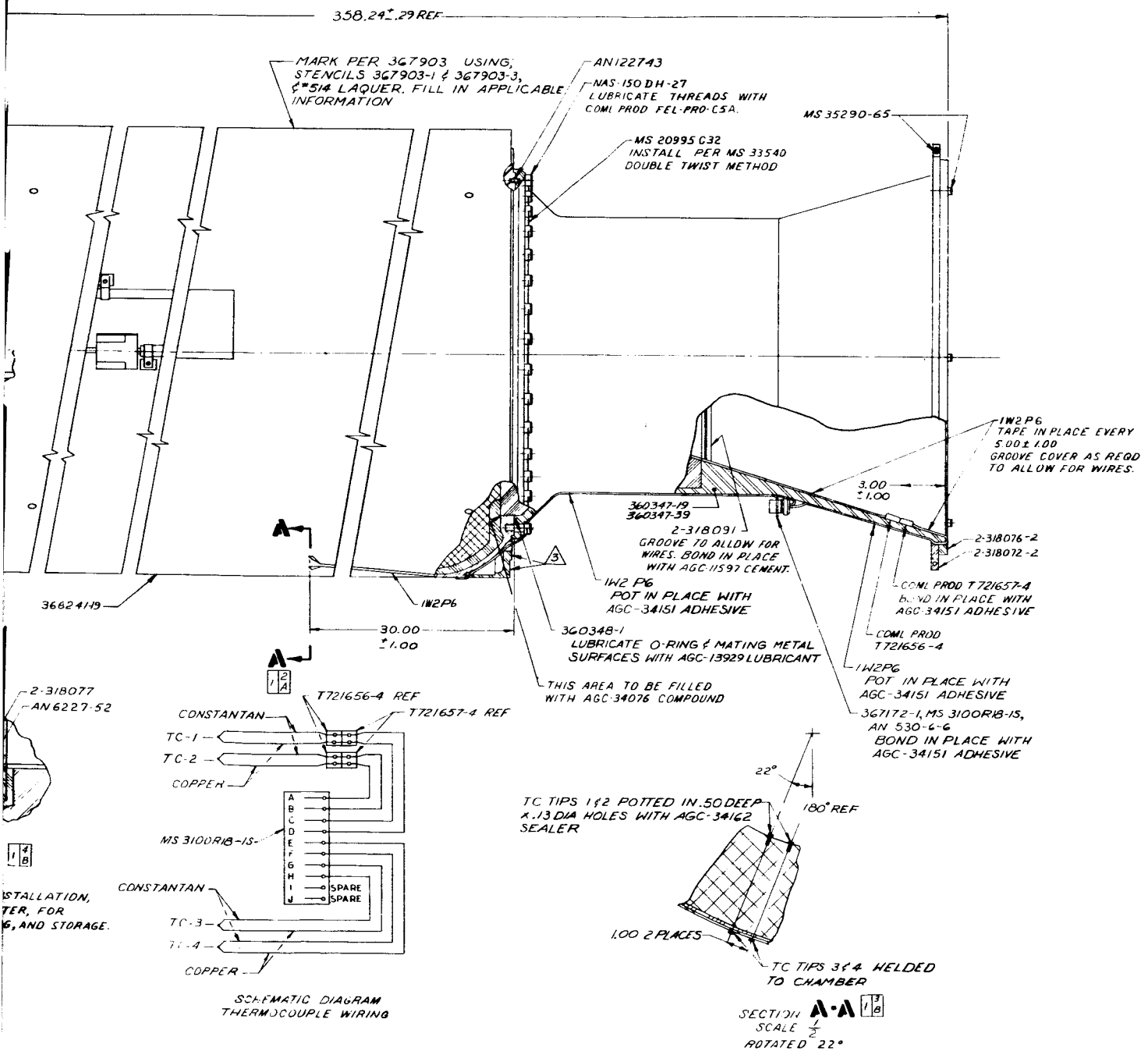


Figure 53, Sheet 1 of 2



Algol ID Mod 1 Motor Assembly

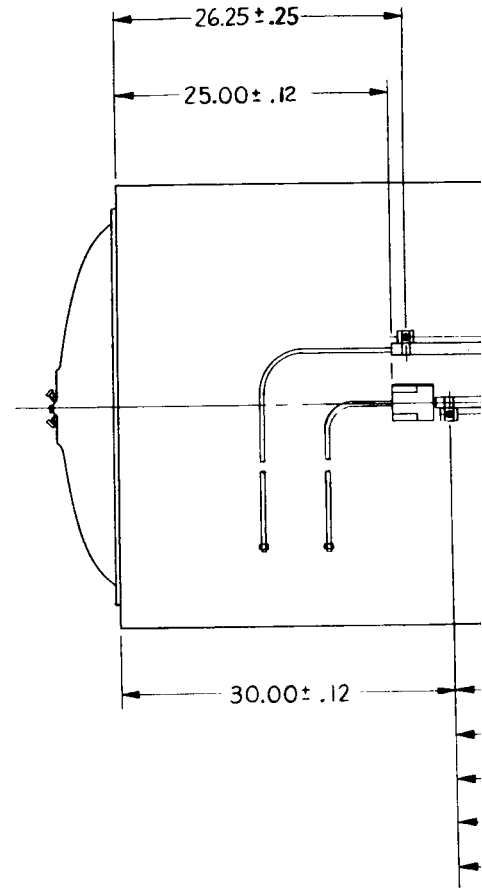
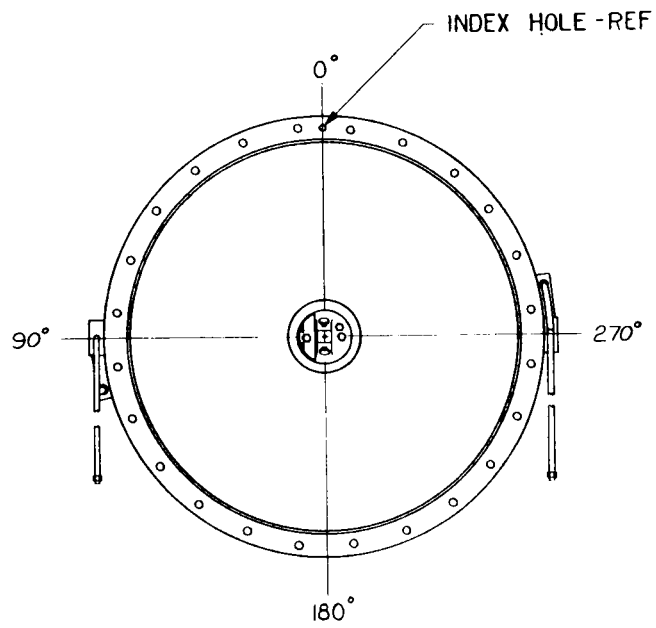


Algol ID Mod 2 Motor Assembly

Figure 54, Sheet 1 of 2

54 (1)

(2)

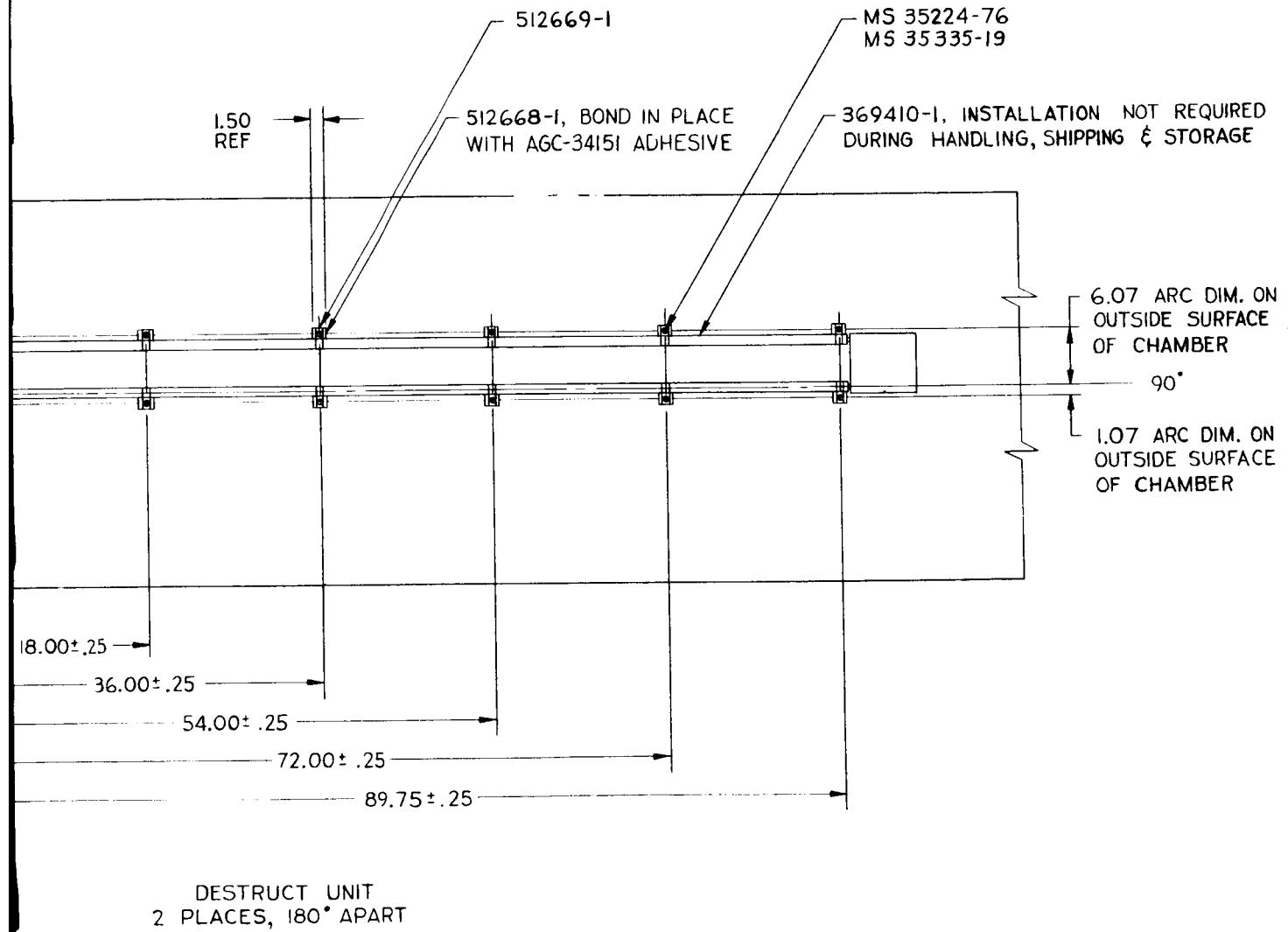


VIEW **C-C** 1 4
C

SCALE $\frac{1}{8}$

54B

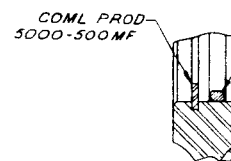
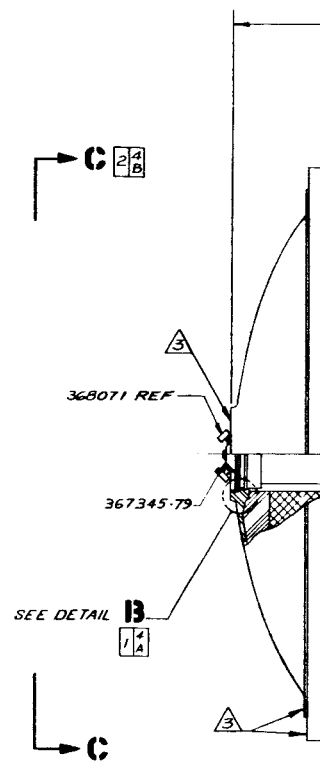
①



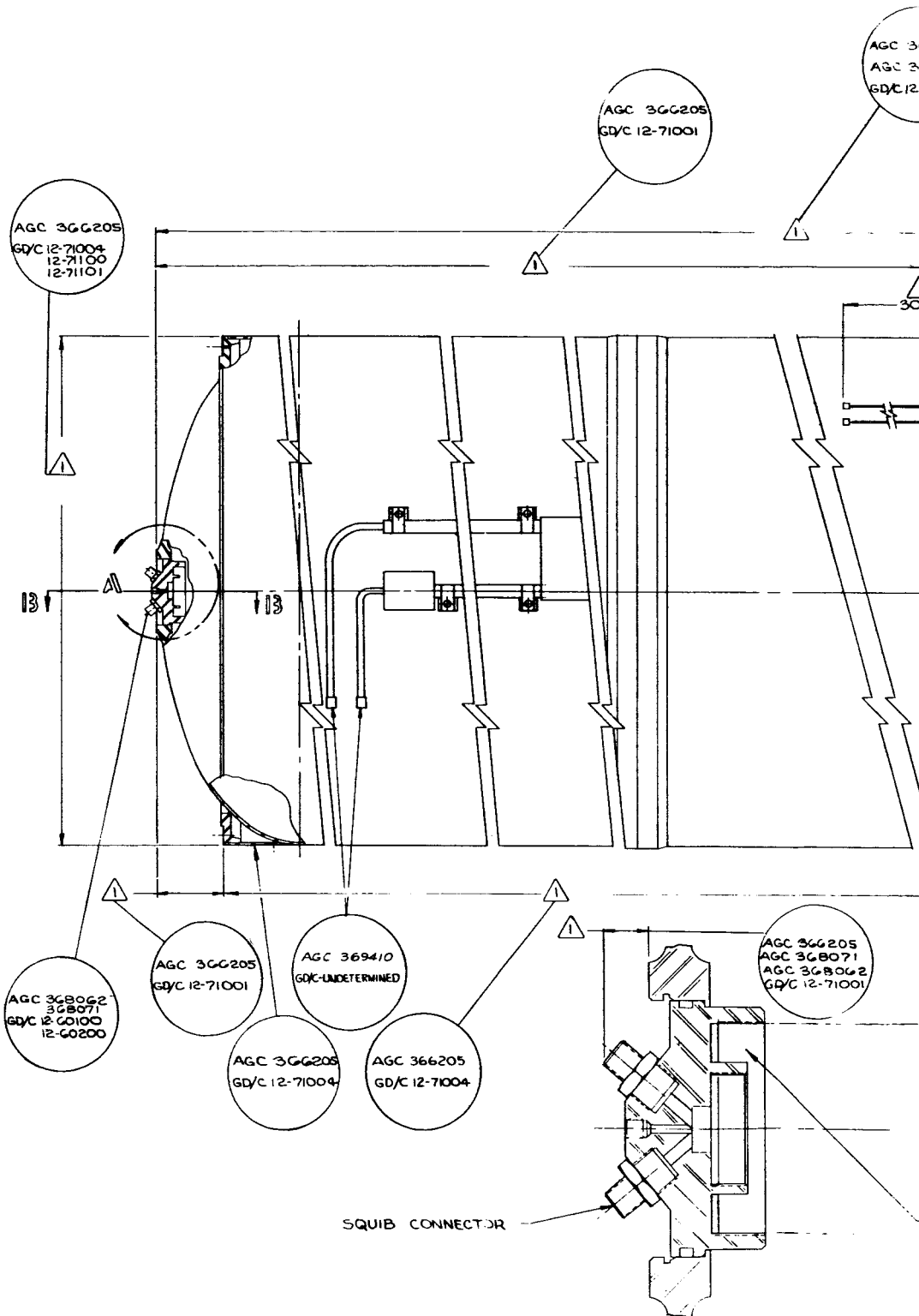
Algol ID Mod 2 Motor Assembly

Figure 54, Sheet 2 of 2

2

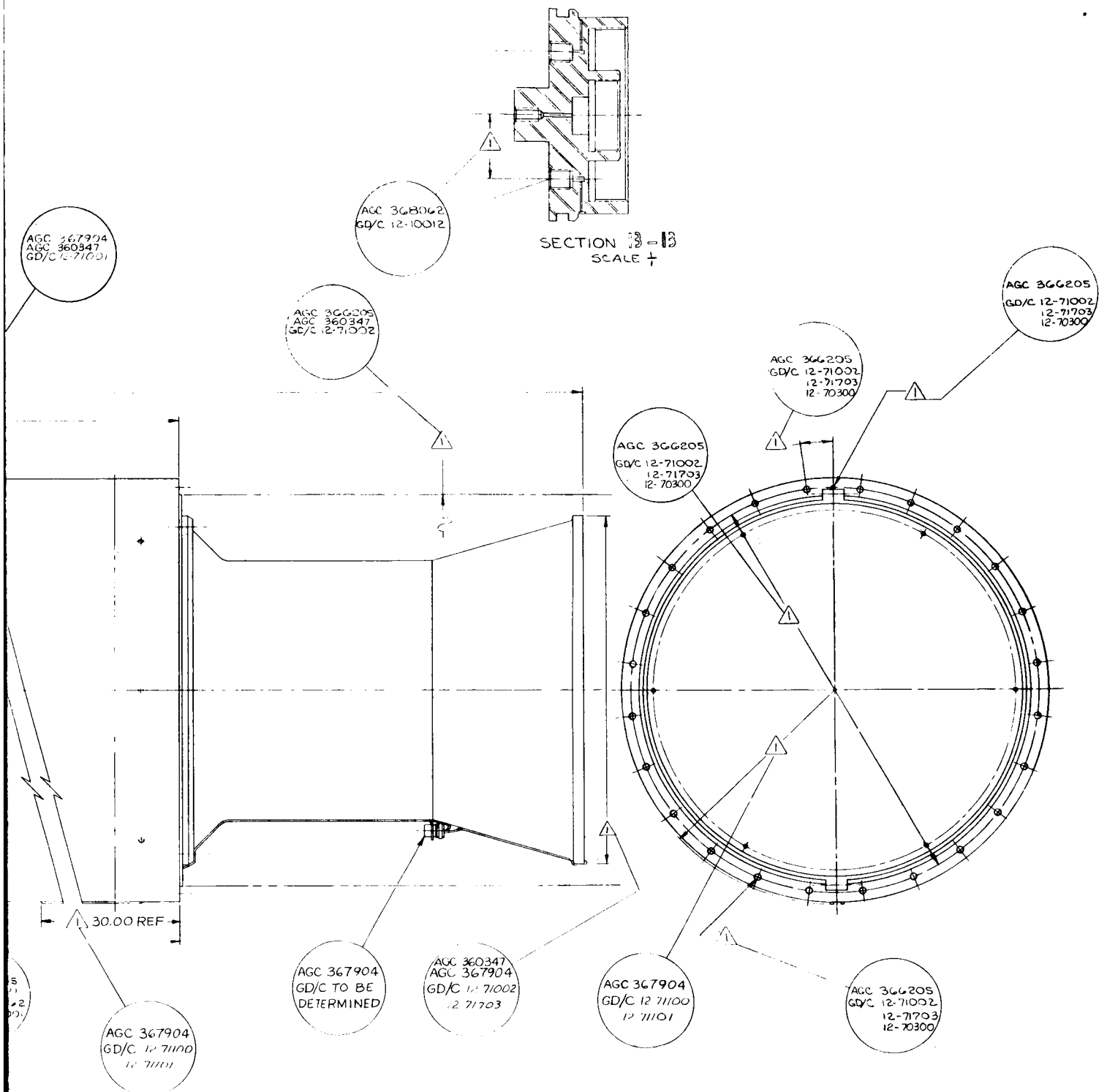


DETAIL B
SCALE 1/1
SHOWING PLUG-IN
IN PLACE OF IGNITION
SHIPPING, HANDLING



55 (1)

DETAIL
SCALE 1

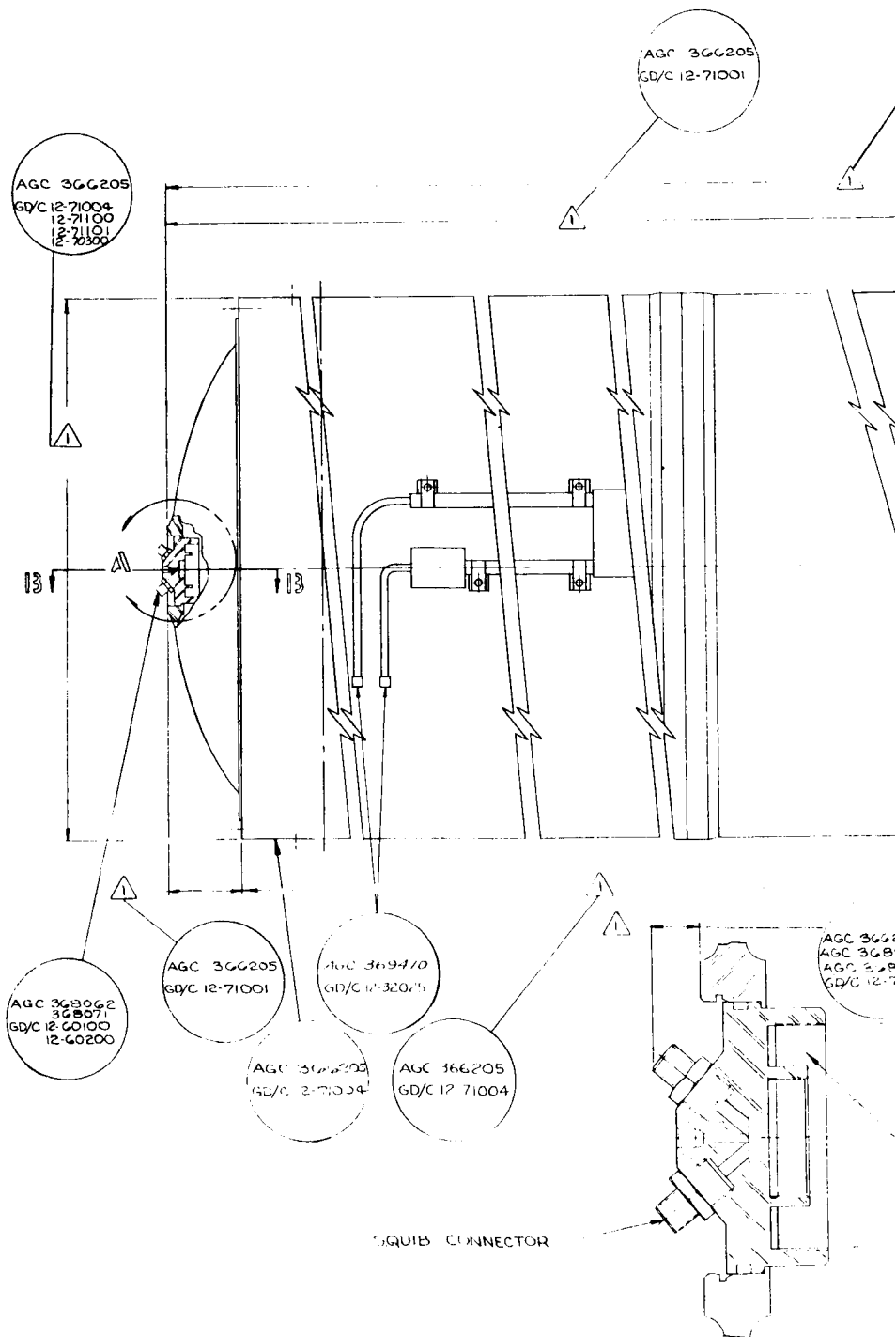


FOR IGNITER SEE AGC 367345

Algol ID Mod 2 Motor Envelope

2

Figure 56



56①

DETAIL
SCALE 1/2"



FOR IGNITER SEE AGC 367345

Algo1 ID Mod 1 Motor Envelope

Figure 55

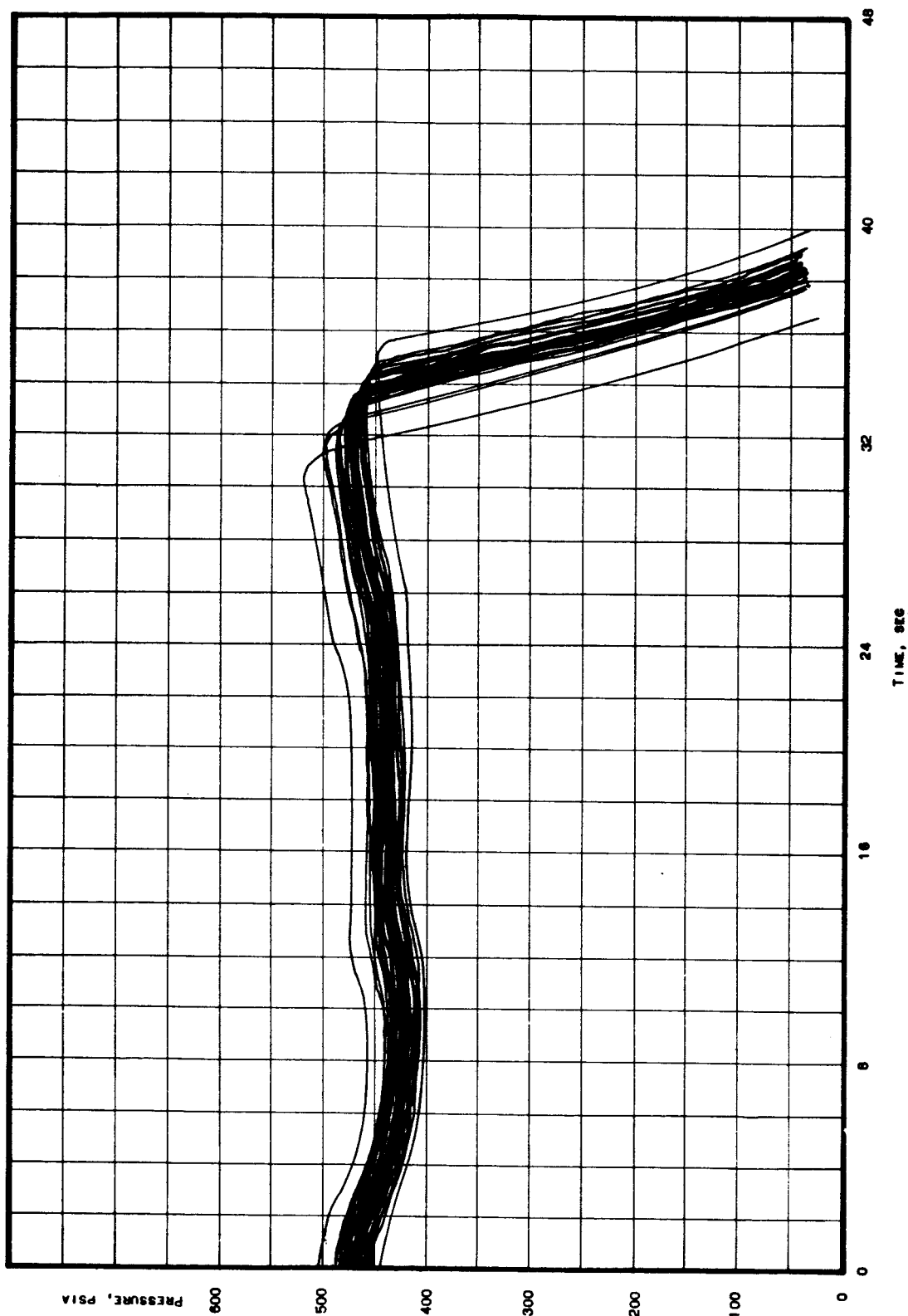
2

<u>DENSITY</u>	<u>MASS FLOW COEFFICIENT</u>	<u>THROAT AREA</u>	<u>BURNING RATE CONSTANT</u>
.060356	.006399	175.328707	.085771
.060327	.006778	175.329025	.086550
.060432	.006628	175.330120	.086550
.060337	.006601	175.328747	.085358
.060428	.006602	175.328547	.085814
.060291	.006624	175.329533	.084874
.060329	.006478	175.332729	.086176
.060199	.006634	175.328318	.086205
.060302	.006412	175.330387	.083014
.060461	.006501	175.327848	.083207
.060387	.006676	175.328468	.084089
.060382	.006671	175.330788	.084030
.060307	.006442	175.329216	.084591
.060450	.006532	175.329241	.083345
.060311	.006633	175.329203	.085858
.060381	.006615	175.329729	.086774
.060458	.006553	175.330301	.083556
.060313	.006700	175.330942	.085390
.060315	.006635	175.329538	.084021
.060416	.006475	175.331779	.084238
.060382	.006518	175.329285	.081067
.060379	.006604	175.329765	.085420
.060327	.006410	175.331118	.086863
.060261	.006609	175.329632	.084848
.060412	.006340	175.328838	.082332
.060299	.006504	175.330025	.085311
.060297	.006522	175.329548	.084049
.060363	.006603	175.330450	.085954
.060329	.006570	175.329729	.083883
.060442	.006486	175.330936	.083724
.060378	.006533	175.330013	.090474
.060342	.006615	175.330322	.086149
.060272	.006661	175.329527	.085738
.060297	.006774	175.332142	.085061
.060336	.006644	175.328350	.083442
.060379	.006316	175.330259	.084765
.060286	.006457	175.330967	.086278
.060243	.006614	175.329714	.084587
.060375	.006565	175.329675	.084745
.060296	.006592	175.330452	.086885
.060455	.006614	175.330559	.082906
.060385	.006549	175.330912	.082623
.060312	.006556	175.328306	.083432
.060390	.006655	175.331236	.086699
.060304	.006732	175.330591	.085996
.060437	.006824	175.329765	.083670
.060345	.006598	175.329277	.085149
.060215	.006438	175.328472	.084686
.060385	.006866	175.329714	.085113
.060239	.006714	175.329575	.086687

Values for Characteristics Used in Computer Program

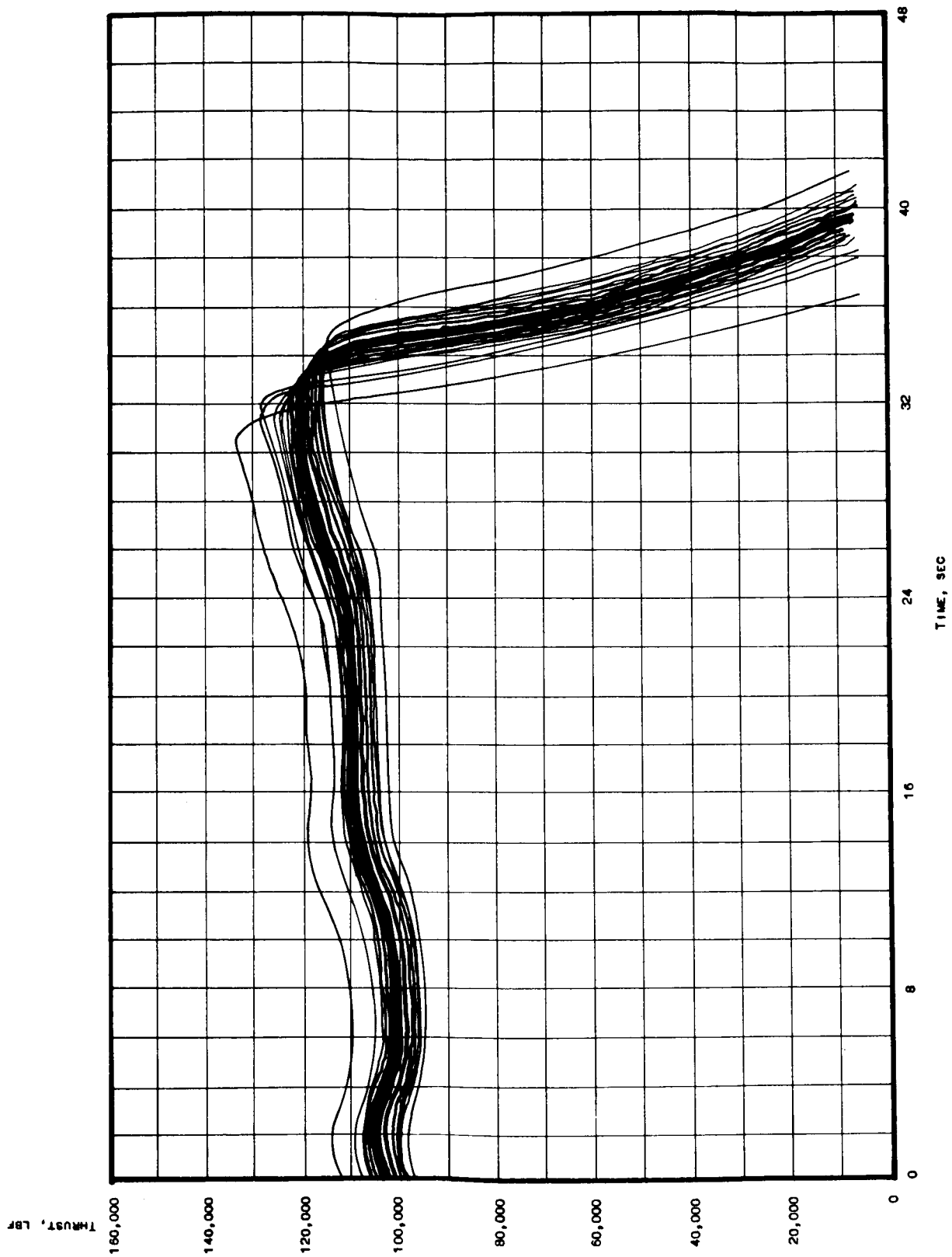
<u>DENSITY*</u>	<u>MASS FLOW COEFFICIENT</u>	<u>THROAT AREA</u>	<u>BURNING RATE CONSTANT</u>
.060396	.006681	175.329145	.085883
.060407	.006538	174.331003	.084336
.060259	.006744	175.330076	.085374
.060187	.006523	175.331028	.083196
.060395	.006693	175.330542	.085270
.060371	.006544	175.327299	.086287
.060237	.006762	175.329830	.082026
.060236	.006644	175.331028	.083929
.060323	.006615	175.331562	.084703
.060402	.006699	175.327579	.084924
.060310	.006662	175.329529	.084977
.060294	.006402	175.330971	.084307
.060308	.006439	175.328012	.085042
.060362	.006748	175.330723	.084111
.060403	.006678	175.329556	.085416
.060395	.006522	175.329481	.084780
.060308	.006523	175.329870	.083510
.060282	.006487	175.330181	.084127
.060315	.006404	175.328957	.082309
.060296	.006729	175.330181	.085406
.060330	.006515	175.329542	.088753
.060225	.006413	175.329260	.086624
.060343	.006751	175.332266	.082676
.060358	.006577	175.332376	.086483
.060390	.006685	175.331135	.087744
.060345	.006685	175.328791	.085144
.060418	.006615	175.328390	.083762
.060221	.006638	175.329311	.084013
.060344	.006836	175.330984	.085218
.060394	.006526	175.327396	.083887
.060372	.006625	175.327736	.085437
.060397	.006614	175.330183	.083966
.060385	.006553	175.330116	.083407
.060383	.006691	175.330036	.082314
.060255	.006547	175.329887	.083326
.060271	.006836	175.329800	.087901
.060470	.006448	175.330328	.082262
.060394	.006476	175.329187	.087531
.060337	.006608	175.330364	.084285
.060313	.006546	175.330582	.084204
.060363	.006456	175.329168	.086330
.060331	.006660	175.330273	.085850
.060399	.006734	175.329914	.083239
.060255	.006761	175.332056	.084355
.060469	.006801	175.330706	.084221
.060340	.006633	175.328684	.085862
.060352	.006726	175.330296	.086258
.060370	.006661	175.330511	.085890
.060455	.006798	175.330774	.082844
.060219	.006683	175.329521	.086329

Values for Characteristics Used in Computer Program



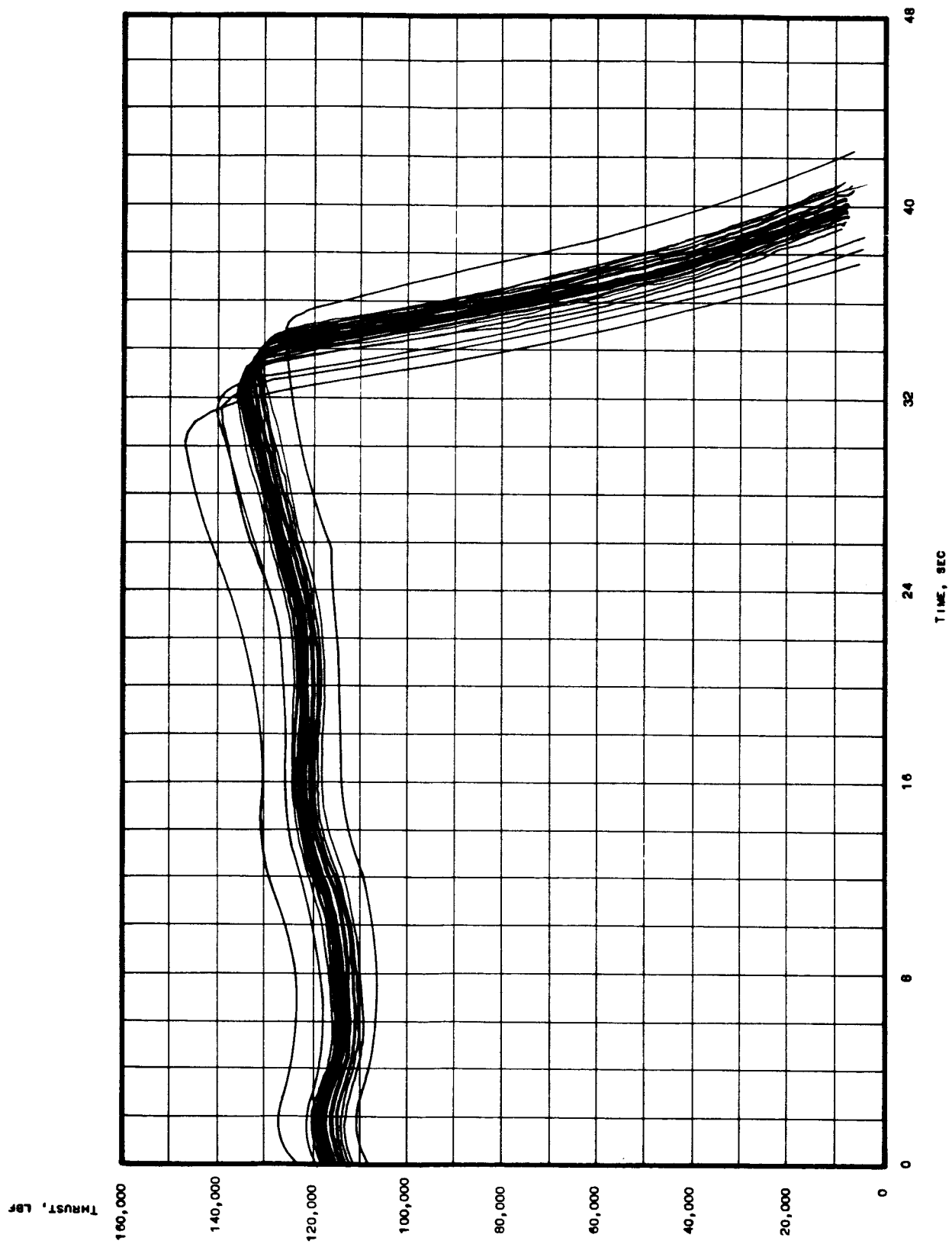
Chamber Pressure vs Time at 70°F, 100 Runs

Figure 58



Sea-Level Thrust vs Time at 70°F, 100 Runs

Figure 59



Altitude Thrust vs Time at 70°F, 100 Runs

Figure 60

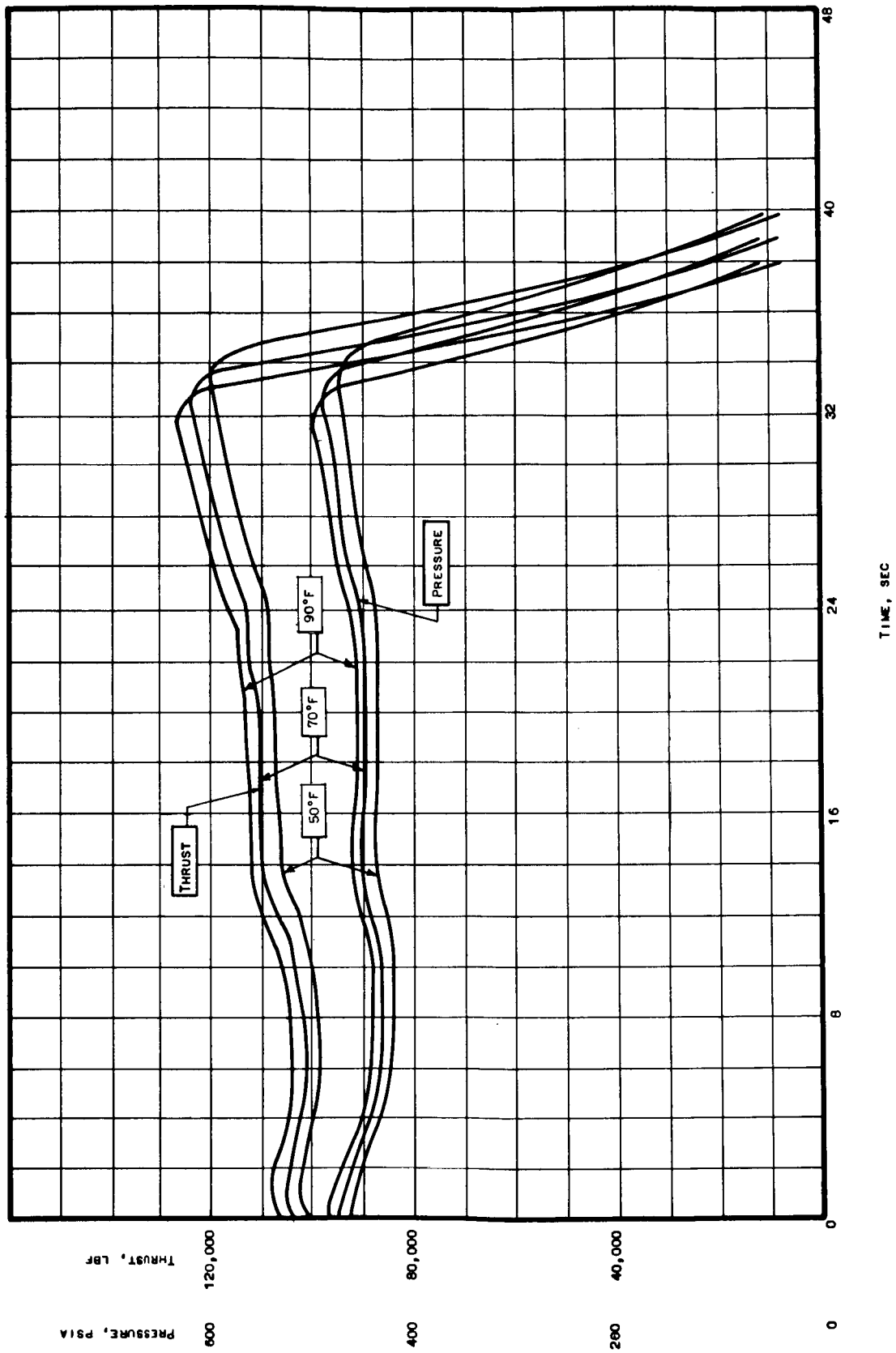
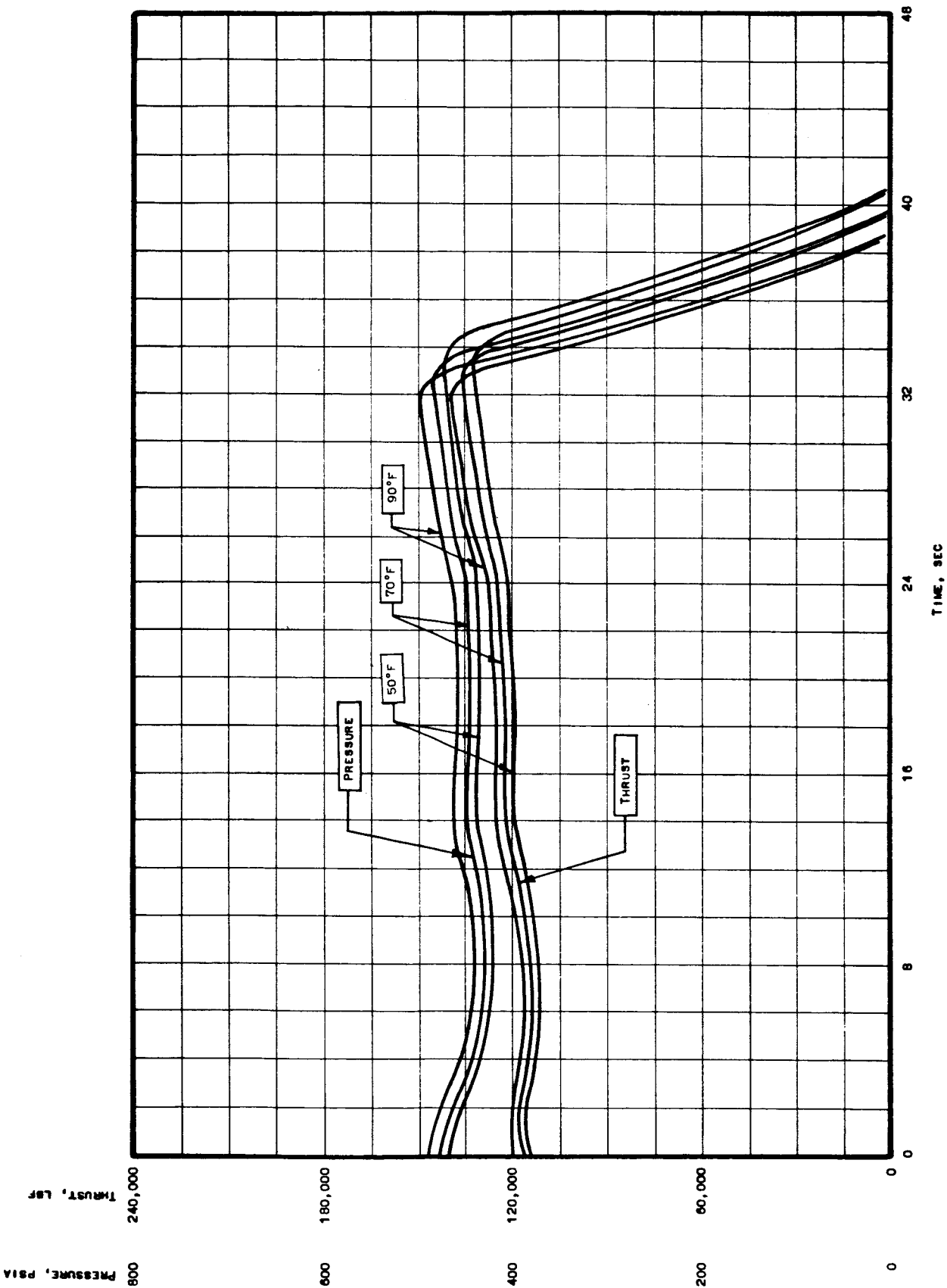


Figure 61

Nominal Thrust and Pressure at 50, 70, and 90°F at Sea Level



Nominal Thrust and Pressure at 50, 70, and 90°F at Altitude

Figure 62

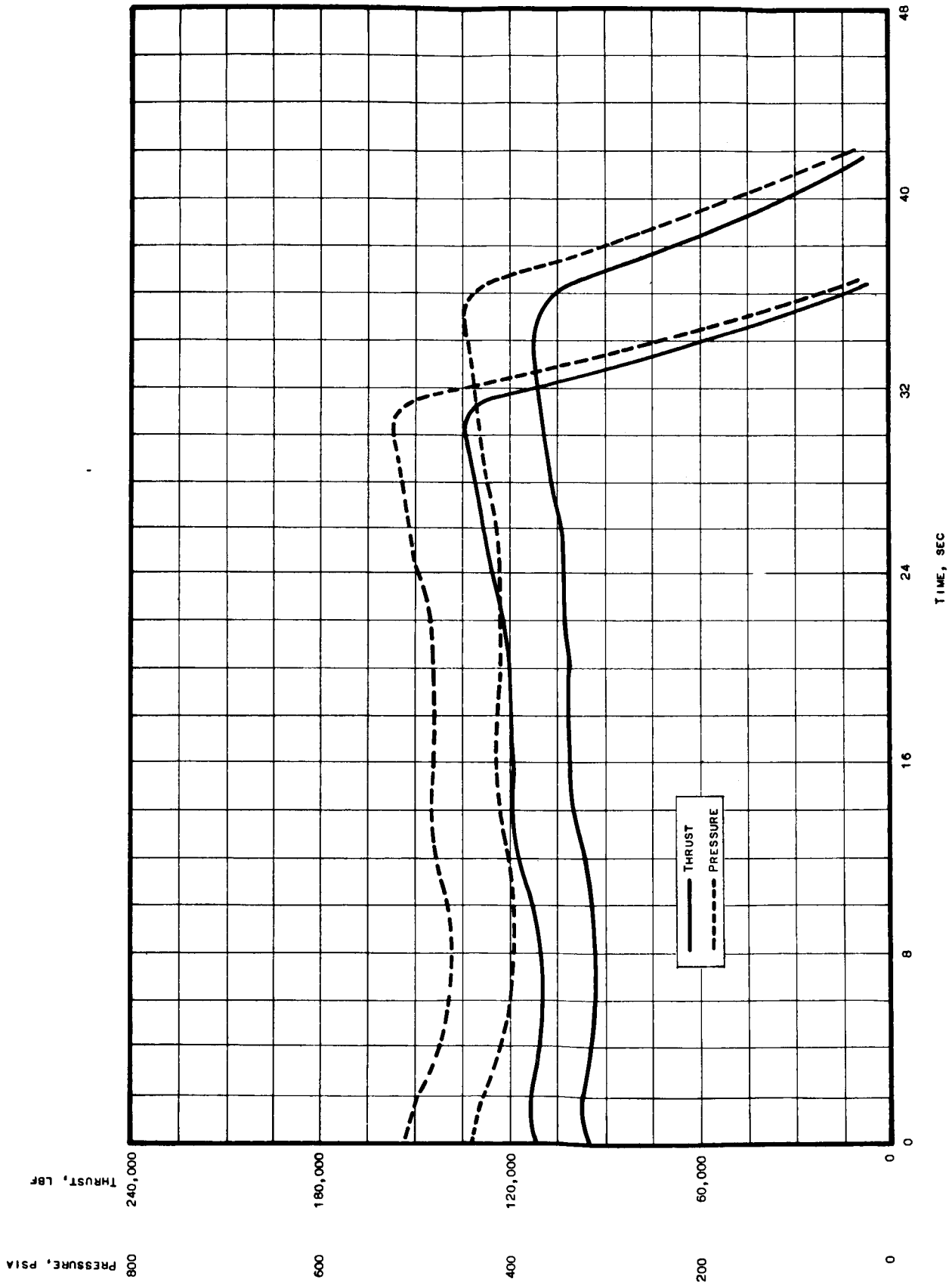
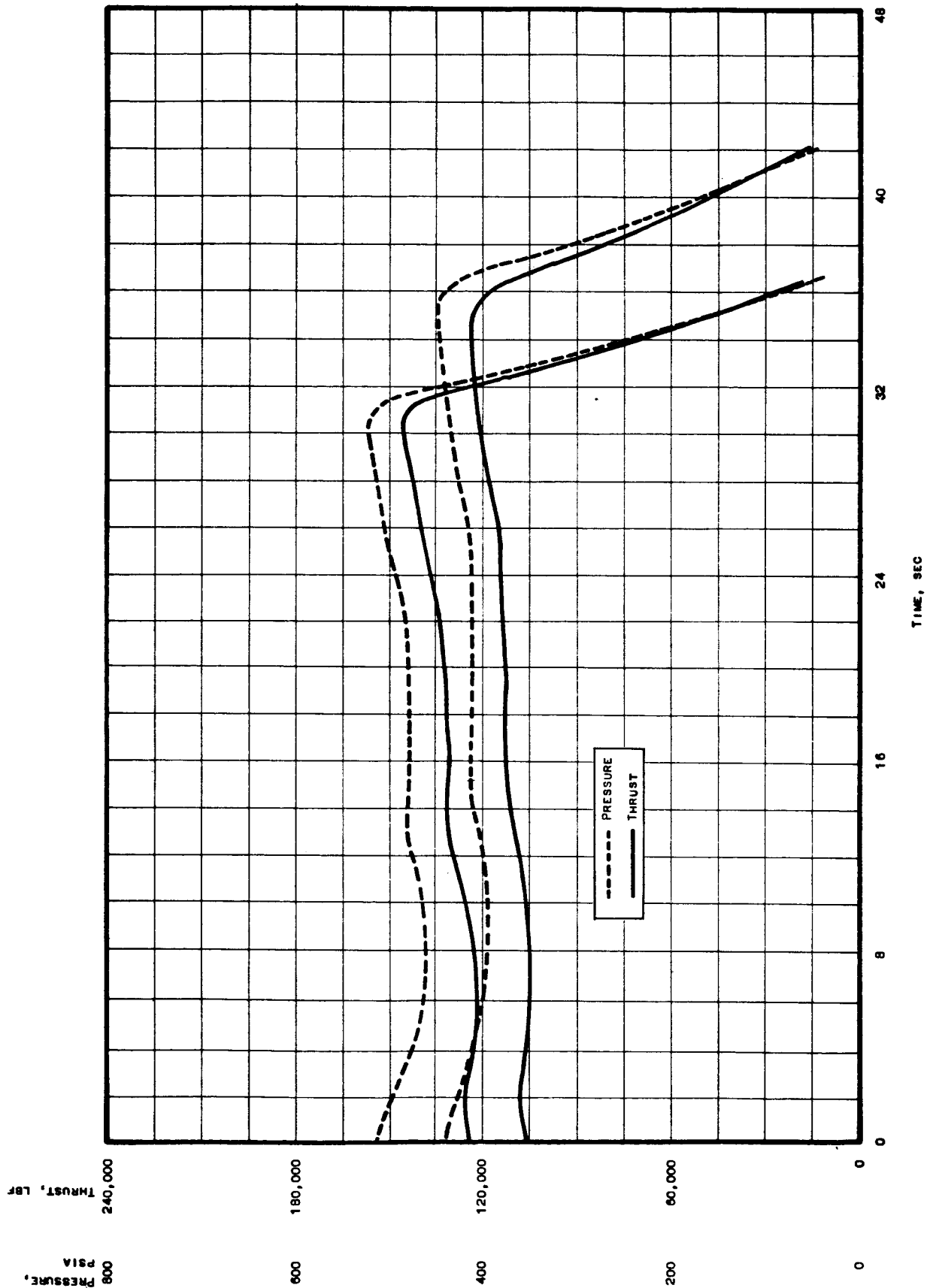


Figure 63

Three-Sigma Limits of Thrust and Pressure at 70°F and Sea Level



Three-Sigma Limits of Thrust and Pressure at 70°F and Altitude

Figure 64

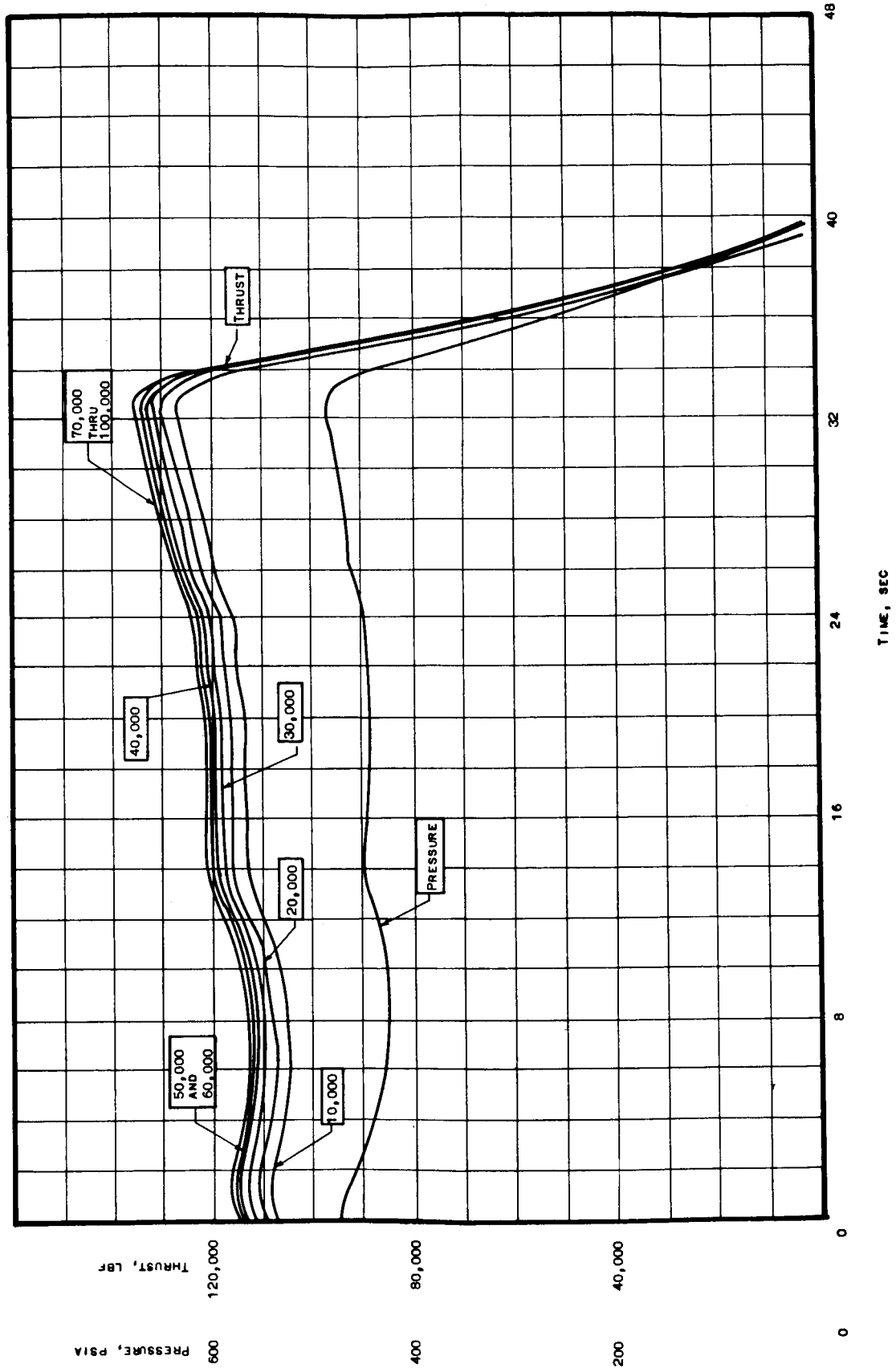
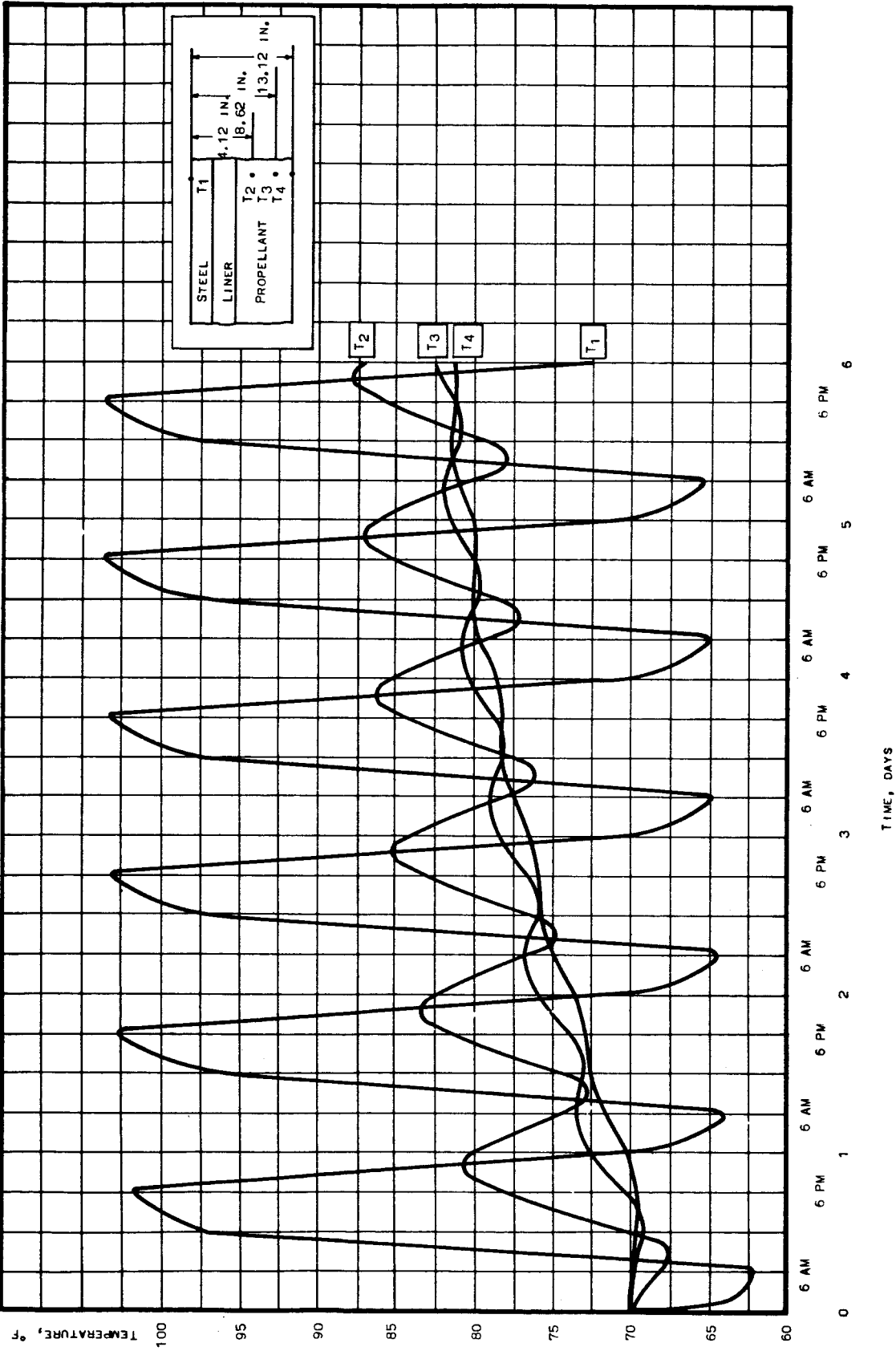


Figure 65

Thrust and Pressure at 70°F From Sea Level to 100,000 ft



Hot-Season Grain-Temperature Gradients

Figure 66

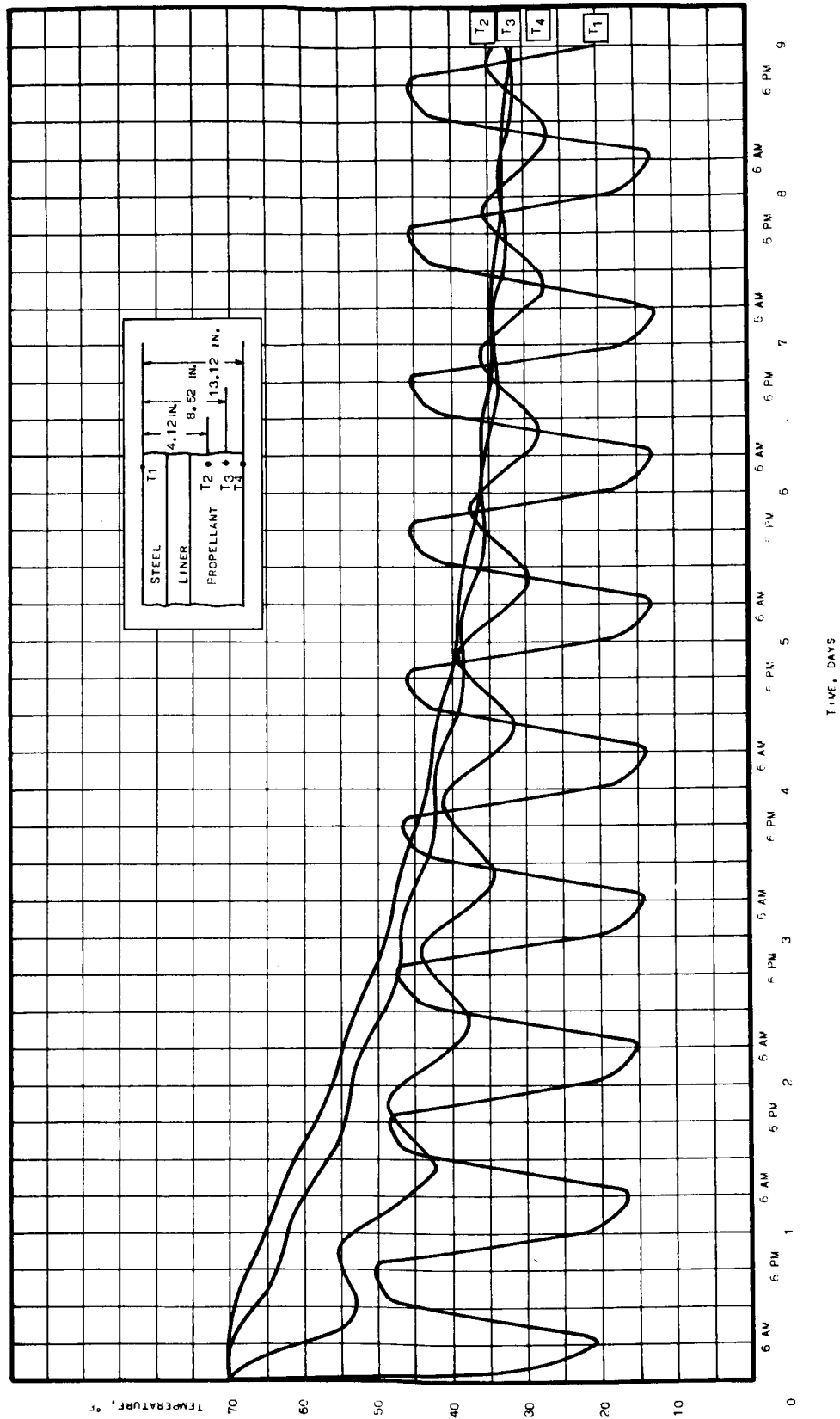
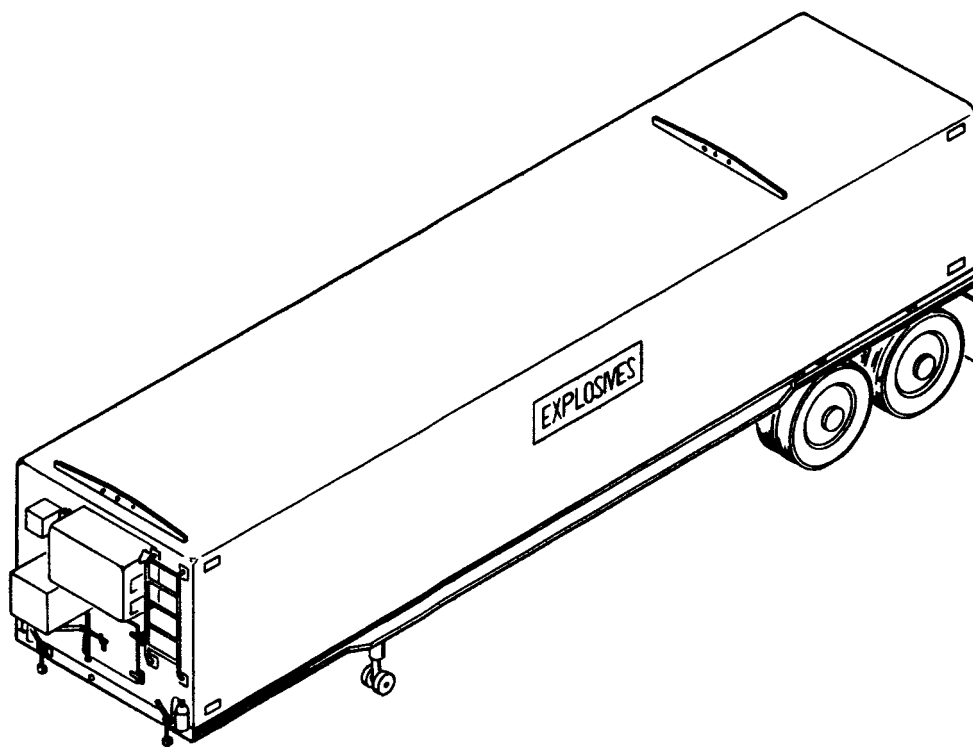


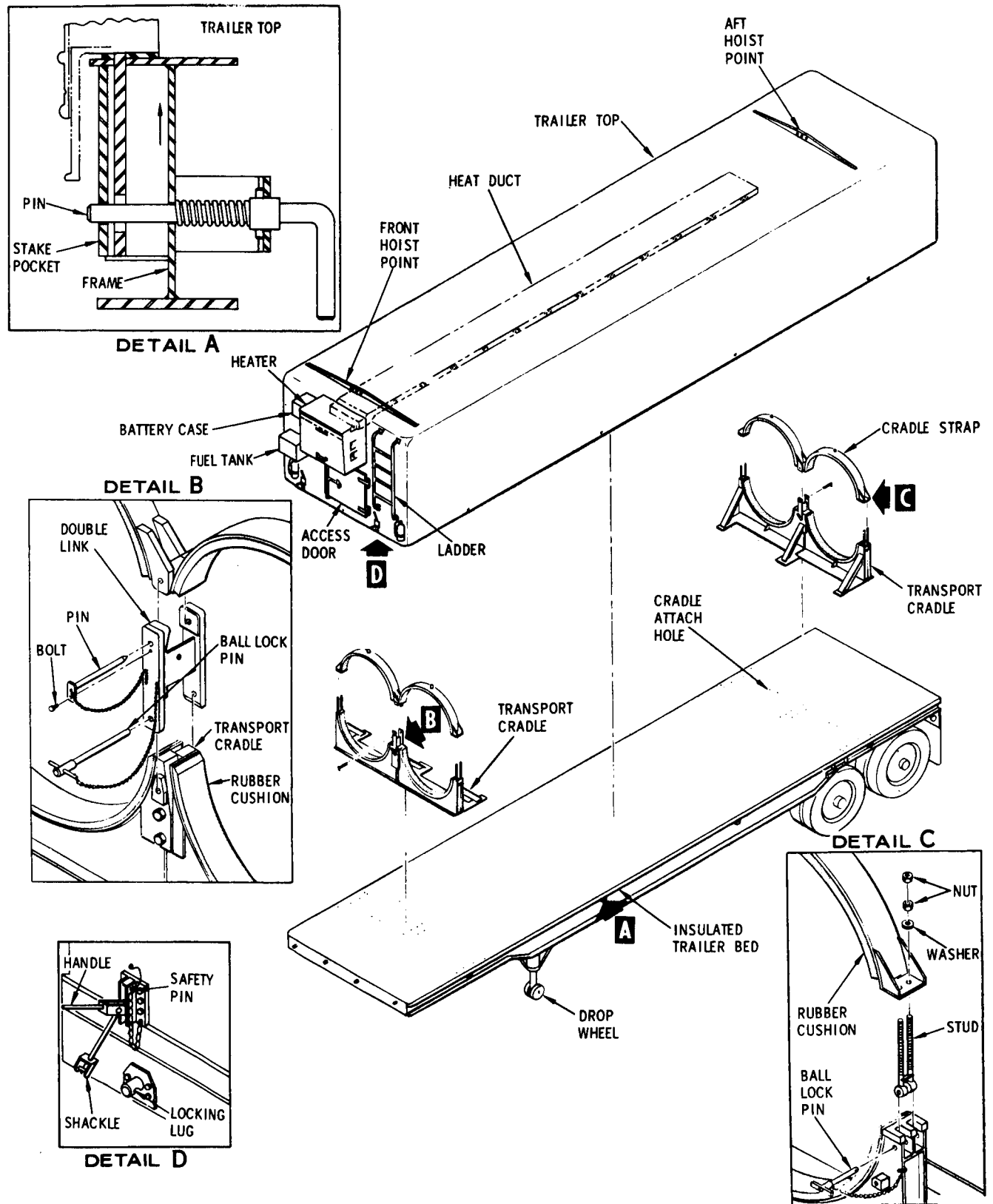
Figure 67

Cold-Season Grain-Temperature Gradients



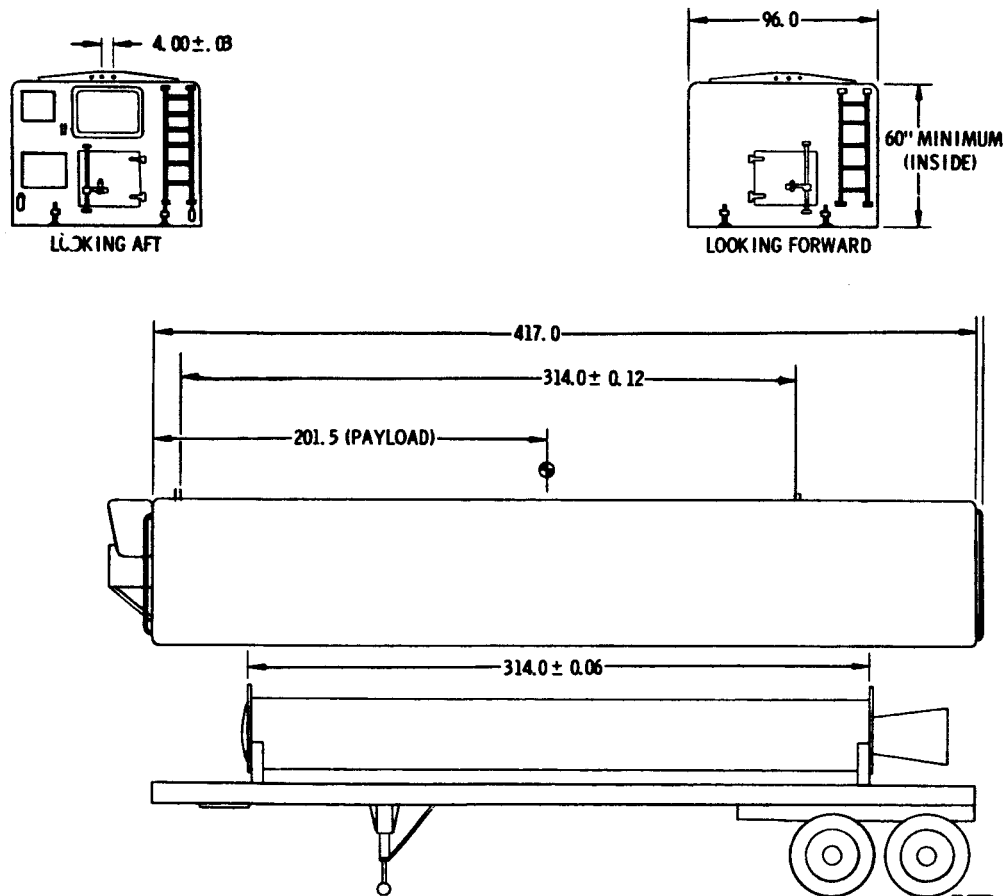
Rocket-Motor Semitrailer

Figure 68



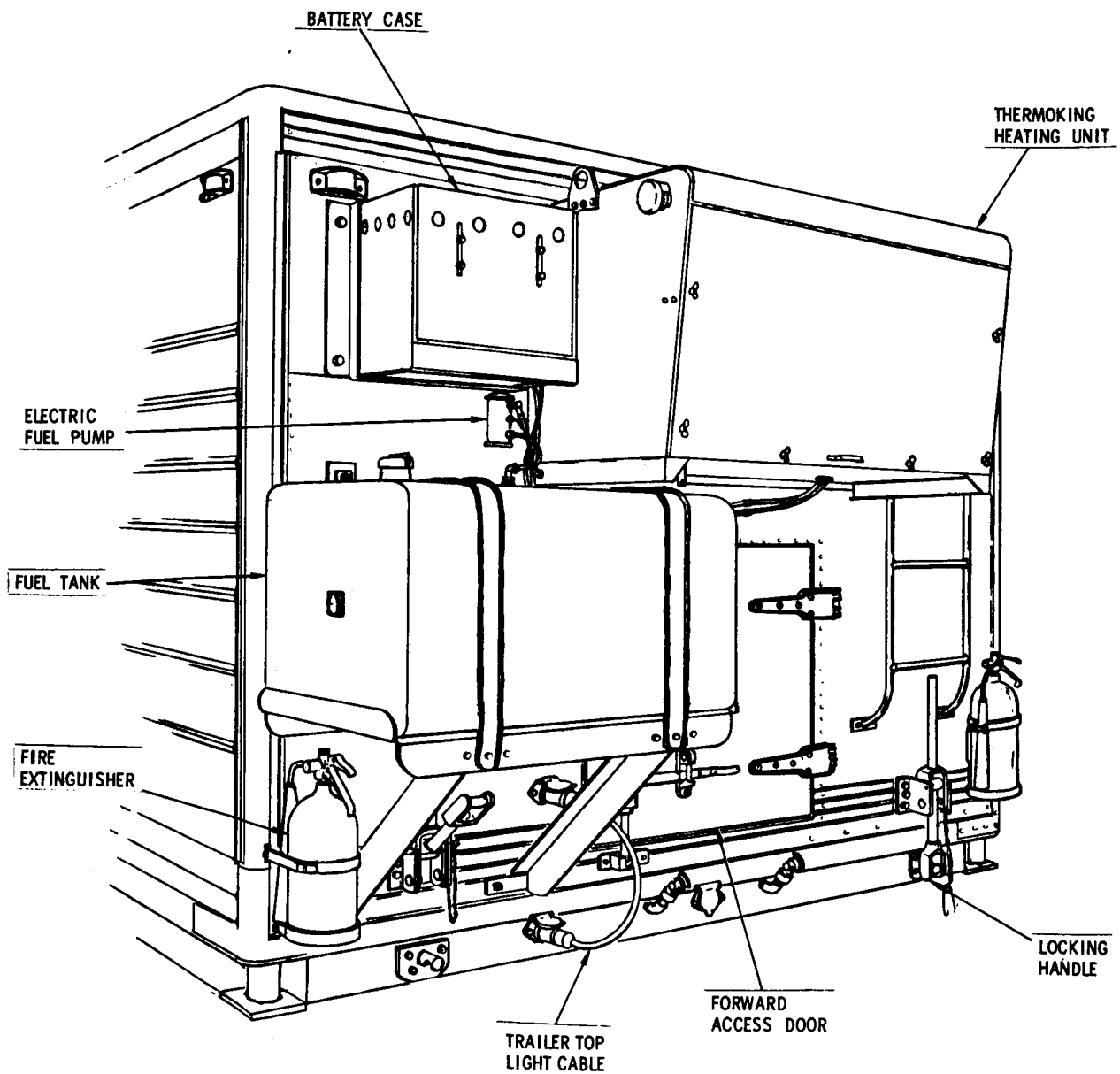
Semitrailer Top

Figure 69



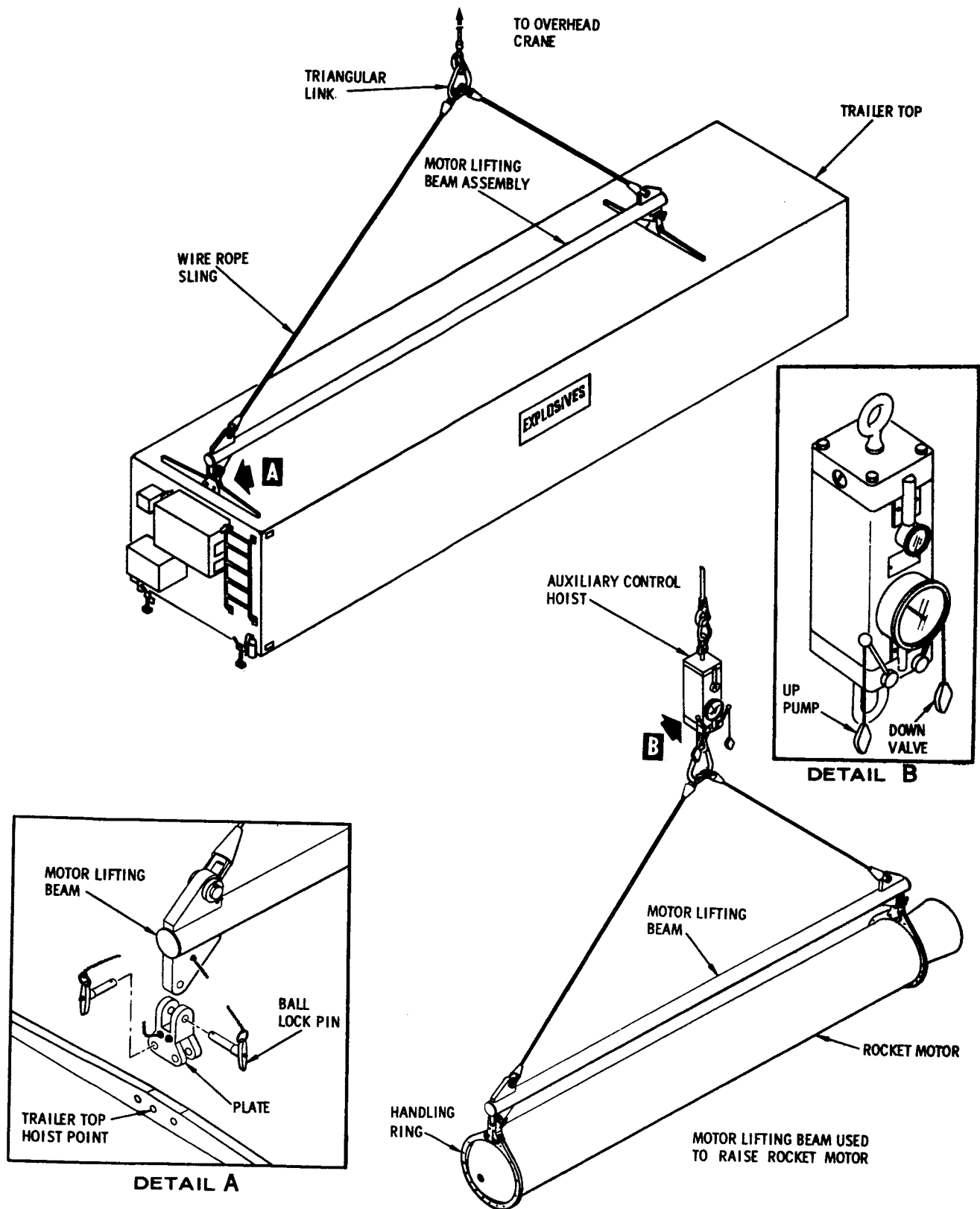
Principal Dimensions of Semitrailer

Figure 70

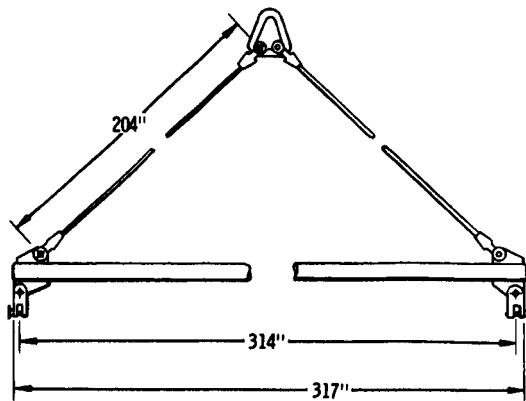


Semitrailer Equipment

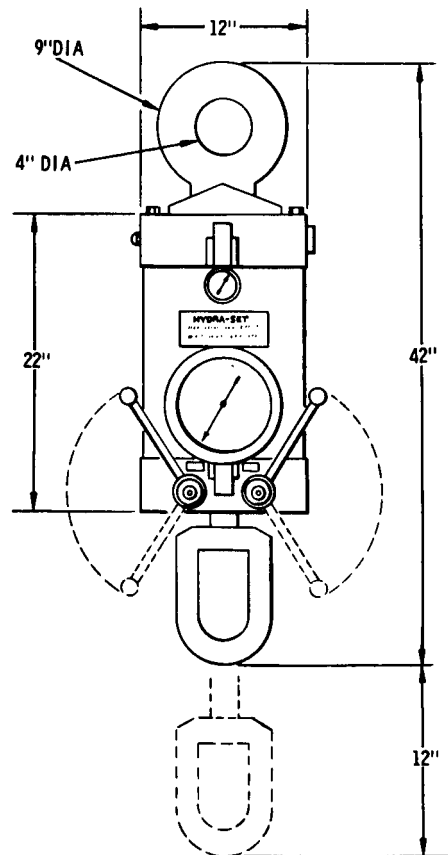
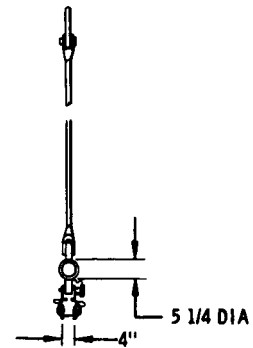
Figure 71



Rocket-Motor Lifting Beam



ROCKET MOTOR LIFTING BEAM



AUXILIARY CONTROL - HOIST

Auxiliary Hoist Control and Principal Dimensions of Lifting Beam

Figure 73

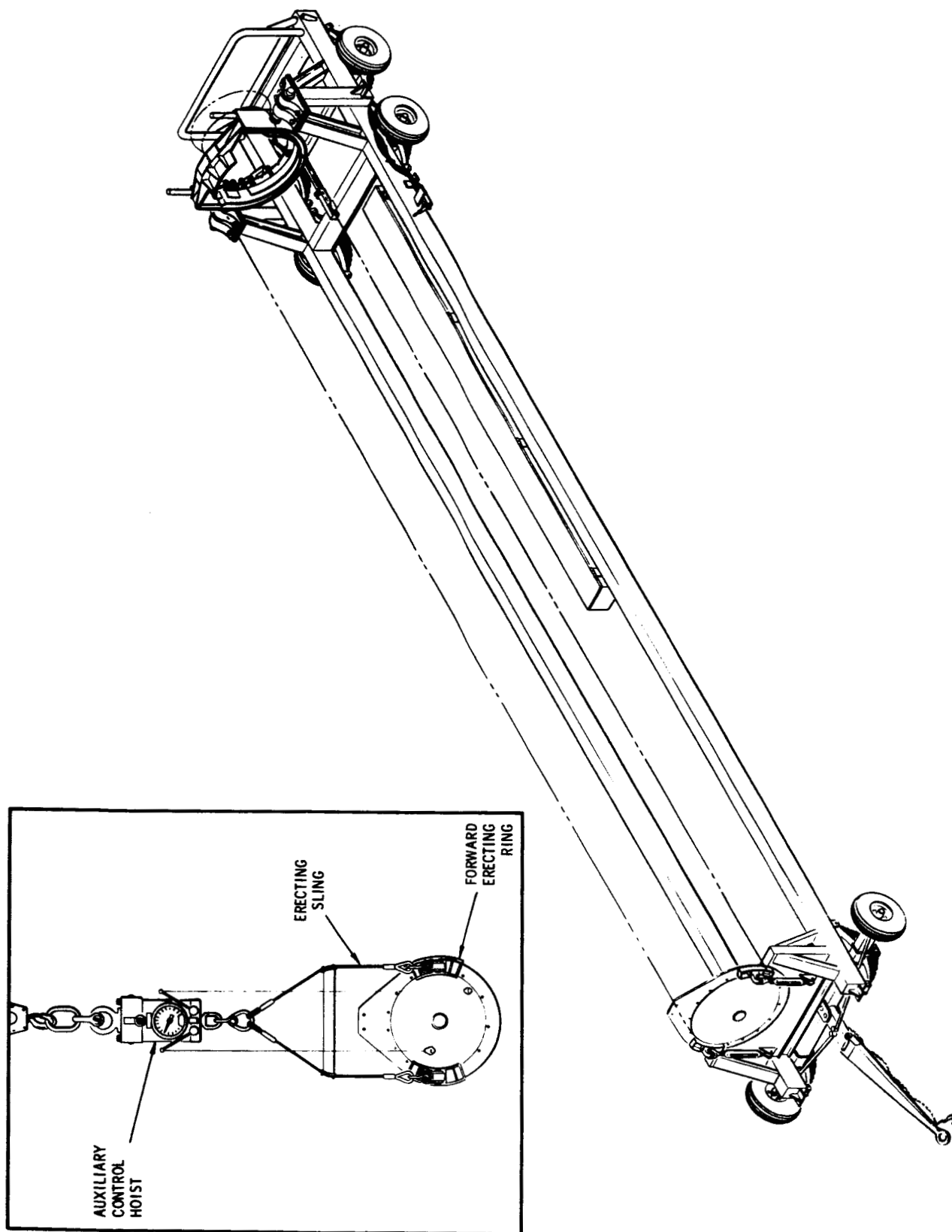
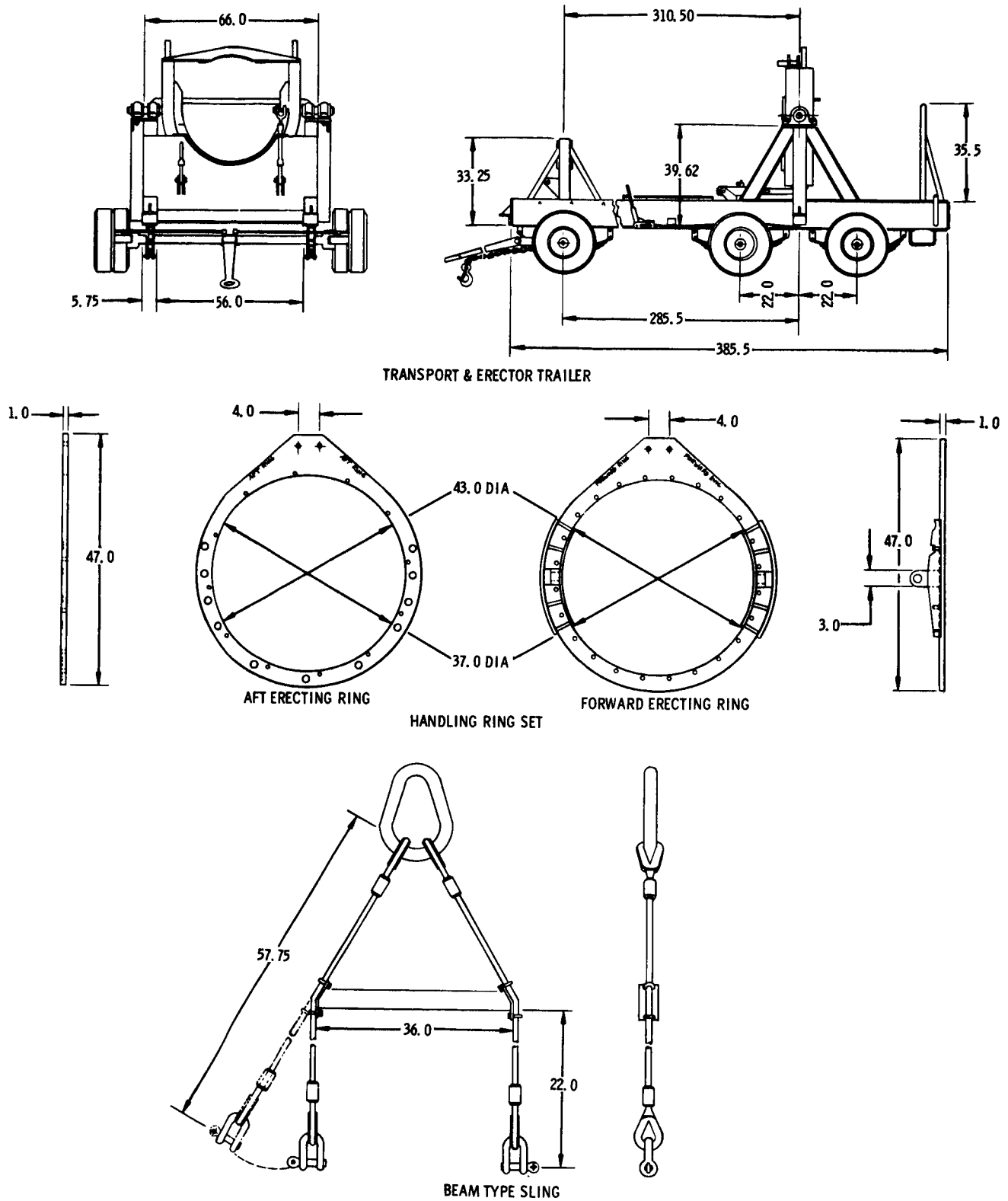
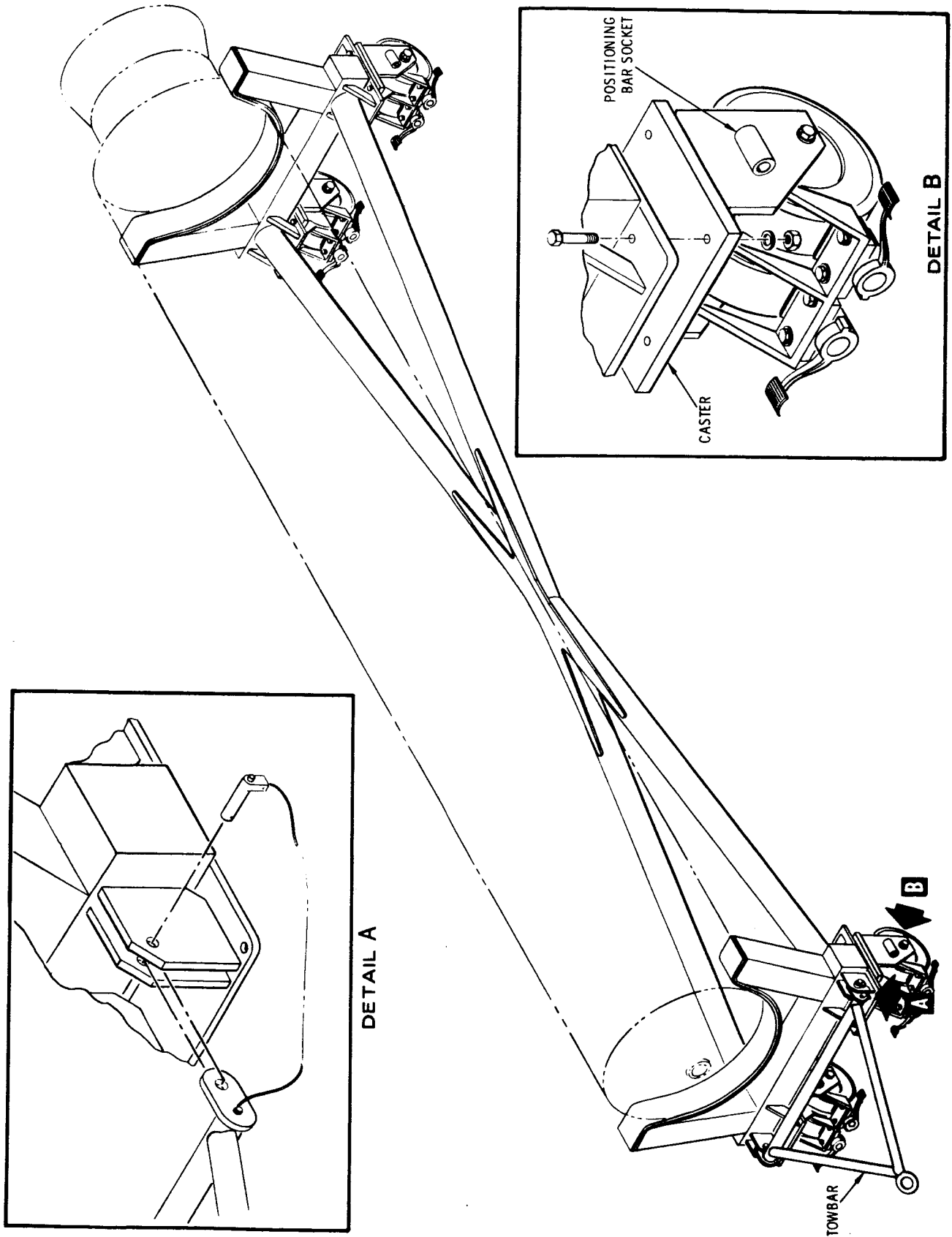


Figure 74



Principal Dimensions of Transport and Erector Trailer

Figure 75



EP 1.032.74.1

Motor Storage Dolly

Figure 76

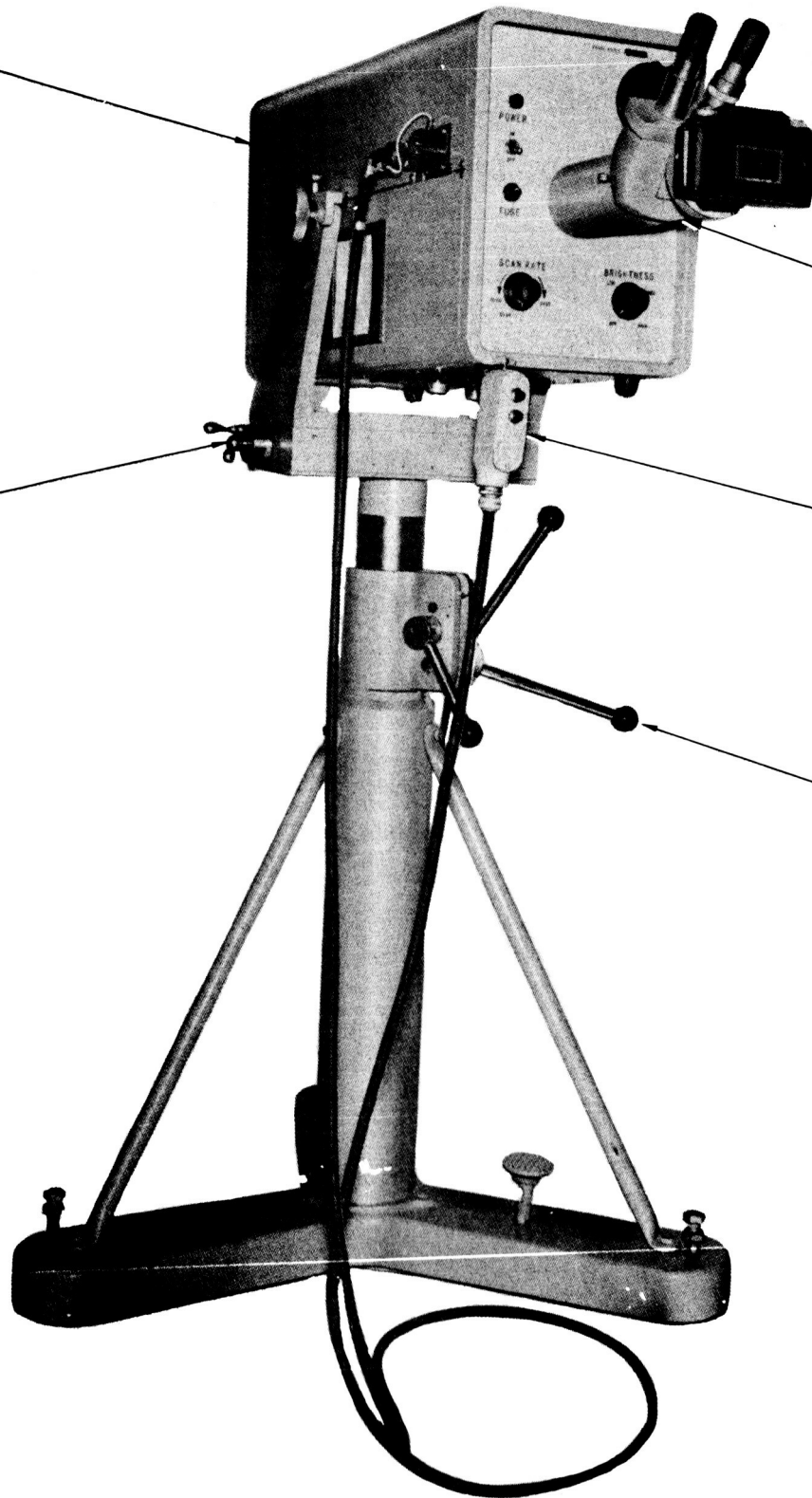
PHOTO AND
OPTICAL ASSEMBLY

TRINOCULAR
ASSEMBLY

LATERAL
ADJUSTMENT
HANDLE

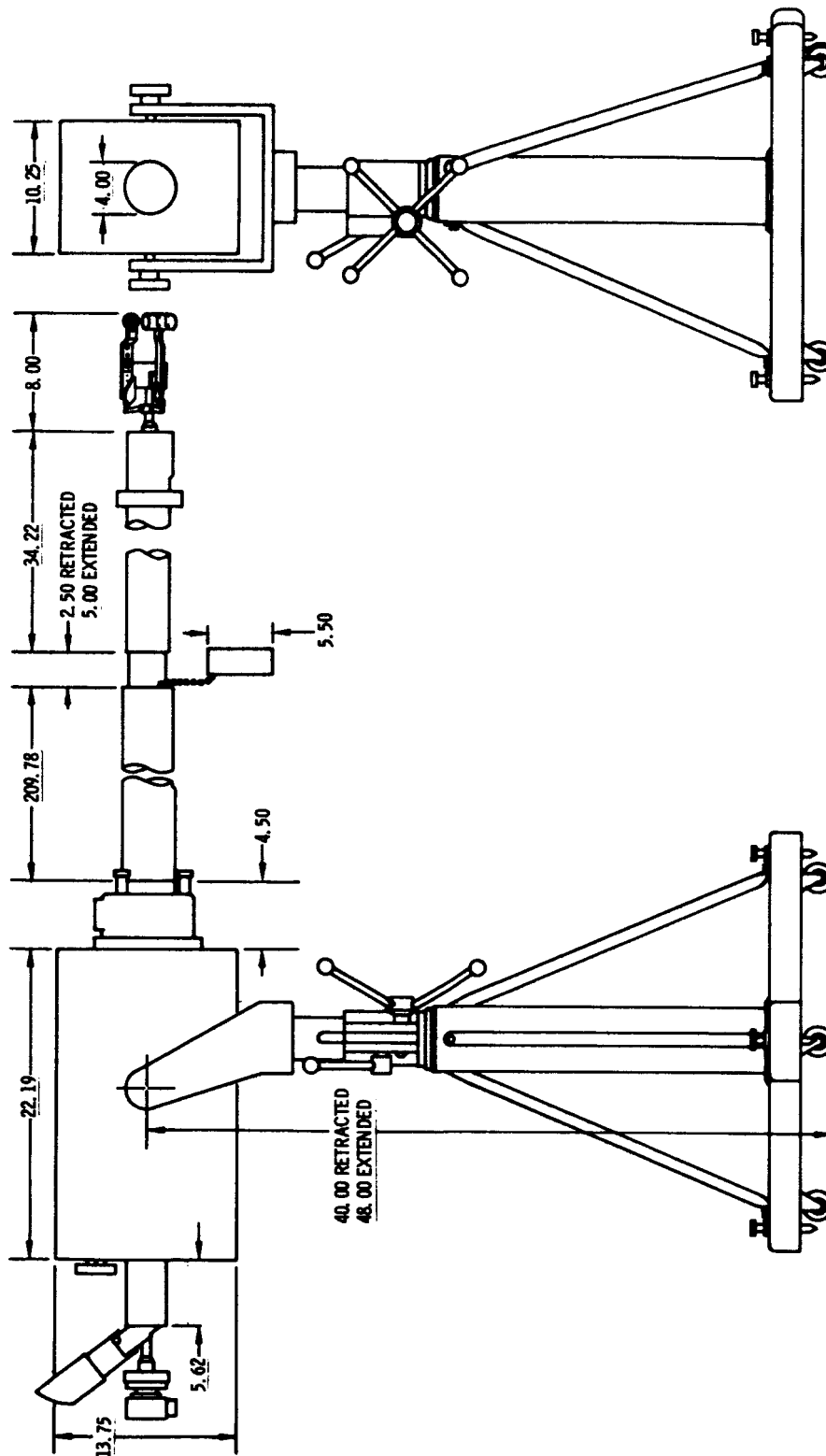
POWER
SUPPLY
CONTROL

VERTICAL
ADJUSTMENT
HANDLE



Rocket-Motor Borescope

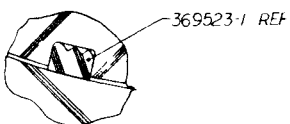
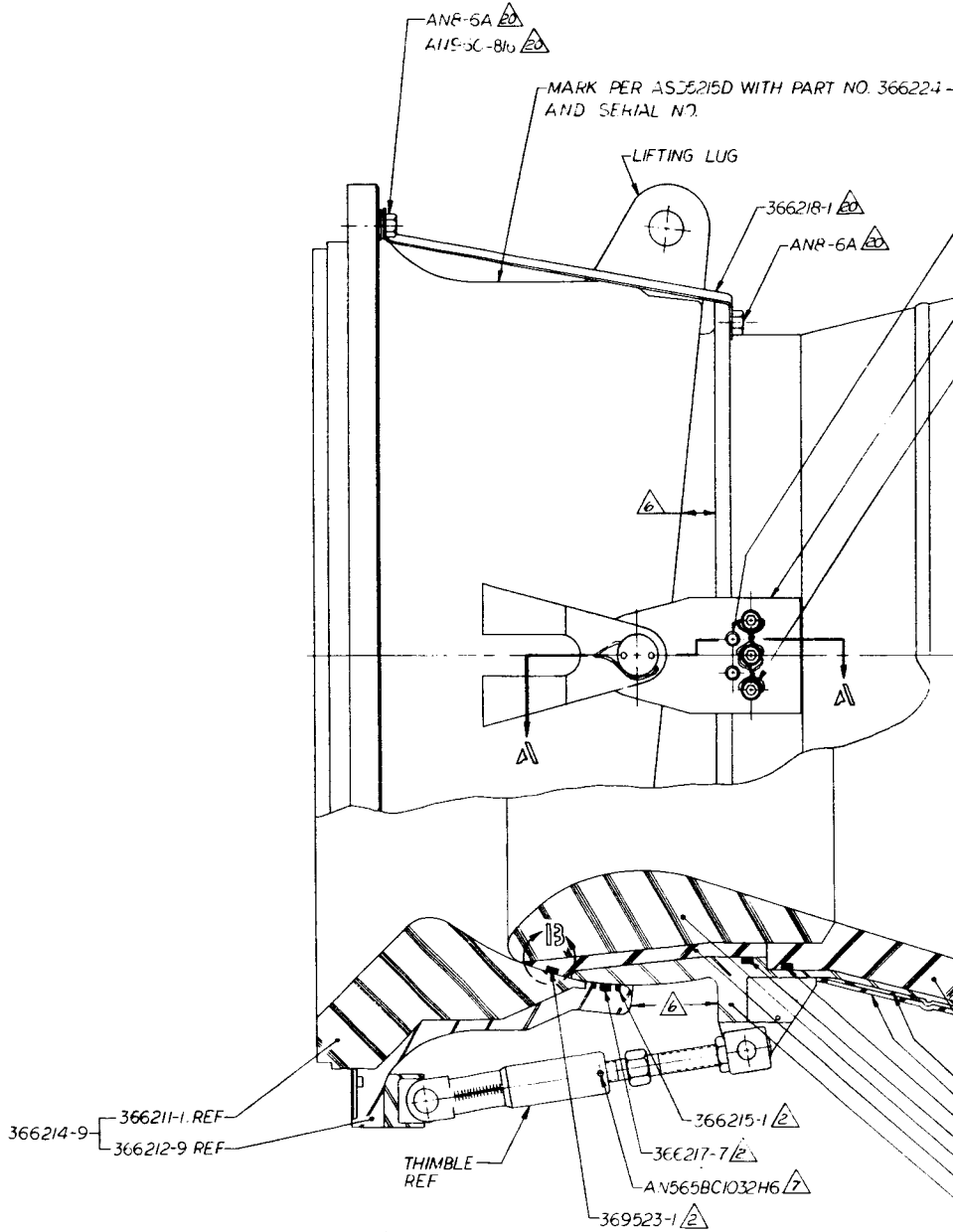
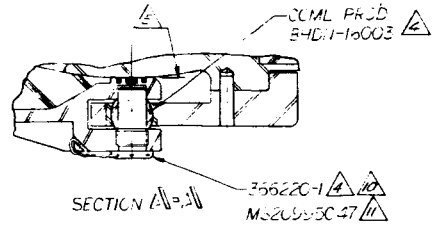
Figure 77



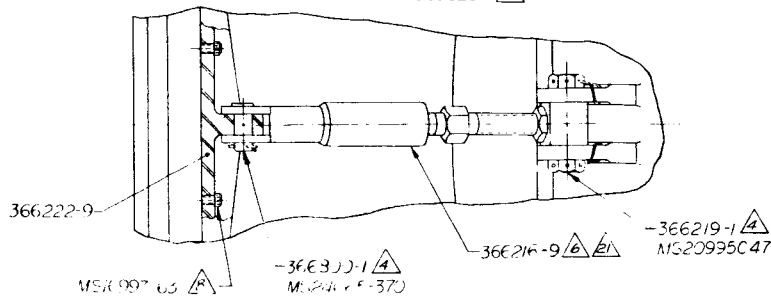
ALL DIMENSIONS IN INCHES

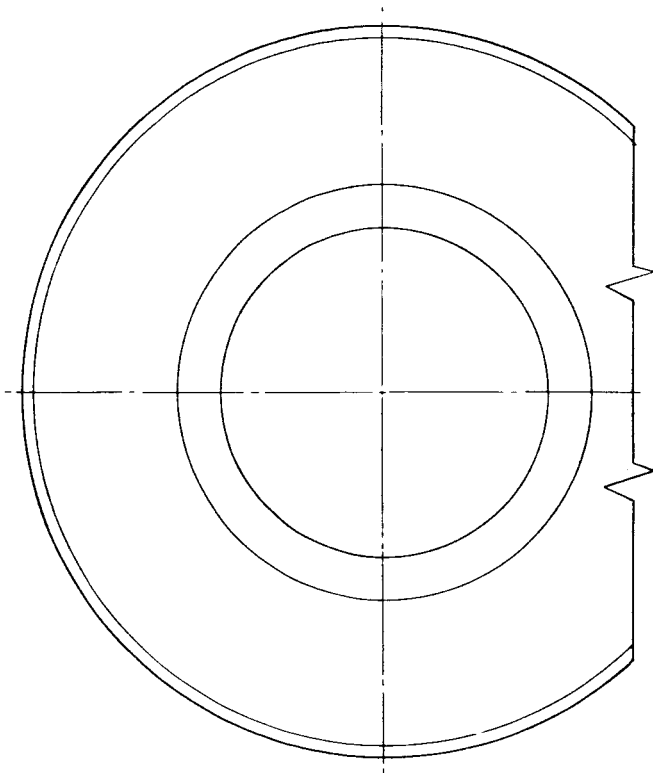
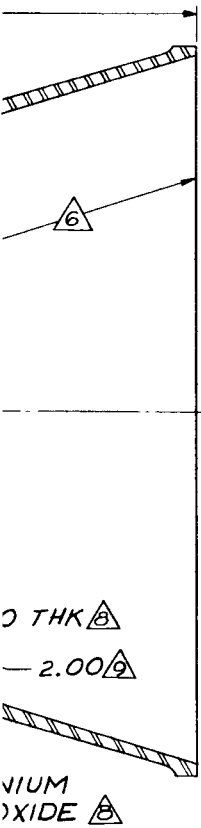
Principal Dimensions of Rocket-Motor Borescope

Figure 78



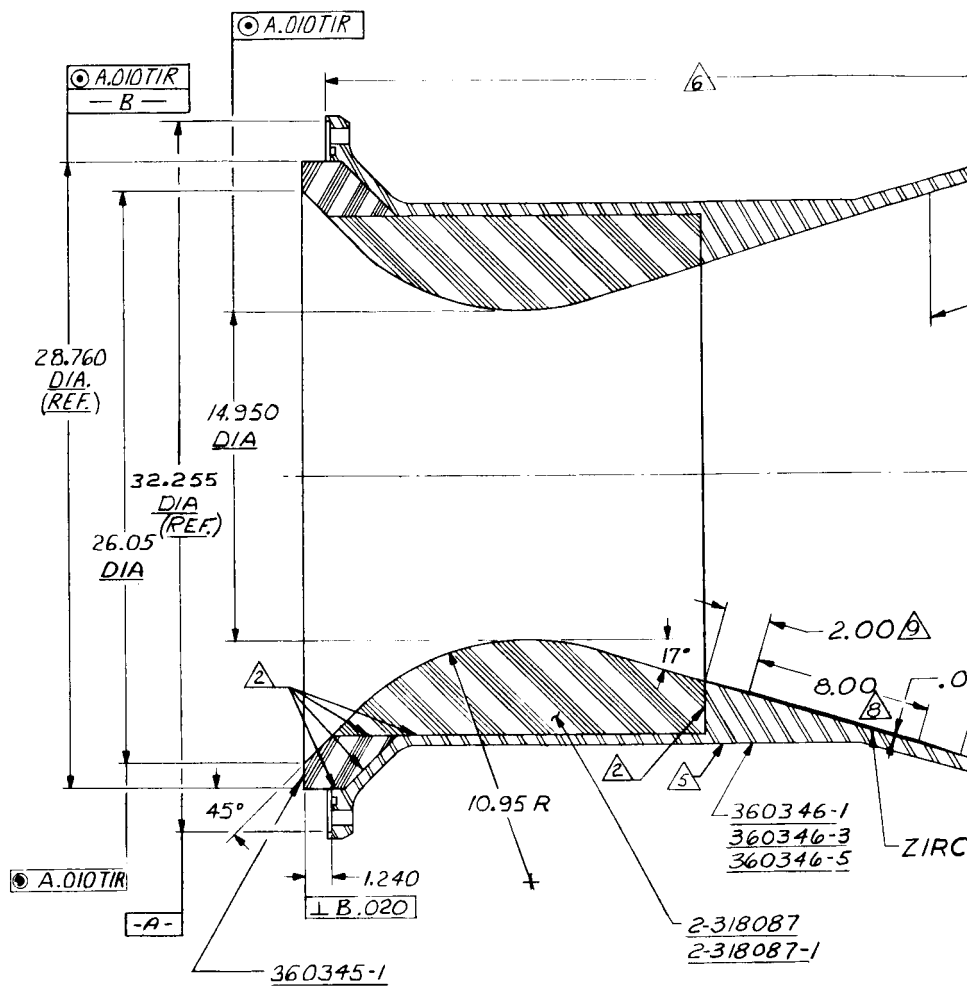
DETAIL 13
SCALE 2



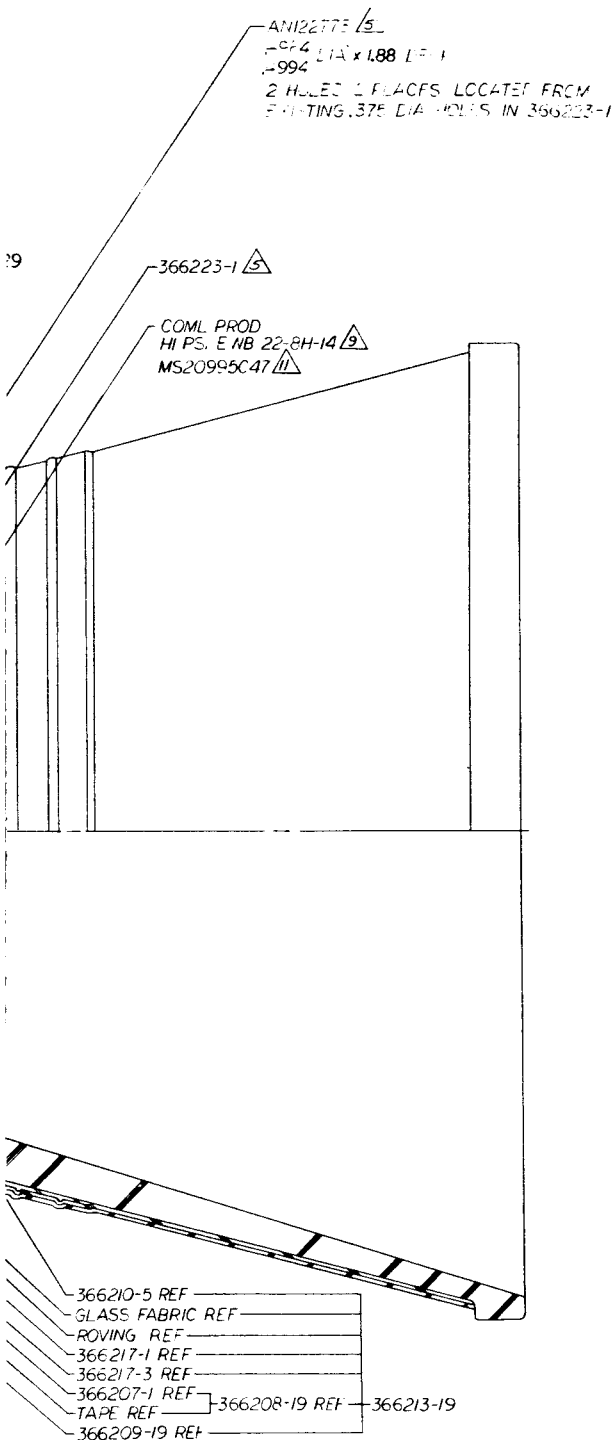


Straight Nozzle

Figure 3



Report 0667-01F



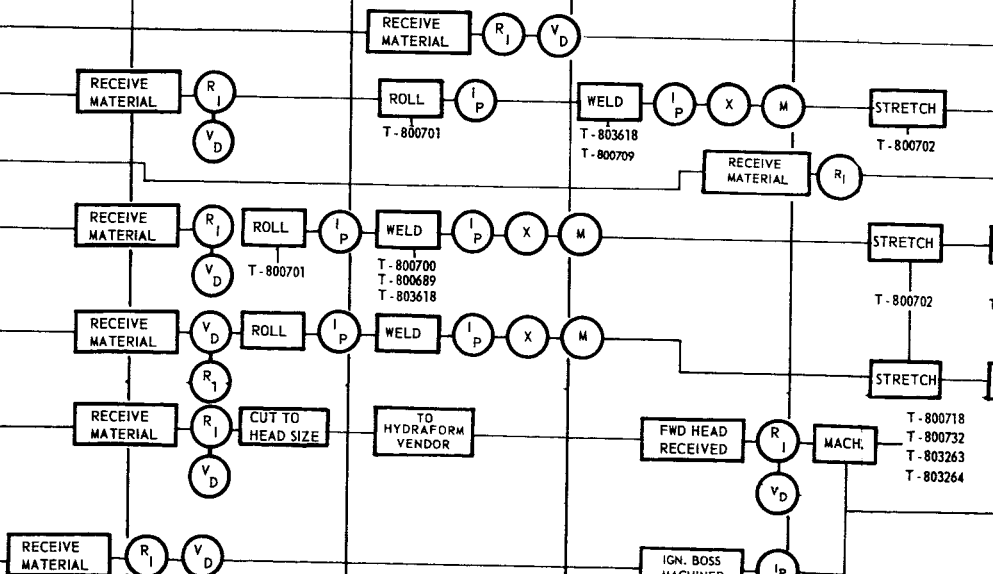
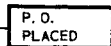
Cantable Nozzle

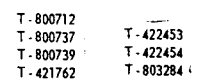
Figure 4

2

**MATERIAL
PROCUREMENT**

**MATERIAL
PROCUREMENT**



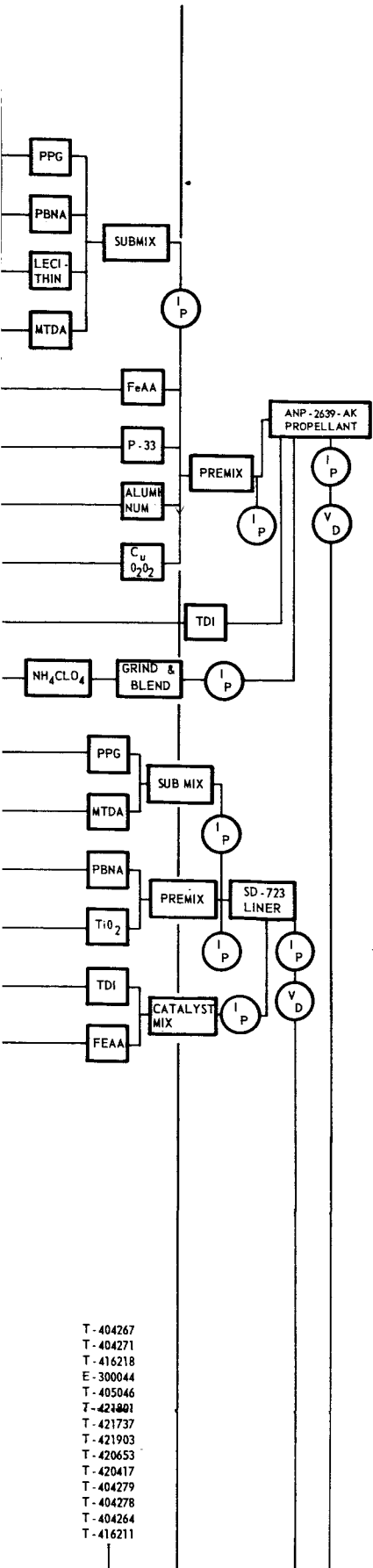


H

Report 0667-01FR-1

Attachment A

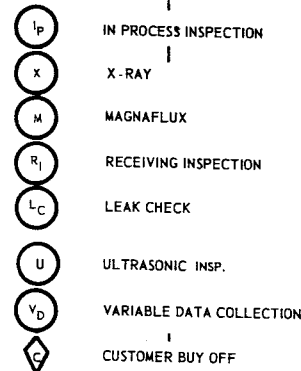
Little Joe II Motor Process Flow Chart



T-404267
T-404271
T-416218
E-300044
T-405046
T-421801
T-421737
T-421903
T-420653
T-420417
T-404279
T-404278
T-404264
T-416211

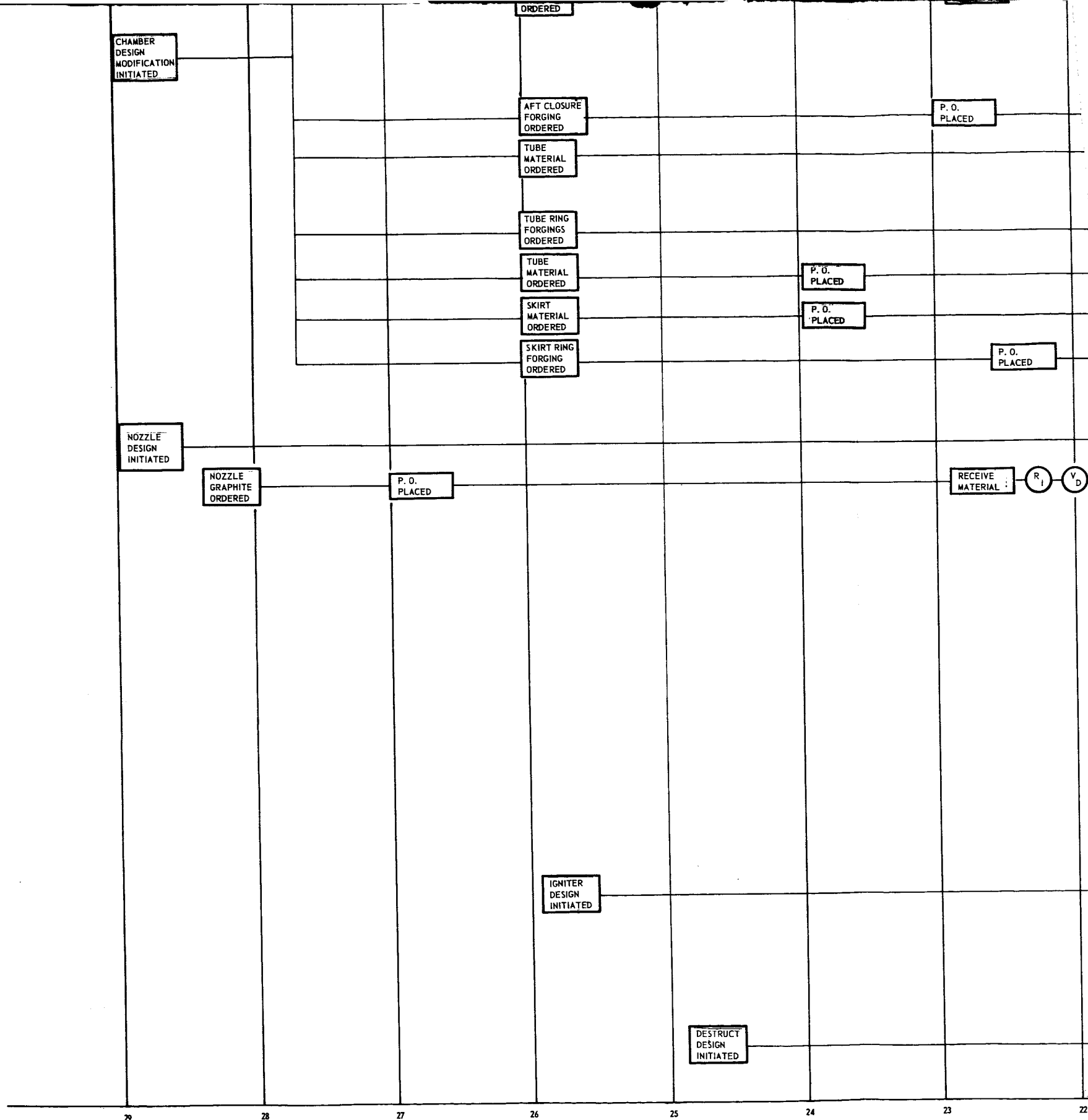
T-405088
T-421760

LITTLE JOE II MOTOR FLOW CHART



E-300044
T-416218
T-404271
T-420689
T-421131
T-404262
T-416219
T-416206
T-416204
T-416235
T-416214
T-421737

TEST
FIRE



CHAMBER
DESIGN
MODIFICATION
COMPLETE

T-800724
T-806000

P. O.
PLACED

RECEIVE
MATERIAL

R_I
V_D

ROLL

I_P

WELD

I_P

X

M

T-800701

T-800700
T-800689
T-803618

RECEIVE
MATERIAL

R_I

V_D

T-800702

STRETCH

TRIM

T-800703
T-800704
T-806263
T-806264
T-800732
T-806001
T-806002

INSULATING
MATERIAL
ORDERED

NOZZLE
DESIGN
SELECTED

RECEIVE
MATERIAL

R_I
V_D

ROLL

I_P

WELD

I_P

X

M

RECEIVE
MATERIAL

R_I
V_D

ROLL

I_P

WELD

I_P

X

M

T-800701

T-803618
T-800705

T-800702

STRETCH

TRIM

MACHINING
T-8007
T-8007
T-8007

RECEIVE
MATERIAL

R_I

V_D

P. O.
PLACED

NOZZLE
DESIGN
COMPLETE

NOZZLES
ORDERED

WEATHER SEAL
DESIGN
COMPLETE

WEATHER SEAL
ORDERED

P. O.
PLACED

BASE HEATING
DESIGN
COMPLETE

BASE HEATING
ORDERED

INSULATING
BOOTS
ORDERED

P. O.
PLACED

MISC. HDWE.
& MATERIAL
ORDERED

BASIC
DESIGN
SELECTED

DESIGN
COMPLETE

BASIC
DESIGN
SELECTED

21

20

19

18

17

16

15

6

